



UPPSALA
UNIVERSITET



UPTEC W 18 026

Examensarbete 30 hp
Augusti 2018

Dissolved organic matter (DOM) quality in
agricultural streams and its impact on carbon
dioxide concentrations in stream water

Karin Broqvist

ABSTRACT

Dissolved organic matter (DOM) quality in agricultural streams and its impact on carbon dioxide concentrations in stream water

Karin Broqvist

Inland waters have lately been recognized to be an important component in the carbon cycle, having a significant role in carbon sequestration and carbon dioxide (CO₂) emissions. Attention has also been drawn to the impact of the quality (i.e. composition and source) of dissolved organic matter (DOM) on CO₂ production.

The objective of this study was to identify geographical and hydrochemical controls on DOM quality and quantity in agricultural streams, and to investigate if DOM quality has an impact on CO₂ concentrations in stream water. Water samples were collected in July-November from ten streams in agricultural catchments in Uppsala, in which partial pressure of CO₂ (pCO₂) had been measured in a related M.Sc. thesis project. Fluorescence measurements and Parallel Factor Analysis (PARAFAC) were carried out to analyse DOM quality. Fluorescence Index (FI), Freshness Index (β/α), Humification Index (HIX) and a five-component PARAFAC model were derived and used to parametrize DOM quality. Dissolved organic carbon (DOC) concentration was used as a measure of DOM quantity.

The fraction of arable land in the catchment was found to be positively correlated with FI, indicating a shift towards more microbially derived DOM with more arable land in the catchment. Two PARAFAC components associated with terrestrial and highly decomposed DOM were found to correlate positively with pCO₂ at one site. Specific discharge and electrical conductivity were correlated with DOM quality and quantity at several sites. The correlations indicated that both the discharge magnitude as well as the flow paths affected the quality and the quantity of DOM.

Keywords: DOM quality, dissolved organic matter, DOC, PARAFAC, fluorescence, streams, agriculture, fluorescence index, freshness index, humification index, carbon dioxide

*Department of Soil and Environment, Swedish University of Agricultural Sciences (SLU),
Lennart Hjelm's väg 9, SE 750 07 Uppsala*

REFERAT

Det lösta organiska materialets (DOM) kvalitet i jordbruksbäckar och dess påverkan på koldioxidkoncentrationer i bäckvatten

Karin Broqvist

Sjöar och vattendrag har på senare tid uppmärksammats som viktiga komponenter i kolcykeln, då de har visats inverka på både inbindningen av kol och på utsläpp av koldioxid (CO₂). Uppmärksamhet har även riktats mot hur kvaliteten, d.v.s. sammansättningen och ursprunget, av det lösta organiska materialet (DOM) påverkar koldioxidproduktionen i inlandsvatten.

Syftet med detta examensarbete var att identifiera geografiska och vattenkemiska variabler som påverkade DOM kvaliteten och kvantiteten i bäckar i jordbrukslandskap, samt att undersöka om DOM kvaliteten hade en påverkan på CO₂-koncentrationen i bäckarna. Vattenprover togs under juli till november från tio jordbruksbäckar i Uppsala, i vilka koncentrationen av CO₂ hade mätts i ett tidigare examensarbete.

DOM kvaliteten analyserades med hjälp av fluorescensmätningar och parallell faktoranalys (PARAFAC). Fluorescence Index (FI), Freshness Index (β/α) och Humification Index (HIX) beräknades och användes tillsammans med en PARAFAC-modell med fem komponenter för att parametrisera DOM kvaliteten. Koncentrationen av löst organiskt kol (DOC) användes som mått på DOM kvantiteten.

Resultaten visade att andelen jordbruksmark i avrinningsområdet var positivt korrelerad med FI, vilket indikerade att mer jordbruksmark i avrinningsområdet skiftar DOM kvaliteten till ett mer mikrobiellt ursprung. Två PARAFAC komponenter var korrelerade med partialtrycket av CO₂ i en av bäckarna. Dessa komponenter var associerade med DOM av terrestriskt ursprung och av hög nedbrytningsgrad. Specifik avrinning och elektrisk konduktivitet korrelerade med DOM kvalitet och kvantitet i flertalet bäckar. Korrelationerna indikerade att både avrinningens storlek och dess flödesvägar påverkade kvaliteten och kvantiteten av DOM.

Nyckelord: DOM kvalitet, löst organiskt material, DOC, PARAFAC, fluorescens, bäckar, jordbruk, fluorescence index, freshness index, humification index, koldioxid

PREFACE

This master thesis corresponds to 30 ECTS and is the final part of the M.Sc. in Environmental and Water Engineering at Uppsala University and the Swedish University of Agricultural Sciences (SLU). Supervisor of this project was Mattias Winterdahl at the Department of Earth Sciences at Uppsala University. Subject reviewer was Magdalena Bierozka at the Department of Soil and Environment at SLU, and examiner was Fritjof Fagerlund at the Department of Earth Sciences at Uppsala University.

I would like to thank Magdalena Bierozka for all the assistance with fluorescence and DOC measurements, and for guiding me with great patience through the complex world of PARAFAC. I would also like to thank Mattias Winterdahl for his guidance and support along the course of this project and for sharing his great expertise, which was of great help for my thesis. Thank you both for your invaluable comments on the report.

I would also like to thank My Osterman for the valuable work of her M.Sc. thesis preceding my project, providing data of CO₂ concentrations and catchment characteristics. Thank you also to Joachim Audet at the Department of Aquatic Sciences and Assessment at SLU for the measuring of hydrochemical variables and collection of water samples. I would also like to thank Marcus Wallin at the Department of Earth Sciences at Uppsala University and Michael Peacock at the Department of Aquatic Sciences and Assessment at SLU for company and assistance in the field.

Finally, I would like to thank my family and friends for all the support and encouragement.

Uppsala, Sweden, July 2018

Karin Broqvist

POPULÄRVETENSKAPLIG SAMMANFATTNING

Sjöar och vattendrag har på senare tid visats spela en aktiv och viktig roll i kolcykeln, d.v.s. kolets transformering och transport i landskapet. Inlandsvatten utgör viktiga miljöer för nedbrytning och transformering av organiskt kol till koldioxid (CO₂) och metan. Både inbindningen av kol i sjösediment och avgången av koldioxid från inlandsvatten till atmosfären har visats vara större än tidigare trott.

Löst organiskt material (DOM) utgörs till största delen av kol och bildas naturligt vid nedbrytning av dött material från växter och djur. DOM kan även härröra från t.ex. mänsklig aktivitet, så som jordbruk och avlopp. I akvatiska miljöer kan DOM påverka ekosystemets dynamik och balans. Det lösta organiska materialet fungerar nämligen som en källa till energi och näring för organismer och kan dessutom påverka ljusförhållandena i vattnet. Förändrade ljusförhållanden i vattnet får i sin tur en effekt på fotosyntetiserande växter och organismer. Ett annat problem kopplat till DOM är att skadliga metaller och föroreningar kan ha lätt att binda till det organiska materialet och på så sätt transporteras vidare i landskapet.

Koldioxidkoncentrationen i vattendrag tros bland annat påverkas av det lösta organiska materialets kvalitet, d.v.s. dess ursprung och sammansättning. Det lösta organiska materialet kan exempelvis härröra från terrestriskt material eller från mikrober och alger, det kan bestå av olika typer av kemiska bindningar och komponenter och det kan ha brutits ned i olika grad. Karaktären på det lösta organiska materialet utifrån dessa egenskaper är det som kallas DOM kvalitet.

I det här examensarbetet studerades huruvida DOM kvaliteten hade någon effekt på koldioxidkoncentrationen i vattnet, samt vilka vattenkemiska och geografiska faktorer som påverkade DOM kvaliteten. Vattenprover samlades in mellan juli och november från tio bäckar, alla belägna i jordbrukslandskap runt Uppsala. För att analysera DOM kvaliteten i vattenproverna användes fluorescensmätningar kombinerat med en multivariat dataanalysteknik kallad PARAFAC. Fluorescens är fenomenet när en molekyl absorberar ljus med hög energi, och därefter sänder ut ljus av lägre energi. Genom att mäta inkommande och utgående ljus vid olika våglängder kan indikationer om kvaliteten av det lösta organiska materialet i vattenproverna fås. Med hjälp av PARAFAC kunde fem komponenter kopplade till olika DOM kvalitet identifieras. Utifrån resultaten av fluorescensmätningarna kunde även tre olika index beräknas. Dessa index gav mått på olika egenskaper hos det organiska materialets kvalitet. Därefter gjordes statistisk analys för att undersöka vilka vattenkemiska och geografiska faktorer som påverkade DOM kvaliteten.

Resultaten indikerade att en högre andel jordbruksmark i avrinningsområdet var kopplad till en högre andel DOM av mikrobiellt ursprung. Inget tydligt mönster kunde ses för hur DOM kvalitet och kvantitet påverkades av mängden näringsämnen i vattnet, däremot verkade både storleken på avrinningen samt avrinningens flödesvägar påverka. Detta skulle kunna bero på att både den totala mängden löst organiskt material och dess kvalitet varierar med markdjupet. Beroende på om avrinningen sker mestadels från ytliga eller från djupa jordlager transporteras olika mängd och olika kvalitet av DOM till vattendragen. Det är möjligt att alla dessa faktorer (andelen jordbruksmark, mängden näringsämnen och avrinningens storlek och flödesvägar) påverkar varandra och även tillsammans får en effekt på DOM kvaliteten och kvantiteten.

Vad gäller det organiska materialets påverkan på koldioxidkoncentrationen kunde inget rumsligt samband ses. För två av de totalt tio undersökta bäckarna fanns tillräckligt med data

för att studera korrelationen mellan DOM kvalitet och CO₂-koncentration över tid. I en av dessa bäckar fanns en korrelation mellan CO₂ och två PARAFAC-komponenter relaterade till terrestriskt organiskt material av hög nedbrytningsgrad. Liknande samband har hittats även i tidigare studier, men orsaken bakom dessa samband är ännu inte klarlagd.

LIST OF ABBREVIATIONS

β/α	freshness index
CO₂	carbon dioxide
DO	dissolved oxygen
DOC	dissolved organic carbon
DOC_{ns}	DOC concentrations in samples analysed within 24 hours
DOC_s	DOC concentration in stored samples
DOM	dissolved organic matter
EC	electric conductivity
EEM	Excitation-Emission Matrix
FI	Fluorescence Index
HIX	Humification index
λ_{em}	emission wavelength
λ_{ex}	excitation wavelength
NH₄⁺-N	ammonium nitrogen
NO₂⁻+NO₃⁻-N	nitrite and nitrate nitrogen
PARAFAC	Parallel Factor Analysis
pCO₂	partial pressure of carbon dioxide
PO₄³⁻-P	phosphate phosphorus
TOC	total organic carbon

TABLE OF CONTENTS

1	Introduction	1
1.1	Objectives and aims	1
1.1.1	Research questions	1
1.1.2	Hypotheses	1
2	Background	2
2.1	Dissolved organic matter	2
2.2	Fluorescent dissolved organic matter	3
2.3	Fluorescence	4
2.3.1	The phenomenon of fluorescence	4
2.3.2	Excitation-Emission Matrix and fluorescence peaks	4
2.3.3	Corrections and normalisation of fluorescence data	5
2.3.4	Fluorescence indices	5
2.4	PARAFAC	6
3	Methods and data	6
3.1	Sites and sampling	6
3.2	Specific discharge	8
3.3	TOC and DOC measurements	8
3.4	Fluorescence	9
3.4.1	Measurements	9
3.4.2	Raman normalisation	9
3.4.3	Calculation of fluorescence indices	9
3.5	PARAFAC	10
3.6	Statistical analysis	10
3.6.1	Storage effect	10
4	Results	11
4.1	DOC	11
4.1.1	Storage effect	11
4.1.2	Site overview	12
4.1.3	Spatial patterns	13
4.1.4	Temporal patterns	14
4.2	Fluorescence indices	17
4.2.1	Site overview	17
4.2.2	Spatial patterns	17

4.2.3	Temporal patterns.....	19
4.3	Components	30
4.3.1	Identification of components.....	30
4.3.2	Spatial patterns	31
4.3.3	Temporal patterns.....	33
5	Discussion	42
5.1	Identification of PARAFAC components.....	42
5.2	Spatial patterns	42
5.3	Temporal patterns	44
5.3.1	DOC	44
5.3.2	Specific discharge and EC.....	45
5.3.3	Temperature	45
5.3.4	Nutrients	46
5.3.5	CO ₂	47
5.4	Sources of error	48
5.4.1	Storage effect.....	48
5.4.2	Sampling period	49
5.4.3	CO ₂ data	49
5.4.4	Specific discharge	49
5.4.5	Fluorescence and PARAFAC.....	50
6	Conclusions	50
	References	51
	Appendix A: Time series and boxplots	54
A.1	DOC time series.....	54
A.2	Nutrients	55
A.2.1	Boxplots	55
A.2.2	NH ₄ ⁺ -N time series.....	56
A.2.3	NO ₂ ⁻ +NO ₃ ⁻ -N time series	57
A.2.4	PO ₄ ³⁻ -P time series	59
A.3	Fluorescence indices.....	60
A.3.1	FI time series	60
A.3.2	β/α time series	61
A.3.3	HIX time series.....	62
A.4	PARAFAC Components	64
A.4.1	C1 time series	64

A.4.2	C2 time series	65
A.4.3	C3 time series	66
A.4.4	C4 time series	67
A.4.5	C5 time series	69
Appendix B:	Significant correlations	71
B.1	DOC: temporal correlations.....	71
B.2	Fluorescence indices.....	73
B.2.1	Spatial correlations	73
B.2.2	FI: Temporal correlations.....	75
B.2.3	β/α : Temporal correlations	76
B.2.4	HIX: Temporal correlations	78
B.3	PARAFAC components	79
B.3.1	Spatial and Temporal correlations.....	79
B.3.2	C1: Temporal correlations.....	84
B.3.3	C2: Temporal correlations.....	85
B.3.4	C3: Temporal correlations.....	86
B.3.5	C4: Temporal correlations.....	87
B.3.6	C5: Temporal correlations.....	88

1 INTRODUCTION

During the last decade, attention has been drawn to the role of inland waters in the carbon cycle. The inland waters' impact on the carbon sequestration and transport from land to sea has been proved to be greater than previously thought (Cole et al., 2007; Tranvik et al., 2009). It has been shown that both carbon dioxide (CO₂) emissions from inland waters to the atmosphere, as well as the storage of carbon in lake sediments, have been underestimated in the global and regional carbon budgets. Inland waters are not only transporting terrestrial carbon to the ocean, as previously thought, they are also an important environment for degradation of organic carbon and transformation into CO₂ and methane (CH₄) (Battin et al., 2009).

Aquatic CO₂ is not only the result of in-stream microbial or photochemical degradation of organic carbon. It can also enter the water body as terrestrially derived CO₂ from soil respiration, transported with ground- and soil water (Hotchkiss et al., 2015; Winterdahl et al., 2016). It has been shown that the main fraction of CO₂ evading from small streams is terrestrially derived CO₂. The contribution of in-stream microbial production of CO₂ by degradation of organic carbon was shown to increase with stream width.

Most studies have focused on CO₂ emissions from streams in forested catchments. In an MSc thesis project by Osterman (2018), CO₂ concentrations were measured in agricultural streams in Uppsala, Sweden. The median concentrations were ranging from 3000 to 10,000 µatm, which is higher than what has been reported from streams in forested catchments. During the project, interest arose about the influence of dissolved organic matter (DOM) quality (i.e. composition and source) on CO₂ concentrations. This relation has been suggested in previous studies (Bodmer et al., 2016). As a result of that, this project was initiated in October 2017.

1.1 OBJECTIVES AND AIMS

The objective of this study was to identify geographical and hydrochemical controls on DOM quality and quantity in agricultural streams, and to investigate if DOM quality has an impact on CO₂ concentration in stream water. The study aims to contribute to an increased understanding of the carbon cycle and the role of stream water in the processing of organic carbon. This is important for the understanding of the dynamics and balances in aquatic ecosystems, and can help in preventing increased CO₂ evasions from inland waters and the losses of ecosystem services.

1.1.1 Research questions

- What geographical and hydrochemical variables can be found to affect the DOM quality and quantity?
- Is there a spatial or temporal correlation between DOM quality and quantity and the CO₂ concentrations in agricultural streams?

1.1.2 Hypotheses

- The fraction of arable land in the catchment area is expected to influence the DOM quality and quantity.
- High nutrient concentrations are expected to enhance DOM of microbial and algal origin.
- Aquatic DOM of terrestrial origin is expected to correlate with CO₂ concentrations.

2 BACKGROUND

2.1 DISSOLVED ORGANIC MATTER

DOM is often defined as organic matter smaller than 0.2-1.2 μm (Coble et al., 2014) and consists mainly of carbon, and to some extent nitrogen (Fellman et al., 2010). Because of this, measurements of dissolved organic carbon (DOC) are often used to quantify DOM (Hansen et al., 2016). DOM is produced by microbes and degraders both in soil and aquatic systems, degrading larger plant- and animal material into organic compounds of lower molecular weight. There are additionally several anthropological sources of DOM, such as agriculture and wastewater. In aquatic systems, DOM is often categorised as allochthonous or autochthonous material, depending on its origin. Allochthonous DOM is material produced outside the system and transported to it, while autochthonous DOM has been produced by organisms within the system (Hudson et al., 2007; Coble et al., 2014). Autochthonous DOM can be produced by photosynthesising organisms (primary production) or by microbial activity. In most streams, the main fraction of DOM is terrestrially derived (Duarte and Prairie, 2005; Wilson and Xenopoulos, 2009).

DOM can affect the dynamics and balance of aquatic ecosystems in several ways. DOM is a source of energy and nutrients for organisms (Fellman et al., 2010). Some DOM compounds absorb light and thus limit the photosynthesis and primary production in the water body (Karlsson et al., 2009). DOM can also be a carrier of metal ions and organic contaminants, since these bind to DOM (Niederer et al., 2007; Pan et al., 2008; Thacker et al., 2005). Primary production within the water body may increase with increasing inputs of nutrients, which may result in a decrease of CO_2 outgassing (Tranvik et al., 2009). An increase in terrestrially derived carbon, transported to the water body, might instead result in an increased heterotrophic respiration, and thus increased CO_2 emissions to the atmosphere (Duarte and Prairie, 2005). The quality of DOM has been shown to be of greater importance than DOM quantity in the production of CO_2 in stream water (D'Amario and Xenopoulos, 2015). Terrestrially derived DOM was shown to be better related than microbial DOM to high CO_2 concentrations.

There is little consensus between research fields in the partitioning of organic matter compounds. DOM is often divided in humic and non-humic substances. Humic substances are partially degraded plant and animal matter, rich in cyclic carbon (aromatic) compounds with strong chemical bonds (Naiman and Bilby, 1998). Non-humic substances are less complex organic compounds derived from e.g. proteins and carbohydrates. Humic substances have traditionally been partitioned into humic acids, fulvic acids and humins, defined by its solubility in water at different pH (Hudson et al., 2007; Eriksson et al., 2011). This partitioning has lately been questioned and criticised, since the separate compounds have only been observed in extraction experiments, and not in natural environments (Lehmann and Kleber, 2015). The concept of humification has also started to be revised. Traditionally, humification is the concept where decomposed organic matter is microbially transformed into larger compounds, more resistant to decay. However, these humified compounds have lately been shown to be decomposable at a faster rate than previously thought. The revised view of humification suggests that humified compounds consist of smaller aggregated molecules, imitating the character of larger molecules (Lehmann and Kleber, 2015).

In natural soils (not impacted by anthropological activities) the top layers are rich in organic matter, mostly derived from plants (Kaiser and Kalbitz, 2012). The organic matter amount is

decreasing with the depth in the soil matrix, and the character of the organic matter is shifted towards older and more mineralised organic matter. When organic matter is decomposed, it loses its charged complex binding functional groups and becomes more soluble in water. Fresher organic matter thus adsorbs to the soil matrix, while more degraded matter can be transported by soil water further down in the profile. The decomposition of the adsorbed organic matter compounds continues, and as the molecular structure of the compounds become more altered, they are transported further down in the soil (Kaiser and Kalbitz, 2012). Thus, in the deeper soil layers, the organic matter is mainly microbially derived, while the top layers contain fresh, plant-derived organic matter. The differences in amount and quality of the DOM in different soil horizons have an effect on the DOM concentration in waters draining the soil. Surface runoff and water in the upper part of the soil might be rich in DOM, while groundwater have low DOM concentrations (Kaiser and Kalbitz, 2012).

In agricultural soils, the organic matter is lower than in natural soils, since the organic matter is removed during harvest. In contrast, the nutrient concentrations in agricultural soils are higher, due to the use of fertilizers. With the vegetation removed, the surface runoff is enhanced and the land is exposed to erosion and leaching. Adding to that, the land is often drained, enhancing the hydraulic conductivity in the soil and hence the leaching of nutrients and minerals to stream waters.

2.2 FLUORESCENT DISSOLVED ORGANIC MATTER

A fraction of the DOM has light absorbing properties. This fraction of the DOM pool is called coloured or chromophoric DOM (CDOM) and can be studied with absorbance measurements. A fraction of the CDOM also has the property of emitting light after absorption; it fluoresces. This sub-fraction of DOM is called fluorescent DOM (FDOM) and the fluorescing compounds are denoted fluorophores (Coble et al., 2014). The optical properties (absorbance and fluorescence) makes it possible to analyse the quality of the DOM compounds in water samples.

FDOM is often categorised as humic-like or protein-like fluorescence. The protein-like fluorescence could also be referred to as amino acid-like fluorescence. Protein-like FDOM is normally associated with autochthonous matter and have been related to microbial activity and more bioavailable DOM (Coble et al., 2014). However, it is not clear if protein-like FDOM is a bioavailable substrate itself or a result of degradation of bioavailable DOM (Hudson et al., 2007). Humic-like material is instead seen as an indicator of less biodegradable DOM. Despite the questioning of the partitioning of humic substances, the notion “fulvic-like” is commonly used in the research field regarding DOM fluorescence.

Stream water is heavily influenced by the surrounding soil organic matter, and several studies have shown that both the amount and the quality of FDOM in natural stream waters vary seasonally (Coble et al., 2014). However, this pattern has not been seen in the same extent for agricultural streams, probably because of different soil biochemistry and runoff characteristics compared to natural streams. Agricultural land is normally drained, giving a higher and faster hydrological response in agricultural streams. Microbially derived DOM has been shown to increase with a greater fraction of agricultural land use in the catchment area (Wilson and Xenopoulos, 2009). This was thought to be due to increased nitrogen concentrations, which have been suggested to enhance bacterial production and CDOM concentrations.

2.3 FLUORESCENCE

2.3.1 The phenomenon of fluorescence

Fluorescence is the phenomenon where a substance is irradiated with short wavelength light and emits light of a longer wavelength. Fluorescence happens in three steps: absorption, vibrational relaxation and fluorescence (Coble et al., 2014). When light hits the molecule, the energy of the photon is *absorbed* by the molecule. If this energy matches the energy gap between the ground electronic state and an energy level in excited state, the electron will be excited. The excited electron will then seek to fall back to the ground state. During the *vibrational relaxation* the excited electron loses energy through vibration and eventually reaches the lowest energy level of the excited state. When the electron returns from the lowest energy level of the excited state to the ground state, fluorescence may occur; the energy of the electron is released as a photon, and light is emitted (Coble et al., 2014). There is however a possibility that the energy is released in other ways, without any light being emitted. The requirement of both excitation and emission to take place is the reason why only a sub-fraction of the CDOM has fluorescent characteristics.

2.3.2 Excitation-Emission Matrix and fluorescence peaks

The emitted photon will have lower energy than the exciting light. The intensity of the fluorescence is measured at pairs of excitation and emission wavelengths. Different fluorophores have different excitation (λ_{ex}) and emission wavelengths (λ_{em}). By combining the results in a three-dimensional Excitation-Emission Matrix (EEM) and analysing the location of the fluorescence intensity peaks, it is possible to identify the underlying typical compound classes in the sample. As a result of aquatic fluorescence studies, commonly occurring peaks in the EEMs have been named and identified (Table 1). The peak wavelengths are not exact and might shift to longer or shorter wavelengths due to chemical and physical interactions, such as pH, photodegradation and the molecular structure of the compound (Coble et al., 2014).

Table 1. Common fluorescence intensity peaks and their interpretation.

Peak	$\lambda_{ex} / \lambda_{em}$ (nm)	Type	Reference
A	237-260/400-500	Humic-like	Hudson et al., 2007
B	225-237/309-321 and 275/310	Protein-like, tyrosine-like. Autochthonous.	Hudson et al., 2007
C	320-365/420-470	Humic-like, fulvic-like	Coble et al., 2014 Baker et al., 2008
M	290-310/370-420	Humic-like. Autochthonous, microbial.	Hudson et al., 2007
T	230/340 and 275/340	Protein-like, tryptophan-like. Autochthonous.	Coble et al., 2014

2.3.3 Corrections and normalisation of fluorescence data

The measured fluorescence intensities must be corrected for inner-filter effects. Inner-filter effects are caused by organic matter in the sample absorbing excited and emitted light during the measurements, causing a loss in the fluorescence intensity signal (Coble et al., 2014). Corrections are also needed for Rayleigh and water Raman scattering. Rayleigh scattering is the effect of light being scattered when hitting for example colloids or bubbles in the sample (Coble et al., 2014). The scatter is not contributing with any fluorescence information. Removal of these lines results in two lines of missing data in the EEMs. The first order Rayleigh line is occurring in the EEMs at the same emission wavelength as the excitation wavelength, while the second order line is occurring at the double emission wavelengths as the excitation wavelength (Hudson et al., 2007). Water Raman scattering is caused by the light's interaction with the water molecules (Coble et al., 2014). By measuring the Raman scatter in a water blank, the Raman signal can be subtracted from the sample and the measured fluorescence intensities normalised to the Raman scatter peak, expressed in Raman Units (R.U.).

2.3.4 Fluorescence indices

To assist in the interpretation of the fluorescence data, a number of fluorescence indices have been developed. The indices are calculated as ratios of different points or areas in the EEMs, representing different fluorophores.

Fluorescence index (FI) is used as an indication of whether the FDOM is of a more microbial or terrestrial origin. It is calculated (Eq (1)) as the ratio of fluorescence intensity at emission wavelengths 470 nm to 520 nm, at excitation wavelength 370 nm (Coble et al., 2014). The calculation is based on the shift in location of peak C, due to the precursor material. For microbially derived fulvic acids, the peak C is shifted to lower emission wavelengths, while fulvic acids with a terrestrial source are shifted to longer emission wavelengths. Thus, a lower FI around 1.2, indicates a predomination of terrestrially derived material. A higher value, around 1.8, indicates material derived from microbial activity.

$$FI = \frac{\text{intensity}(\lambda_{em}470nm \lambda_{ex}370nm)}{\text{intensity}(\lambda_{em}520nm \lambda_{ex}370nm)} \quad \text{Eq (1)}$$

Freshness index (β/α) is used as an indication of how recently produced the FDOM is (Coble et al., 2014). It is calculated (Eq (2)) as the ratio of the intensity at emission wavelength 380 nm (representing recently produced DOM) to the maximum intensity at emission wavelengths between 420 and 435 nm (representing older DOM), at excitation wavelength 310 nm. Thus, a higher value indicates a greater amount of freshly produced organic matter, while a lower value indicates a greater contribution of more decomposed organic matter.

$$\beta/\alpha = \frac{\text{intensity}(\lambda_{em}380nm \lambda_{ex}310nm)}{\text{max intensity}(\lambda_{em}420-435nm \lambda_{ex}310nm)} \quad \text{Eq (2)}$$

Humification index (HIX) is defined (Eq (3)) as the sum of fluorescence intensity for emission wavelengths 435-480 nm at excitation 254 nm, divided by the sum of fluorescence intensity for emission wavelengths 300-345 nm + 435-480 nm at excitation wavelength 254 nm (Ohno, 2002). A higher HIX indicates a higher degree of humification.

$$HIX = \frac{\sum \text{intensity}(\lambda_{em}435-480nm \lambda_{ex}254nm)}{\sum (\text{intensity}(\lambda_{em}300-345nm \lambda_{ex}254nm) + \text{intensity}(\lambda_{em}435-480nm \lambda_{ex}254nm))} \quad \text{Eq (3)}$$

2.4 PARAFAC

Parallel Factor Analysis (PARAFAC) is a multivariate data analysis technique, often used in combination with fluorescence measurements to identify underlying FDOM components in the EEMs (Stedmon et al., 2003; Stedmon & Bro, 2008). The EEMs of several samples are combined into a three-dimensional array (sample \times excitation wavelength \times emission wavelength), and PARAFAC is applied to model the peak fluorescence data. For each component found, a unitless score related to the intensity of the fluorophore is calculated. This score is not only dependant on the concentration of the fluorophore, but also on the physical and chemical attributes of the fluorophore and its surrounding environment.

3 METHODS AND DATA

3.1 SITES AND SAMPLING

During the period 2017-07-06 until 2017-11-08, CO₂ measurements and water sampling were carried out in ten agricultural streams located around Uppsala, Sweden (Figure 1). Water samples were taken manually every second week, while stream water CO₂ concentrations were measured every 30 minutes with floating chambers. The CO₂ measurements were initiated in June, as part of another MSc thesis project (Osterman, 2018). Since the outlines of this study was not clear at the time, no water samples were taken in June. A further description of the method for CO₂ measurements can be found in Osterman (2018). The sites were chosen with regard to accessibility, arable land in the catchment area and small risk of drying of the streams. However, site 3 and 4 did get dry during the sampling period. Site 3 is therefore missing data from the three sampling occasions in August, from 2017-08-03 until 2017-08-30. For site 4, water samples could be collected from 2017-10-11 and onwards, resulting in data from only three sampling occasions. On 2017-09-26, CO₂ measurements at site 6 had to be cancelled due to interference with the floating chamber and damaging of the sensor. Because of this, water sampling at site 6 was cancelled as well. The catchments of the ten streams differed in size and land use distribution (Table 2). Upstream of site 5, a small wastewater treatment plant is located.

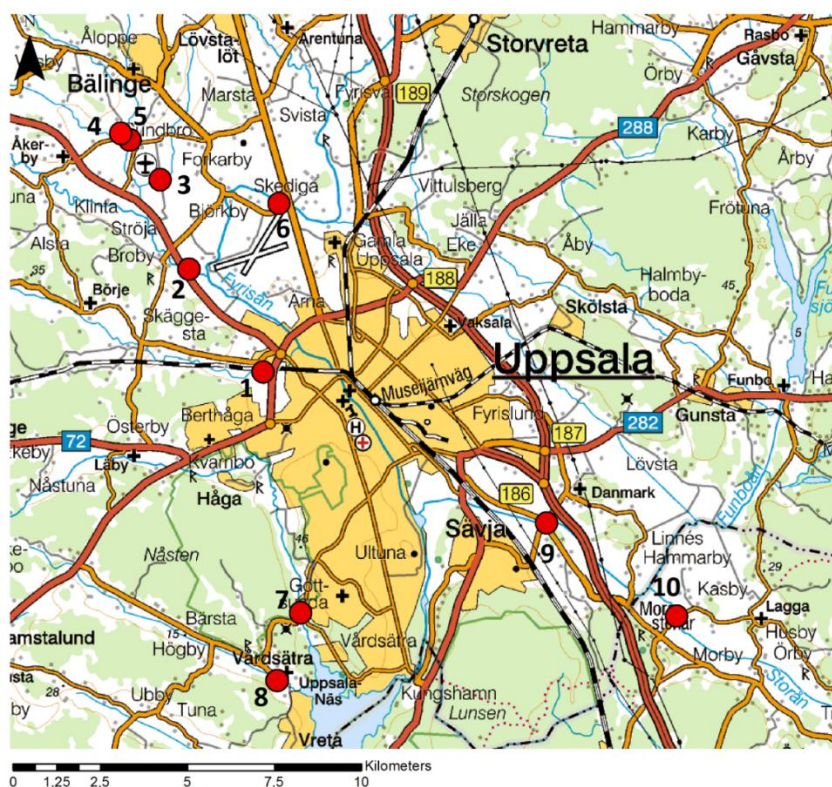


Figure 1. Location of the ten sampling sites (red dots). With permission from Osterman (2018).

Table 2. Catchment characteristics for the ten sites. Numbers used with permission from Osterman (2018).

Site	Catchment area [km ²]	% arable land	% forest	% urban	% lakes and wetland
1	25	52.0	44.6	1.9	0.0
2	200	41.6	56.1	0.7	1.3
3	9	91.3	5.0	3.7	0.0
4	14	56.4	43.5	0.0	0.0
5	21	45.8	44.7	5.0	0.0
6	780	34.5	59.4	2.2	3.6
7	105	29.7	62.4	6.1	0.6
8	23	38.9	59.4	0.0	0.0
9	741	34.7	62.5	1.0	1.5
10	209	39.5	57.5	1.4	1.2

Water samples were manually collected in clean 250 ml plastic bottles. The bottles were rinsed with stream water before sample collection. Two sets of samples were collected on each site and transported in a cooling box to the lab. One set was brought to the SWEDAC accredited Geochemical laboratory at the Department of Aquatic Sciences and Assessment at the Swedish

University of Agricultural Sciences (SLU) in Uppsala, where DOC concentration, ammonium nitrogen ($\text{NH}_4^+\text{-N}$), nitrite and nitrate nitrogen ($\text{NO}_2^- + \text{NO}_3^-\text{-N}$) and phosphate phosphorus ($\text{PO}_4^{3-}\text{-P}$) were measured within 24 hours from the sampling. The other set of samples was stored unfiltered in the dark at 4 °C for later DOC and fluorescence measurements. The time of storage varied for the samples (Table 3). Electrical conductivity (EC), pH, temperature and dissolved oxygen (D.O.) were measured in-situ on the same sampling occasions as the water sampling, using a Hach-Lange multiprobe.

Table 3. Schedule of sampling occasion and the number of days the sample was stored unfiltered.

Sampling occasion	Sampling date	Days of storage
1	2017-07-06	105
2	2017-07-19	92
3	2017-08-03	77
4	2017-08-15	66
5	2017-08-30	51
6	2017-09-14	36
7	2017-09-26	24
8	2017-10-11	9
9	2017-10-25	1
10	2017-11-08	1

3.2 SPECIFIC DISCHARGE

Stream discharge measurements were obtained from SMHI Vattenwebb (2018) for the stations Stabby, Sävjaån and Vattholma, and converted to specific discharge by dividing by the catchment area. Specific discharge data from Stabby were used for site 7 and 8, while data from Sävjaån were used for site 9 and 10, and data from Vattholma for site 1-6.

3.3 TOC AND DOC MEASUREMENTS

Ca 100 ml of each sample was filtered through 0.45 μm polyethersulfone (PES) membrane filters, using a 60 ml plastic syringe. Total organic carbon (TOC) concentrations were measured on unfiltered samples, and dissolved organic carbon (DOC) concentrations were measured on filtered samples. Fluorescence was then measured on both filtered and unfiltered samples.

TOC and DOC concentrations were measured with a Shimadzu Corporation TOC-V CPH analyser, programmed for low concentration measurement up to 20 mg/l. Two standards were used: 20 mg/l potassium hydrogen phthalate (KHP) used for calibration, and 10 mg/l EDTA as check standard. Both standards were acidified using 1 ml 2 M hydrochloric acid (HCl). The analyser was programmed to measure calibration concentrations of 0, 2, 5, 10 and 20 mg/l. The 20 mg/l KHP solution was poured in two vials, and the machine internally diluted the injected volume 10, 4, 2 or 0 times to measure the concentrations 2, 5, 10 and 20 mg/l respectively. For 0 mg/l calibration, Milli-Q water was used.

Four vials were filled with Milli-Q water, serving as blanks. All samples and standards were shaken before poured in 24 ml vials. Ca $\frac{3}{4}$ of the vial was filled. 200 μl HCl was added to each

vial containing sample or blank. With all vials prepared, a magnet was added to each vial for stirring. The vial rack was put in the analyser and the automatized measurements were started.

The injection volume in the analyser was 80 μ l. Three measurements on each sample were made, and the result was given as the mean concentration of these. When the standard deviation was more than 0.1 and the coefficient of variance (CV) greater than 2%, an extra measurement was made until the requirements were met. A maximum of 5 measurements on each sample could be made in total.

3.4 FLUORESCENCE

3.4.1 Measurements

Fluorescence intensity was measured with a Horiba Scientific Aqualog, with excitation wavelengths ranging from 240 nm to 600 nm with 2 nm intervals, and emission wavelengths ranging from 212 nm to 619 nm with 3.2 nm intervals. The integration time was 1 second. Along with the fluorescence measurements, absorbance was measured for the same excitation wavelengths.

At the start of each measuring session, the Aqualog measuring set-ups were made. Using a sealed cuvette containing MilliQ water, the Raman signal and a blank was measured. The Raman signal was measured three times. The results of the Raman signal and blank were saved and used for correction of the fluorescence data for the same day.

The water sample bottles were shaken before pouring the sample in a 10x10 mm Quartz Suprasil cuvette. Before placing the sample in the Aqualog, the cuvette was wiped on the outside with extra soft tissues to remove water drops, fingerprints and other impurities. Between each measurement, the cuvette was first rinsed thoroughly with Milli-Q water and then rinsed with the water that was to be analysed.

The results of the fluorescence measurements were given as fluorescence intensities at different pairs of excitation and emission wavelengths, in an EEM, with the blank subtracted. Using built-in Aqualog software tools the resulting fluorescence intensities were corrected for inner-filter effects, and the 1st and 2nd order Rayleigh lines were removed and replaced with zeros.

3.4.2 Raman normalisation

To be able to compare the results from different measurements, the fluorescence intensities were converted to Raman units by normalising the results to the Raman peak area measured at the beginning of each measuring session. The Raman peak of interest occurs between emission wavelengths 380 nm and 420 nm. The peak area was calculated for all three Raman measurements, and the resulting area was given as the mean value. All measured intensities were then divided by the resulting Raman peak area for the corresponding measuring session. The calculations were carried out in MATLAB R2017b.

3.4.3 Calculation of fluorescence indices

Since the fluorescence intensity was measured with a 3.2 nm interval for emission wavelengths, the exact wavelengths of interest for calculation of FI, β/α and HIX were not measured. Instead, the measured wavelength closest to the wavelength of interest was used for calculating the indices. FI was therefore calculated as the ratio of the fluorescence intensity at emission wavelength 468.6 nm to the intensity at emission wavelength 518.6 nm. β/α was calculated as the intensity at emission wavelength 379.7 nm divided by the maximum intensity between emission wavelengths 419.0 nm and 435.5 nm. For calculations of HIX, the emission

wavelengths used were 435.5 nm to 478.6 nm, and 298.6 nm to 343.8 nm. All three indices were calculated on Raman-normalised fluorescence intensity data corrected for inner-filter effects and with 1st and 2nd Rayleigh scatter lines removed. Calculations were performed in MATLAB R2017b.

3.5 PARAFAC

The PARAFAC modelling was computed in MATLAB R2017b with the open source toolbox DOMFluor version 1.7 (Stedmon & Bro, 2008). The corrected and normalised EEMs were loaded to MATLAB, and all zero values were converted to Not a Number (NaN). The EEMs for all 172 samples were then plotted and analysed for possible measurement errors. This resulted in one sample being removed. Thus, the total amount of samples being used for the PARAFAC modelling was 171. Non-negativity constraints were set for the fluorescence intensity, and unimodality constraints were set for both emission and excitation wavelengths, allowing the modelled components to only contain one peak in fluorescence intensity.

Seven models, with the number of components ranging from 1 to 7, were derived. Ten iterations on each model were computed in order to get the lowest residual error. The models were then validated by a combination of split-half validation, sum of squared error and spectral inspection of the plots of the components. The split-half validation was done following the procedure further explained by Stedmon & Bro (2008), though, the script for the data split was modified by adding an element of randomness to the split of the data. The scores of the components in the model chosen were saved for further statistical analysis.

3.6 STATISTICAL ANALYSIS

Statistical analyses were computed in the open source program RStudio version 1.1.383. Since the data set was relatively small and not all variables were normally distributed, Kendall's tau was used for checking correlations, and median value and IQR (inter quartile range) were used as statistical measures of central tendency and spread. To analyse the effect of catchment characteristics, median values for DOC, water chemistry variables, fluorescence indices and PARAFAC components were correlated with total catchment area and fraction of arable land in the catchment area. To identify spatial patterns, correlation was analysed between site median values of the depending variables DOC, fluorescence indices and PARAFAC components and median values of the independent water chemistry variables. To identify temporal patterns, the correlation was checked in each stream for the dependent and independent variables.

The consistency of CO₂ data differed between sites, and for a majority of the sites data were missing at the end of the sampling period. For the spatial correlation tests between pCO₂ and other variables, median values for observations in July were used, since this was the month where CO₂ data was most consistent. Due to the lack of CO₂ data, temporal correlations could only be tested at site 1 and 5. Daily median CO₂ concentrations were derived for the days when water samples had been collected, and these values were used in correlation tests on temporal scale within sites. The median was derived from CO₂ measurements during the 24 hours preceding the water sampling.

3.6.1 Storage effect

Since DOC had been measured on two sets of samples, of which one set had been stored unfiltered, the differences between these measurements were analysed for a potential storage effect on the DOC concentration. The DOC concentration differences (Δ DOC) were calculated, for each sampling event at each site, as the difference between the concentration in the samples

that had not been stored (DOC_{ns}) and the concentration in the samples that had been stored (DOC_s), see Eq (4).

$$\Delta DOC = DOC_{ns} - DOC_s \quad \text{Eq (4)}$$

The calculated differences from the same sampling event were then grouped together, resulting in ten groups. The non-parametric Kruskal-Wallis test was then computed on the log-transformed differences, to check if all ten groups were identical. To find which groups that could be said to be identical, a post hoc Kruskal-Wallis multiple comparison test was computed, using the *kruskalmc* test in the R package *pgirmess* version 1.6.7 (Giraudox, 2017). The theory behind the post hoc test is further explained by Siegel and Castellan (1988).

4 RESULTS

4.1 DOC

4.1.1 Storage effect

The null hypothesis of the Kruskal-Wallis test could be rejected ($p = 4.053e-05$), meaning that the ten groups were not all identical. The post hoc multiple comparison test gave that four pairs of sample events were significantly different from each other: sampling event 1 and 8; 1 and 10; 7 and 8; 7 and 10.

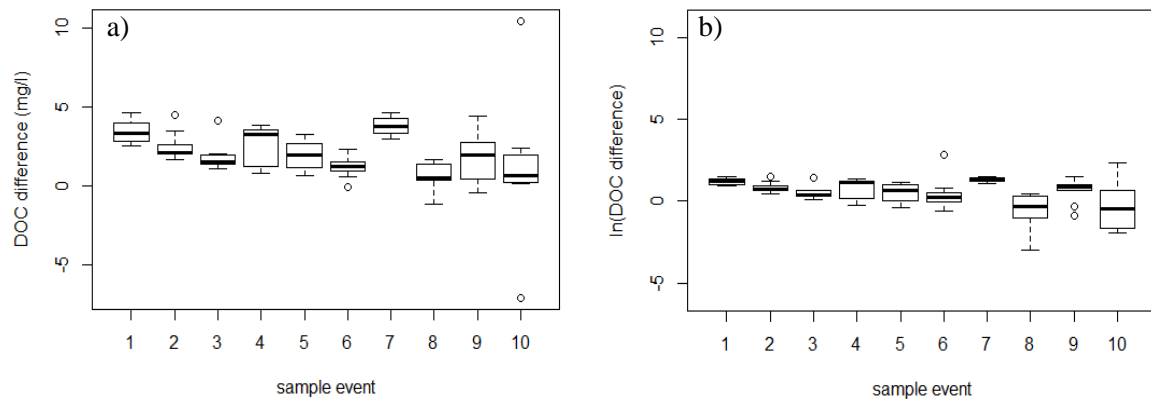


Figure 2. a) Boxplot of DOC differences grouped after sampling event 1-10. b) Boxplot of log-transformed DOC differences grouped after sampling event 1-10.

At some sites, the difference between DOC in stored samples (DOC_s) and DOC in samples that had not been stored (DOC_{ns}) could be seen to decrease over time, while no such pattern could be seen at other sites (Figure 3).

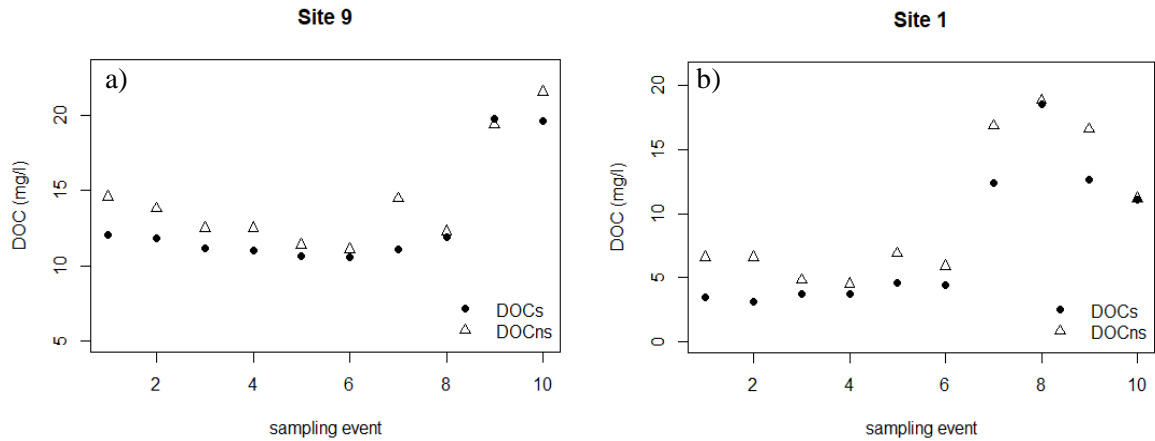


Figure 3. DOC_s and DOC_{ns} at site 9 and site 1. a) At site 9, the difference between DOC_{ns} and DOC_s seems to decrease from sampling event 1 to 6. b) At site 1, no clear trend can be seen in the difference between DOC_{ns} and DOC_s .

4.1.2 Site overview

Median and IQR of measured DOC values varied among the ten sites (Figure 4, Table 4). Time series of DOC_s , DOC_{ns} and nutrient concentrations at each site can be found in Appendix A.1 and Appendix A.2.

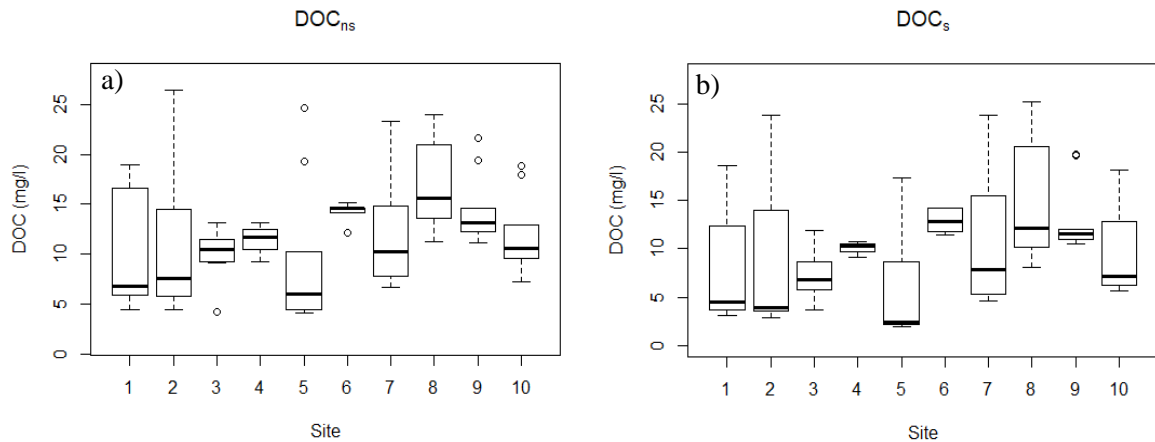


Figure 4. Boxplot of a) DOC_{ns} and b) DOC_s at each site.

Table 4. Median and IQR for DOC_{ns} and DOC_s at each site.

Site	DOC_{ns}		DOC_s	
	Median (mg/l)	IQR	Median (mg/l)	IQR
1	6.8	9.2	4.5	8.4
2	7.6	7.1	3.9	8.0
3	10.5	2.2	6.8	2.9
4	11.7	2.0	10.3	0.8
5	6.1	4.7	2.4	5.0
6	14.6	0.3	12.8	2.0
7	10.2	6.9	7.9	9.3
8	15.7	6.7	12.1	8.9
9	13.2	2.2	11.5	0.98
10	10.6	3.3	7.2	5.7

4.1.3 Spatial patterns

No significant correlation was found between median DOC_{ns} and catchment area ($p = 0.29$, $\tau = 0.29$), with the fraction of arable land in the catchment area ($p = 0.32$, $\tau = -0.25$), median pCO_2 ($p = 1$, $\tau = 0.047$) or with specific discharge ($p = 0.85$, $\tau = 0.05$). No significant correlations were found between median DOC_{ns} and any of the water chemistry variables (Table 5).

Table 5. Correlations between DOC and water chemistry variables. Kendall's tau (τ) and significance level (p) is presented.

	DOC_{ns} (mg/l)
NH_4^+-N ($\mu g/l$)	$p = 0.61$ $\tau = -0.17$
$NO_2^-+NO_3^- -N$ ($\mu g/l$)	$p = 0.12$ $\tau = -0.42$
$PO_4^{3-} -P$ ($\mu g/l$)	$p = 0.61$ $\tau = -0.17$
EC ($\mu S/cm$)	$p = 0.60$ $\tau = -0.16$
DO (mg/l)	$p = 0.48$ $\tau = -0.2$
pH	$p = 0.86$ $\tau = -0.07$
Temp ($^{\circ}C$)	$p = 0.38$ $\tau = 0.24$

4.1.4 Temporal patterns

No significant correlation was found between DOC_{ns} and pCO₂ at site 1 ($p = 0.23$, $\tau = 0.37$, $n = 8$) nor at site 5 ($p = 0.72$, $\tau = 0.2$, $n = 6$). Temporal correlations with CO₂ were only tested at site 1 and 5, since the CO₂ data were insufficient for the other sites. At site 1, half of the CO₂ observations hit the upper instrumental detection limit and therefore the exact concentration was not known for these observations.

At six of the sites, DOC and specific discharge were significantly correlated (Table 6). All correlations were positive. The result differed slightly between DOC_s and DOC_{ns}. At site 1, DOC_{ns} was significantly correlated while DOC_s was not, and vice versa at site 8. However, the correlations looked similar when plotted (Appendix B.1 Figure B1).

Table 6. Correlation between specific discharge (mm/day) and DOC (stored and not stored). Number of observations (n), Kendall's tau (τ) and significance level (p) is presented. Significant correlations ($p < 0.05$) are in bold.

Site	n	Specific discharge (mm/day)	
		DOC _s (mg/l)	DOC _{ns} (mg/l)
1	10	$p = 0.072$ $\tau = 0.45$	$p = 0.02$ $\tau = 0.57$
2	10	$p = 0.007$ $\tau = 0.67$	$p = 0.03$ $\tau = 0.54$
3	7	$p = 0.38$ $\tau = -0.33$	$p = 0.56$ $\tau = -0.24$
4	3	$p = 1$ $\tau = -0.33$	$p = 1$ $\tau = -0.33$
5	10	$p = 0.0003$ $\tau = 0.90$	$p = 0.004$ $\tau = 0.72$
6	6	$p = 0.70$ $\tau = -0.14$	$p = 0.56$ $\tau = -0.21$
7	10	$p = 0.047$ $\tau = 0.51$	$p = 0.048$ $\tau = 0.49$
8	10	$p = 0.047$ $\tau = 0.51$	$p = 0.11$ $\tau = 0.42$
9	10	$p = 0.009$ $\tau = 0.64$	$p = 0.02$ $\tau = 0.58$
10	10	$p = 0.0001$ $\tau = 0.87$	$p = 0.001$ $\tau = 0.87$

Significant correlations were found between DOC_{ns} and at least one of the water chemistry variables at all sites except for site 4 and 6 (Table 7). The largest number of significant correlations were found at site 5, where DOC_{ns} was correlated with four variables: NO₂⁻+NO₃⁻-N, DO, pH and temperature. The variable which correlated with DOC_{ns} at the largest number of sites was temperature, which was significantly correlated at four sites (site 2, 5, 7 and 8). The correlations between DOC and DO were all positive, while the correlations between DOC and EC, and DOC and temperature were all negative (Figure 5).

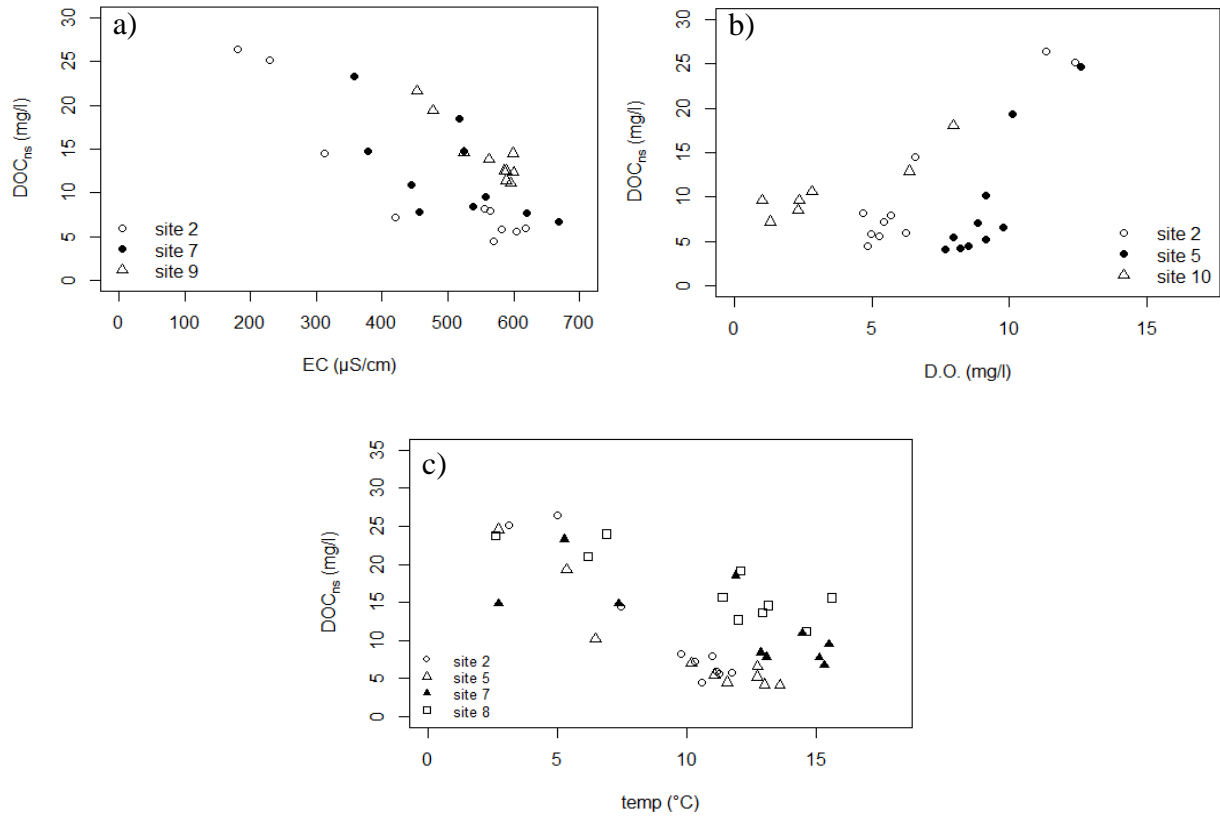


Figure 5. Plots of DOC_{ns} against a) EC, b) DO and c) temperature at sites where correlations were significant.

Table 7. Correlations between DOC_{ns} and water chemistry variables at each site. Kendall's tau (τ) and significance level (p) are given. Significant correlations ($p < 0.05$) are in bold.

Site	DOC_{ns} (mg/l)													
	NH_4^+-N ($\mu g/l$)		$NO_2^-+NO_3^- -N$ ($\mu g/l$)		$PO_4^{3-} -P$ ($\mu g/l$)		EC ($\mu S/cm$)		DO (mg/l)		pH		Temp ($^{\circ}C$)	
1	p = 0.038 $\tau = - 0.52$		p = 0.07 $\tau = 0.45$		p = 0.79 $\tau = - 0.07$		p = 0.37 $\tau = - 0.23$		p = 0.21 $\tau = 0.32$		p = 0.53 $\tau = - 0.17$		p = 0.37 $\tau = - 0.23$	
2	p = 0.47 $\tau = 0.18$		p = 0.48 $\tau = - 0.18$		p = 0.86 $\tau = - 0.05$		p = 0.005 $\tau = - 0.67$		p = 0.028 $\tau = 0.56$		p = 0.38 $\tau = 0.24$		p = 0.005 $\tau = - 0.69$	
3	p = 0.38 $\tau = 0.33$		p = 0.24 $\tau = 0.43$		p = 0.033 $\tau = 0.68$		p = 1 $\tau = - 0.05$		p = 0.38 $\tau = - 0.33$		p = 0.27 $\tau = - 0.47$		p = 0.38 $\tau = 0.33$	
4	p = 0.22 $\tau = - 0.82$		p = 1 $\tau = - 0.33$		p = 1 $\tau = - 0.33$		p = 1 $\tau = - 1$		p = 1 $\tau = - 1$		N/A		p = 1 $\tau = 1$	
5	p = 0.59 $\tau = - 0.14$		p = 0.017 $\tau = - 0.6$		p = 0.21 $\tau = - 0.32$		p = 0.16 $\tau = - 0.38$		p = 0.002 $\tau = 0.73$		p = 0.046 $\tau = - 0.55$		p = 0.0004 $\tau = - 0.82$	
6	p = 0.44 $\tau = - 0.28$		p = 0.06 $\tau = - 0.69$		p = 0.17 $\tau = 0.5$		p = 0.25 $\tau = - 0.41$		p = 0.06 $\tau = - 0.69$		p = 0.70 $\tau = - 0.14$		p = 0.44 $\tau = 0.28$	
7	p = 0.53 $\tau = 0.16$		p = 0.020 $\tau = 0.58$		p = 0.07 $\tau = 0.45$		p = 0.012 $\tau = - 0.63$		p = 0.072 $\tau = 0.45$		p = 0.92 $\tau = - 0.056$		p = 0.020 $\tau = - 0.58$	
8	p = 0.29 $\tau = - 0.29$		p = 0.11 $\tau = 0.42$		p = 0.005 $\tau = - 0.69$		p = 0.11 $\tau = - 0.42$		p = 0.11 $\tau = 0.42$		p = 0.60 $\tau = 0.14$		p = 0.047 $\tau = - 0.51$	
9	p = 0.37 $\tau = 0.23$		p = 0.11 $\tau = 0.41$		p = 0.93 $\tau = - 0.02$		p = 0.009 $\tau = - 0.66$		p = 0.37 $\tau = 0.23$		p = 0.008 $\tau = 0.73$		p = 0.32 $\tau = - 0.25$	
10	p = 0.010 $\tau = 0.71$		p = 0.005 $\tau = 0.76$		p = 0.17 $\tau = 0.38$		p = 0.54 $\tau = 0.20$		p = 0.015 $\tau = 0.78$		p = 0.36 $\tau = 0.29$		p = 0.07 $\tau = - 0.59$	
Total no. of sign. corr	+	-	+	-	+	-	+	-	+	-	+	-	+	-
	1	1	2	1	1	1	0	3	3	0	1	1	0	4

4.2 FLUORESCENCE INDICES

4.2.1 Site overview

The median values of FI for the ten sites varied between 1.48 and 1.69 (Table 8), indicating a mix of microbial and terrestrial matter. The median β/α were relatively similar among sites and all lower than 1, indicating a large fraction of older material. The median HIX were around 0.9 for all sites, indicating a high degree of humification.

Table 8. Median values for Fluorescence index, β/α and Humification index for each site.

Site	n	FI		β/α		HIX	
		Median	IQR	Median	IQR	Median	IQR
1	10	1.63	0.0996	0.633	0.292	0.902	0.106
2	10	1.55	0.080	0.630	0.365	0.907	0.124
3	7	1.69	0.040	0.737	0.008	0.908	0.0089
4	3	1.56	0.048	0.592	0.032	0.937	0.0013
5	10	1.61	0.077	0.696	0.303	0.892	0.099
6	6	1.48	0.022	0.632	0.078	0.899	0.034
7	10	1.53	0.031	0.632	0.230	0.915	0.081
8	10	1.60	0.074	0.635	0.269	0.918	0.0899
9	10	1.51	0.018	0.629	0.017	0.911	0.011
10	10	1.56	0.027	0.612	0.031	0.929	0.007

4.2.2 Spatial patterns

A significant correlation was found between FI and catchment area, and fraction of arable land (Table 9). The correlation with catchment area was negative, while the correlation with fraction of arable land was positive. Linear regressions for the two correlations were found to be significant (Figure 6). However, the catchment area and the fraction of arable land were significantly correlated ($p = 0.0089$, $\tau = -0.659$, $n = 10$), which could be the reason for both parameters being correlated with FI. The residuals of the linear regression model for FI and the fraction of arable land were not correlated with the catchment area ($p = 0.156$, $\tau = -0.378$, $n = 10$). None of the three fluorescence indices were correlated with median CO_2 concentration, nor with median specific discharge.

Table 9. Correlation between median values of fluorescence indices and catchment area, land use, CO₂ concentration and specific discharge. Kendall's tau (τ) and significance level (p) is presented. Significant correlations ($p < 0.05$) are written in bold.

Median	Catchment area (km ²)	Arable land (%)	pCO ₂ (μ atm)	Spec. discharge (mm/day)
FI	p = 0.0092 $\tau = -0.64$	p = 0.0089 $\tau = 0.66$	p = 0.77 $\tau = -0.14$	p = 0.36 $\tau = 0.24$
β/α	p = 0.11 $\tau = -0.42$	p = 0.42 $\tau = 0.21$	p = 0.77 $\tau = 0.14$	p = 0.46 $\tau = 0.19$
HIX	p = 0.73 $\tau = -0.11$	p = 0.93 $\tau = -0.02$	p = 0.56 $\tau = -0.24$	p = 0.2 $\tau = 0.33$

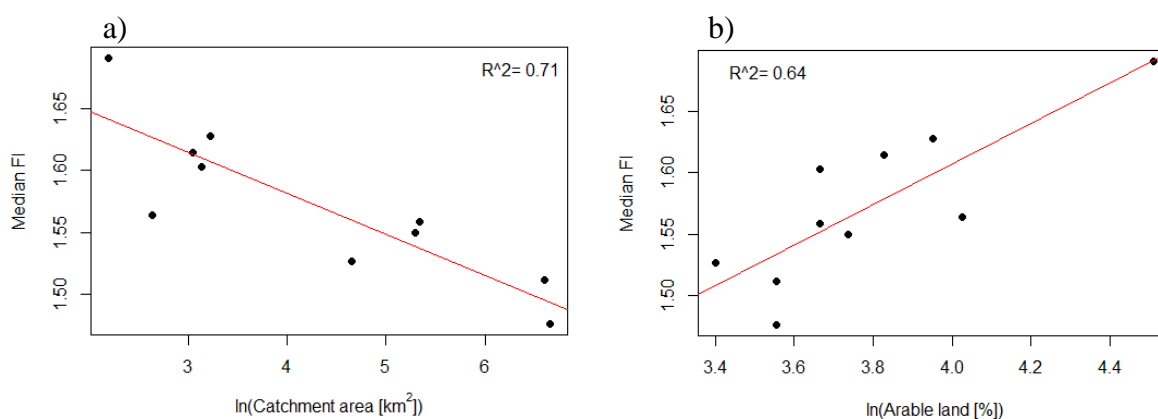


Figure 6. a) Linear regression for FI vs catchment area ($FI = 1.71423 - 0.03316 * \ln(\text{Catchment area})$, $p = 0.0013$, $n = 10$). b) Linear regression for FI vs fraction of arable land ($FI = 0.94686 - 0.16506 * \ln(\% \text{ arable land})$, $p = 0.0033$, $n = 10$).

FI and β/α were both significantly and positively correlated with NH₄⁺-N and PO₄³⁻-P (Table 10). HIX was not correlated with any of the water chemistry variables, and none of the indices were correlated with NO₂⁻+NO₃⁻-N, EC, DO or pH. A negative correlation was found between FI and temperature. No significant correlations were found between median DOC and any of the three fluorescence indices (Table 10). Plots for the significant correlations can be found in Appendix B.2.

Table 10. Correlations between median values of fluorescence indices and water chemistry variables, and DOC. Kendall's tau (τ) and significance level (p) is presented. Significant correlations ($p < 0.05$) are in bold. The number of observations (n) was 10 for all c

Median	FI	β/α	HIX
NH₄⁺-N ($\mu\text{g/l}$)	p = 0.045 $\tau = 0.56$	p = 0.0024 $\tau = 0.78$	p = 0.36 $\tau = -0.28$
NO₂⁻+NO₃⁻-N ($\mu\text{g/l}$)	p = 0.12 $\tau = 0.423$	p = 0.17 $\tau = 0.37$	p = 0.25 $\tau = -0.31$
PO₄³⁻-P ($\mu\text{g/l}$)	p = 0.045 $\tau = 0.56$	p = 0.013 $\tau = 0.67$	p = 0.36 $\tau = -0.28$
EC ($\mu\text{S/cm}$)	p = 0.11 $\tau = 0.42$	p = 0.29 $\tau = 0.29$	p = 0.86 $\tau = 0.067$
DO (mg/l)	p = 0.29 $\tau = 0.29$	p = 0.38 $\tau = 0.24$	p = 0.73 $\tau = 0.11$
pH	p = 1 $\tau = -0.022$	p = 1 $\tau = 0.022$	p = 0.86 $\tau = 0.067$
temp ($^{\circ}\text{C}$)	p = 0.017 $\tau = -0.6$	p = 0.73 $\tau = -0.11$	p = 0.60 $\tau = -0.16$
DOC_s (mg/l)	p = 0.16 $\tau = -0.38$	p = 0.60 $\tau = -0.16$	p = 0.22 $\tau = 0.33$
DOC_{ns} (mg/l)	p = 0.29 $\tau = -0.29$	p = 0.60 $\tau = -0.16$	p = 0.11 $\tau = 0.42$

4.2.3 Temporal patterns

All three indices were correlated with CO₂ at site 1 (Table 11). The correlations with FI and β/α were negative, while the correlation with HIX was positive. For site 5, a negative significant correlation was found between CO₂ and β/α . Since half of the CO₂ observations had the value of the upper detection limit, the linearity of the correlations could not be examined properly (Figure 7).

Table 11. Correlations between fluorescence indices (FI, β/α , HIX) and CO₂.

	Site 1	Site 5
FI	p = 0.017 $\tau = -0.73$	p = 0.47 $\tau = 0.33$
Freshness	p = 0.0079 $\tau = -0.81$	p = 0.017 $\tau = -0.87$
HIX	p = 0.017 $\tau = 0.73$	p = 0.14 $\tau = 0.6$

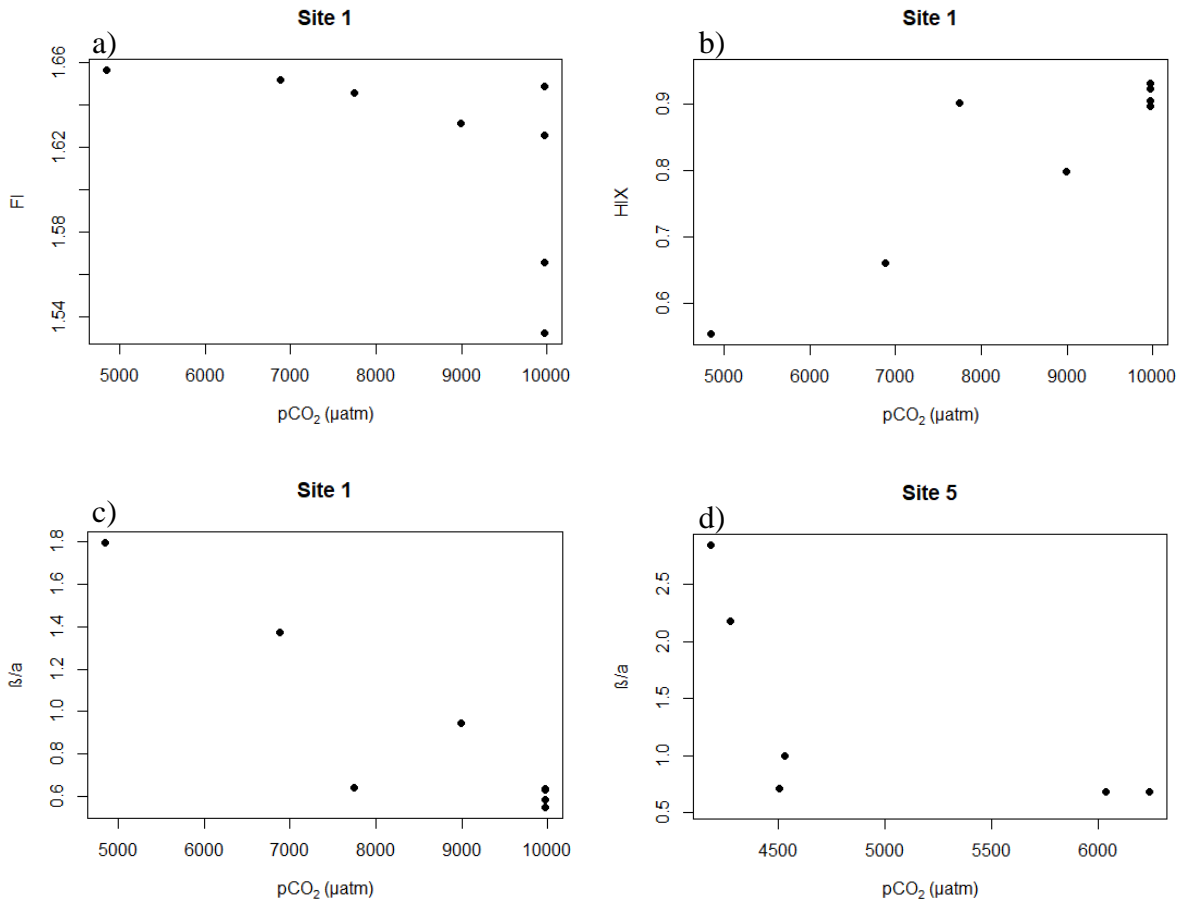


Figure 7. Plots of significant correlations between fluorescence indices and pCO₂ at site 1 and site 5. a) FI vs pCO₂ at site 1, b) HIX vs pCO₂ at site 1, c) β/α vs pCO₂ at site 1 and d) β/α vs pCO₂ at site 5.

At five of the sites (1, 2, 5, 7 and 8) both FI and β/α were negatively correlated with specific discharge (Table 12). HIX was positively correlated at four sites (1, 7, 8 and 10). For each correlation, the data for all significant sites were plotted together to identify possible common trends (Figure 8).

Table 12. Correlations between specific discharge and fluorescence indices. Kendall's tau (τ) and significance level (p) is presented. Significant correlations ($p < 0.05$) are written in bold.

Specific discharge (mm/day)			
Site	FI	β/α	HIX
1	p = 0.048 $\tau = -0.49$	p = 0.048 $\tau = -0.49$	p = 0.048 $\tau = 0.49$
2	p = 0.020 $\tau = -0.58$	p = 0.048 $\tau = -0.49$	p = 0.15 $\tau = 0.36$
3	p = 0.56 $\tau = 0.24$	p = 0.77 $\tau = 0.14$	p = 0.77 $\tau = -0.14$
4	p = 0.33 $\tau = -1$	p = 1 $\tau = -0.33$	p = 1 $\tau = 0.33$
5	p = 0.0071 $\tau = -0.67$	p = 0.031 $\tau = -0.54$	p = 0.15 $\tau = 0.36$
6	p = 0.44 $\tau = 0.28$	p = 0.70 $\tau = 0.14$	p = 1 $\tau = 0$
7	p = 0.017 $\tau = -0.6$	p = 0.0022 $\tau = -0.73$	p = 0.0091 $\tau = 0.64$
8	p = 0.0022 $\tau = -0.73$	p = 0.017 $\tau = -0.6$	p = 0.0091 $\tau = 0.64$
9	p = 1 $\tau = 0.022$	p = 0.22 $\tau = -0.33$	p = 0.073 $\tau = 0.47$
10	p = 0.48 $\tau = -0.2$	p = 0.60 $\tau = -0.16$	p = 0.029 $\tau = 0.56$

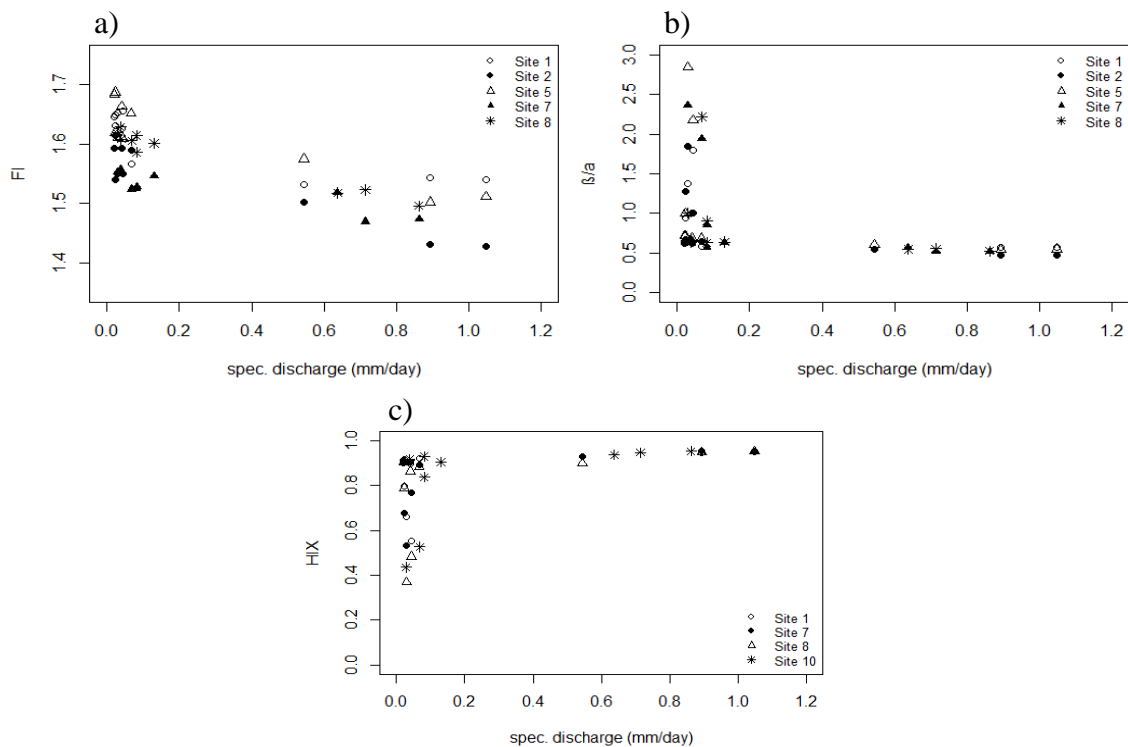


Figure 8. Plots of significant correlations between a) FI and specific discharge b) β/α and specific discharge and c) HIX and specific discharge.

At site 1 and 8, DOC_s was correlated with all three fluorescence indices (Table 13). All significant correlations between DOC_s and the indices were consistent in the sign of the correlation coefficient: negative for FI; negative for β/α ; positive for HIX. The correlations between FI and DOC were of linear character, while the correlation between β/α and DOC was negatively non-linear (Figure 9). The linearity of the correlation between HIX and DOC differed between sites. At site 1 and 8 the correlations were non-linear, while it was more linear at site 10 (Figure 9). At site 4, 6 and 9, no significant correlations were found between any of the fluorescence indices and DOC_s. For site 4 and 6, this might be due to a smaller sample size.

Table 13. Correlations between DOCs and fluorescence indices. Kendall's tau (τ), significance level (p) and number of observations (n) is presented. Significant correlations ($p < 0.05$) in bold.

DOC _s (mg/l)				
Site	n	FI	β/α	HIX
1	10	p = 0.0022 $\tau = - 0.73$	p = 0.00095 $\tau = - 0.78$	p = 0.0047 $\tau = 0.69$
2	10	p = 0.00036 $\tau = - 0.82$	p = 0.22 $\tau = - 0.33$	p = 0.48 $\tau = 0.2$
3	7	p = 0.030 $\tau = - 0.71$	p = 0.56 $\tau = - 0.24$	p = 0.56 $\tau = 0.24$
4	3	p = 1 $\tau = 0.33$	p = 1 $\tau = - 0.33$	p = 0.33 $\tau = -1$
5	10	p = 0.00095 $\tau = - 0.78$	p = 0.017 $\tau = - 0.6$	p = 0.38 $\tau = 0.24$
6	6	p = 0.14 $\tau = - 0.6$	p = 1 $\tau = - 0.067$	p = 1 $\tau = - 0.067$
7	10	p = 0.0091 $\tau = - 0.64$	p = 0.11 $\tau = - 0.42$	p = 0.22 $\tau = 0.33$
8	10	p = 0.00095 $\tau = - 0.78$	p = 0.0022 $\tau = - 0.73$	p = 0.0047 $\tau = 0.69$
9	10	p = 1 $\tau = 0.022$	p = 0.38 $\tau = - 0.244$	p = 0.16 $\tau = 0.38$
10	10	p = 0.22 $\tau = - 0.33$	p = 0.29 $\tau = - 0.29$	p = 0.017 $\tau = 0.6$

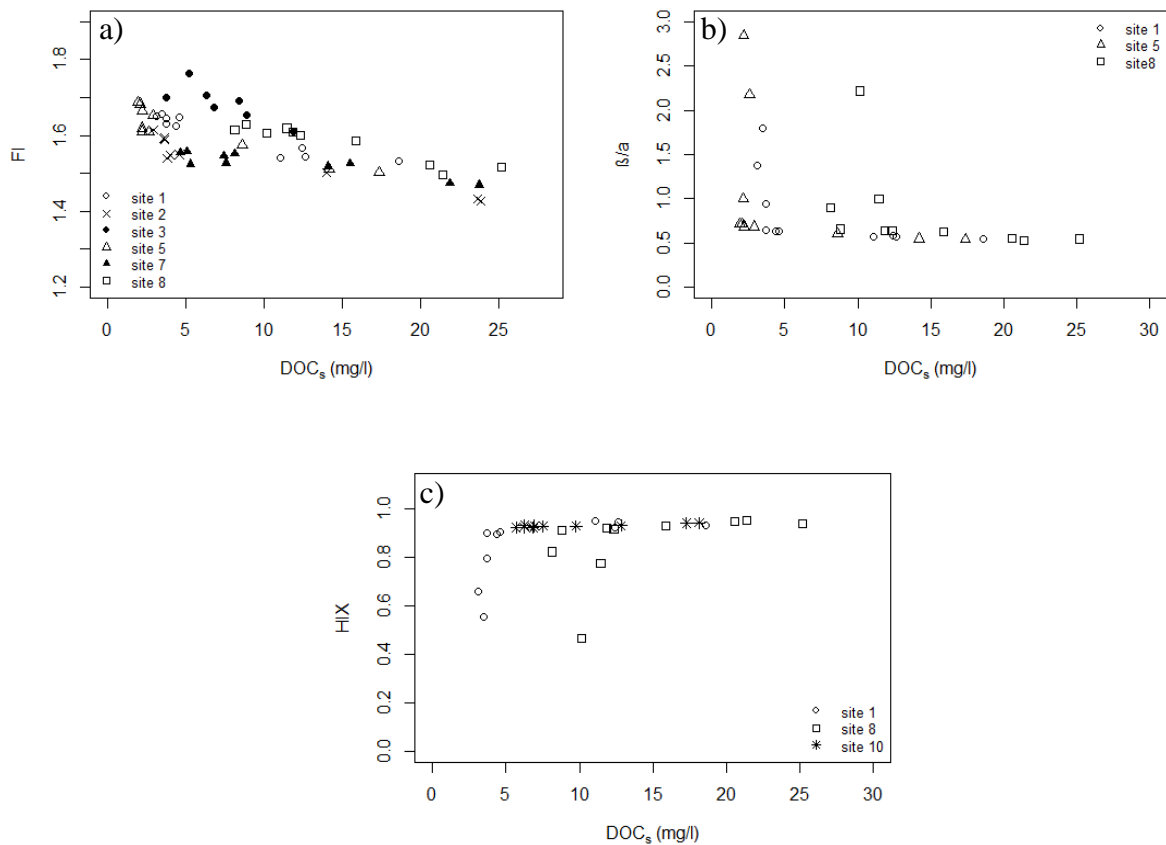


Figure 9. Plots of fluorescence indices against DOCs concentration at sites where correlations were significant. a) FI against DOCs, b) β/α against DOCs and c) HIX against DOCs.

Significant correlations were found between FI and $\text{NH}_4^+\text{-N}$ at two sites (Table 14). The correlations were positive at both sites. Significant correlations were found between FI and $\text{NO}_2^- + \text{NO}_3^- \text{-N}$ at three sites, where two of the correlations were negative and one positive (Table 14). Between FI and $\text{PO}_4^{3-}\text{-P}$, significant correlations were found at three sites. The correlation was negative at two sites, and positive at one. At three of the sites, positive correlations were found between FI and EC. Positive correlations between FI and temperature were found at two sites. Data from these sites were plotted together to check whether the correlations were similar between sites (Figure 10). For dissolved oxygen, a significant correlation was found at site 8 (Table 14). No significant correlations were found with pH. Plots of all significant correlations between FI and the water chemistry variables can be found in Appendix B.2.2.

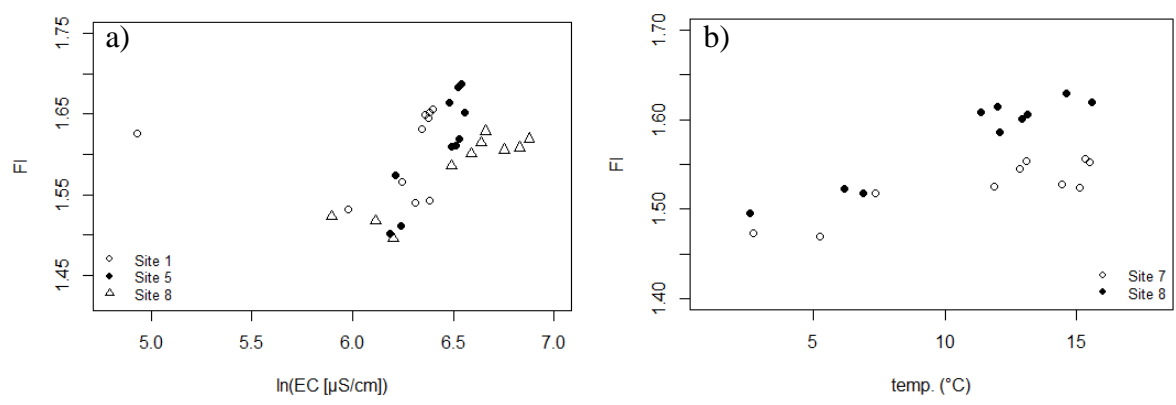


Figure 10. Plot of significant correlations between a) FI and EC, b) FI and temperature.

Table 14. Correlations between FI and water chemistry variables at the ten sites. Kendall's tau (τ) and significance level (p) are given. Significant correlations ($p < 0.05$) in bold.

	Site	NH ₄ ⁺ -N ($\mu\text{g/l}$)	NO ₂ ⁻ +NO ₃ ⁻ -N ($\mu\text{g/l}$)	PO ₄ ³⁻ -P ($\mu\text{g/l}$)	EC ($\mu\text{S/cm}$)	DO (mg/l)	pH	Temp ($^{\circ}\text{C}$)
FI	1	p = 0.031 $\tau = 0.54$	p = 0.38 $\tau = -0.24$	p = 0.59 $\tau = 0.14$	p = 0.047 $\tau = 0.51$	p = 0.073 $\tau = -0.47$	p = 0.92 $\tau = -0.028$	p = 0.16 $\tau = 0.38$
	2	p = 0.59 $\tau = -0.14$	p = 0.11 $\tau = 0.41$	p = 1 $\tau = 0$	p = 0.11 $\tau = 0.42$	p = 0.16 $\tau = -0.38$	p = 0.51 $\tau = -0.18$	p = 0.22 $\tau = 0.33$
	3	p = 1 $\tau = 0.048$	p = 0.24 $\tau = -0.43$	p = 0.033 $\tau = -0.68$	p = 0.56 $\tau = 0.24$	p = 0.14 $\tau = 0.52$	p = 0.72 $\tau = 0.2$	p = 0.38 $\tau = -0.33$
	4	p = 1 $\tau = 0$	p = 1 $\tau = 0.33$	p = 1 $\tau = 0.33$	p = 1 $\tau = -1$	p = 1 $\tau = -1$	N/A	p = 1 $\tau = 1$
	5	p = 0.59 $\tau = -0.14$	p = 0.017 $\tau = 0.6$	p = 0.86 $\tau = 0.045$	p = 0.0092 $\tau = 0.64$	p = 0.073 $\tau = -0.47$	p = 0.60 $\tau = 0.14$	p = 0.16 $\tau = 0.38$
	6	p = 1 $\tau = -0.067$	p = 0.27 $\tau = 0.47$	p = 0.022 $\tau = -0.83$	p = 0.056 $\tau = 0.73$	p = 0.056 $\tau = 0.73$	p = 0.72 $\tau = 0.2$	p = 1 $\tau = -0.067$
	7	p = 0.15 $\tau = -0.36$	p = 0.0047 $\tau = -0.69$	p = 0.11 $\tau = -0.42$	p = 0.073 $\tau = 0.47$	p = 0.073 $\tau = -0.47$	p = 0.76 $\tau = -0.11$	p = 0.017 $\tau = 0.6$
	8	p = 0.047 $\tau = 0.51$	p = 0.0091 $\tau = -0.64$	p = 0.0092 $\tau = 0.64$	p = 0.0092 $\tau = 0.64$	p = 0.002 $\tau = -0.73$	p = 0.075 $\tau = -0.48$	p = 0.0092 $\tau = 0.64$
	9	p = 0.79 $\tau = 0.068$	p = 0.52 $\tau = -0.17$	p = 0.72 $\tau = -0.090$	p = 0.21 $\tau = 0.32$	p = 0.60 $\tau = -0.16$	p = 1 $\tau = 0$	p = 0.28 $\tau = 0.27$
	10	p = 0.15 $\tau = -0.37$	p = 0.60 $\tau = -0.16$	p = 0.42 $\tau = 0.21$	p = 0.11 $\tau = 0.5$	p = 0.90 $\tau = 0.071$	p = 0.55 $\tau = 0.21$	p = 0.55 $\tau = -0.21$
Total no. of sign. corr.		+ -	+ -	+ -	+ -	+ -	+ -	+ -
		2 0	1 2	1 2	3 0	0 1	0 0	2 0

β/α and $\text{NH}_4^+\text{-N}$ concentration were significantly correlated at one site, site 5 (Table 15). This correlation was positive and non-linear. Significant correlations were also found between β/α and $\text{NO}_2^- + \text{NO}_3^- \text{-N}$ and $\text{PO}_4^{3-} \text{-P}$ at site 5, 7 and 8. Both for $\text{NO}_2^- + \text{NO}_3^- \text{-N}$ and $\text{PO}_4^{3-} \text{-P}$, the correlations were positive at one site, and negative at the two other sites. β/α and EC were positively correlated at two sites, site 2 and 8 (Table 15). These correlations were positive and non-linear. DO was significantly correlated with β/α at three sites, all correlations were negative and non-linear. pH and β/α were significantly correlated at site 5. This correlation was positive and non-linear. Significant correlation between β/α and temperature was found at five sites. All these correlations were positive. Plots of all significant correlations between β/α and water chemistry variables are found in Appendix B.2.3.

Table 15. Correlation between β/α and water chemistry variables. Kendall's tau (τ) and significance level (p) are given. Significant correlations ($p < 0.05$) in bold.

	Site	NH ₄ ⁺ -N ($\mu\text{g/l}$)		NO ₂ ⁻ +NO ₃ ⁻ -N ($\mu\text{g/l}$)		PO ₄ ³⁻ -P ($\mu\text{g/l}$)		EC ($\mu\text{S/cm}$)		DO (mg/l)		pH		Temp ($^{\circ}\text{C}$)	
β/α	1	p = 0.11 τ = 0.41		p = 0.73 τ = - 0.11		p = 0.72 τ = 0.090		p = 0.073 τ = 0.47		p = 0.11 τ = - 0.42		p = 0.75 τ = 0.085		p = 0.22 τ = 0.33	
	2	p = 0.37 τ = 0.23		p = 0.37 τ = 0.23		p = 0.15 τ = 0.36		p = 0.0022 τ = 0.73		p = 0.047 τ = - 0.51		p = 0.66 τ = - 0.12		p = 0.00036 τ = 0.82	
	3	p = 1 τ = - 0.05		p = 0.77 τ = - 0.14		p = 0.54 τ = - 0.20		p = 1 τ = - 0.048		p = 0.24 τ = 0.43		p = 0.72 τ = 0.2		p = 0.56 τ = - 0.24	
	4	p = 0.22 τ = 0.83		p = 0.33 τ = 1		p = 0.33 τ = 1		p = 1 τ = 1		p = 1 τ = 1		N/A		p = 1 τ = -1	
	5	p = 0.048 τ = 0.49		p = 0.047 τ = 0.51		p = 0.012 τ = 0.63		p = 0.16 τ = 0.38		p = 0.073 τ = - 0.47		p = 0.0024 τ = 0.82		p = 0.00036 τ = 0.82	
	6	p = 1 τ = - 0.067		p = 0.72 τ = 0.2		p = 0.44 τ = - 0.28		p = 0.72 τ = 0.2		p = 1 τ = - 0.067		p = 0.72 τ = 0.2		p = 0.72 τ = 0.2	
	7	p = 0.59 τ = 0.14		p = 0.0022 τ = - 0.73		p = 0.0092 τ = - 0.64		p = 0.11 τ = 0.42		p=0.00012 τ = - 0.87		p = 0.76 τ = - 0.11		p < 0.00003 τ = 0.91	
	8	p = 0.16 τ = 0.38		p = 0.047 τ = - 0.51		p = 0.020 τ = 0.6		p = 0.017 τ = 0.6		p = 0.047 τ = - 0.51		p = 0.25 τ = - 0.31		p = 0.0047 τ = 0.69	
	9	p = 0.058 τ = - 0.48		p = 0.052 τ = - 0.50		p = 0.11 τ = - 0.41		p = 0.59 τ = 0.14		p = 0.22 τ = - 0.33		p = 0.83 τ = - 0.057		p = 0.012 τ = 0.63	
	10	p = 0.47 τ = - 0.18		p = 0.73 τ = - 0.11		p = 0.93 τ = - 0.023		p = 0.40 τ = 0.29		p = 0.40 τ = 0.29		p = 0.72 τ = - 0.14		p = 1 τ = 0	
Total no. of sign. corr.	+ -		+ -		+ -		+ -		+ -		+ -		+ -		
	1 0		1 2		2 1		2 0		0 3		1 0		5 0		

No significant correlation could be found between HIX and NH_4^+ -N concentration at any site (Table 16). HIX and $\text{NO}_2^- + \text{NO}_3^-$ -N was however significantly correlated at three sites, all three correlations were positive and non-linear (Appendix B.2.4 Figure B10). PO_4^{3-} -P was positively correlated with HIX at one site, and negatively correlated at two sites. The correlations were not linear. The significant correlations found between HIX and EC, and HIX and temperature, were all negative. HIX and EC was correlated at two sites, while HIX and temperature were correlated at five sites (Table 16). HIX and DO were significantly positively correlated at four sites, but no common pattern could be seen between the correlations. A negative, non-linear significant correlation between HIX and pH was found at site 5. Plots of significant correlations between HIX and water chemistry variables can be found in Appendix B.2.4.

Table 16. Correlations between HIX and water chemistry variables at the ten sites. Kendall's tau (τ) and significance level (p) are given. Significant correlations ($p < 0.05$) in bold.

	Site	NH ₄ ⁺ -N ($\mu\text{g/l}$)		NO ₂ ⁻ +NO ₃ ⁻ -N ($\mu\text{g/l}$)		PO ₄ ³⁻ -P ($\mu\text{g/l}$)		EC ($\mu\text{S/cm}$)		DO (mg/l)		pH		Temp ($^{\circ}\text{C}$)	
HIX	1	p = 0.15 τ = - 0.36		p = 0.29 τ = 0.29		p = 0.47 τ = - 0.18		p = 0.29 τ = - 0.29		p = 0.047 τ = 0.51		p = 0.60 τ = - 0.14		p = 0.11 τ = - 0.42	
	2	p = 0.47 τ = - 0.18		p = 0.47 τ = - 0.18		p = 0.11 τ = - 0.41		p = 0.0047 τ = - 0.69		p = 0.029 τ = 0.56		p = 1 τ = 0		p = 0.0047 τ = - 0.69	
	3	p = 0.24 τ = 0.43		p = 0.77 τ = 0.14		p = 0.54 τ = 0.20		p = 0.77 τ = - 0.14		p = 0.069 τ = - 0.62		p = 0.27 τ = - 0.47		p = 0.56 τ = 0.24	
	4	p = 0.22 τ = 0.82		p = 1 τ = 0.33		p = 1 τ = 0.33		p = 1 τ = 1		p = 1 τ = 1		N/A		p = 1 τ = -1	
	5	p = 0.59 τ = - 0.14		p = 0.22 τ = - 0.33		p = 0.031 τ = - 0.54		p = 0.48 τ = - 0.2		p = 0.073 τ = 0.47		p = 0.016 τ = - 0.65		p = 0.0092 τ = - 0.64	
	6	p = 1 τ = - 0.067		p = 1 τ = - 0.067		p = 0.70 τ = 0.14		p = 1 τ = - 0.067		p = 0.72 τ = 0.2		p = 1 τ = - 0.067		p = 1 τ = - 0.067	
	7	p = 0.59 τ = - 0.14		p = 0.0092 τ = 0.64		p = 0.029 τ = 0.56		p = 0.11 τ = - 0.42		p = 0.00012 τ = 0.87		p = 0.48 τ = 0.22		p = 0.00036 τ = - 0.82	
	8	p = 0.22 τ = - 0.33		p = 0.073 τ = 0.47		p = 0.0092 τ = - 0.64		p = 0.0092 τ = - 0.64		p = 0.029 τ = 0.56		p = 0.35 τ = 0.25		p = 0.0022 τ = - 0.73	
	9	p = 0.18 τ = 0.34		p = 0.033 τ = 0.55		p = 0.21 τ = 0.32		p = 0.28 τ = - 0.27		p = 0.073 τ = 0.47		p = 0.67 τ = 0.11		p = 0.020 τ = - 0.58	
	10	p = 0.069 τ = 0.46		p = 0.017 τ = 0.6		p = 0.24 τ = 0.30		p = 0.55 τ = 0.22		p = 0.28 τ = 0.36		p = 0.55 τ = 0.21		p = 0.28 τ = - 0.36	
Total no. of sign. corr.		+	-	+	-	+	-	+	-	+	-	+	-	+	-
		0	0	3	0	1	2	0	2	4	0	0	1	0	5

4.3 COMPONENTS

4.3.1 Identification of components

A five-component PARAFAC model could be split-half validated and found to be the most suitable model. Three of the components (C1, C2 and C5) were identified as humic-like FDOM, and two as protein-like (C3 and C4) (Figure 11-12, Table 17).

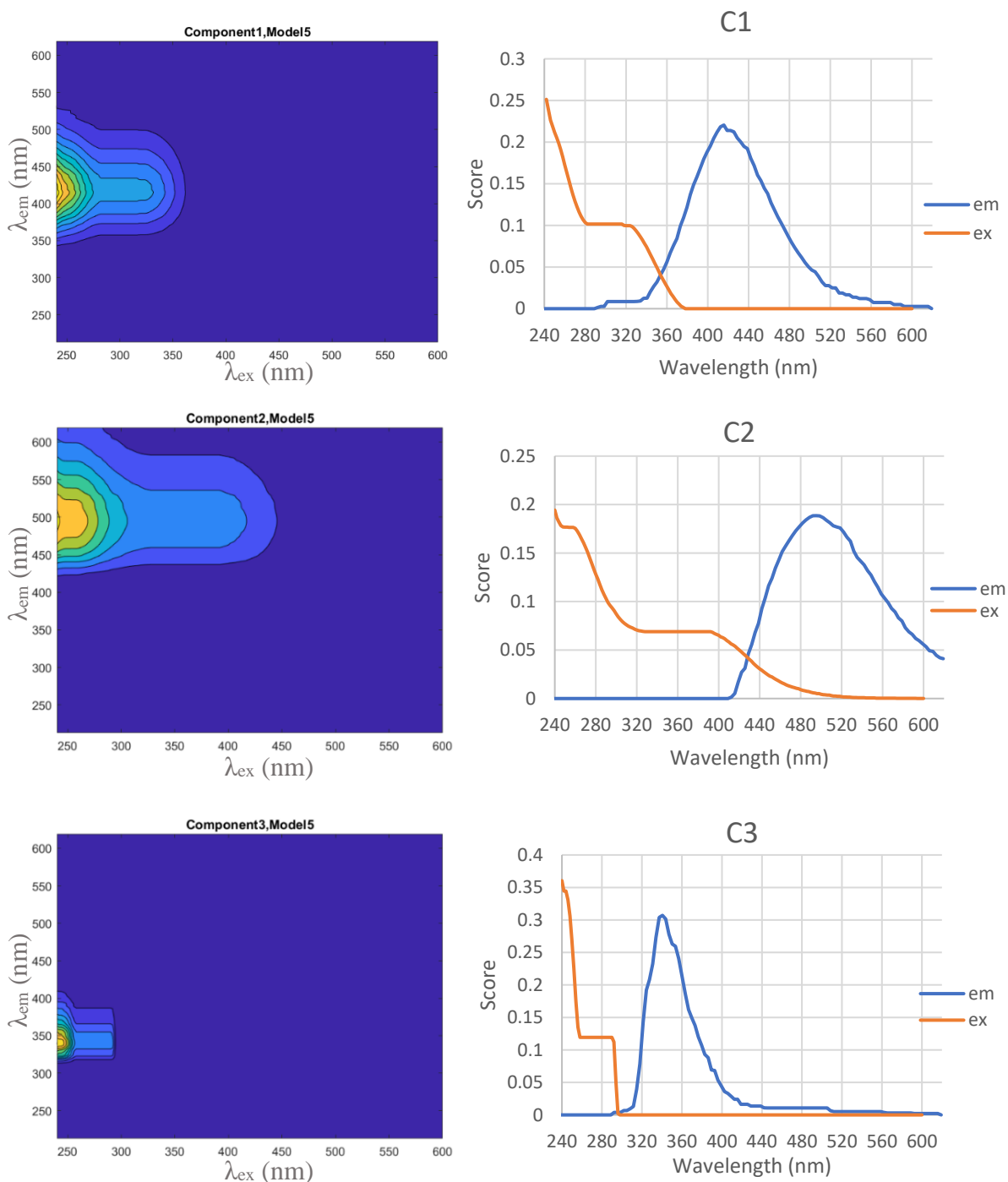


Figure 11. EEMs and plots of emission (λ_{em}) and excitation (λ_{ex}) wavelengths of the fluorescence intensity peaks of components C1, C2 and C3.

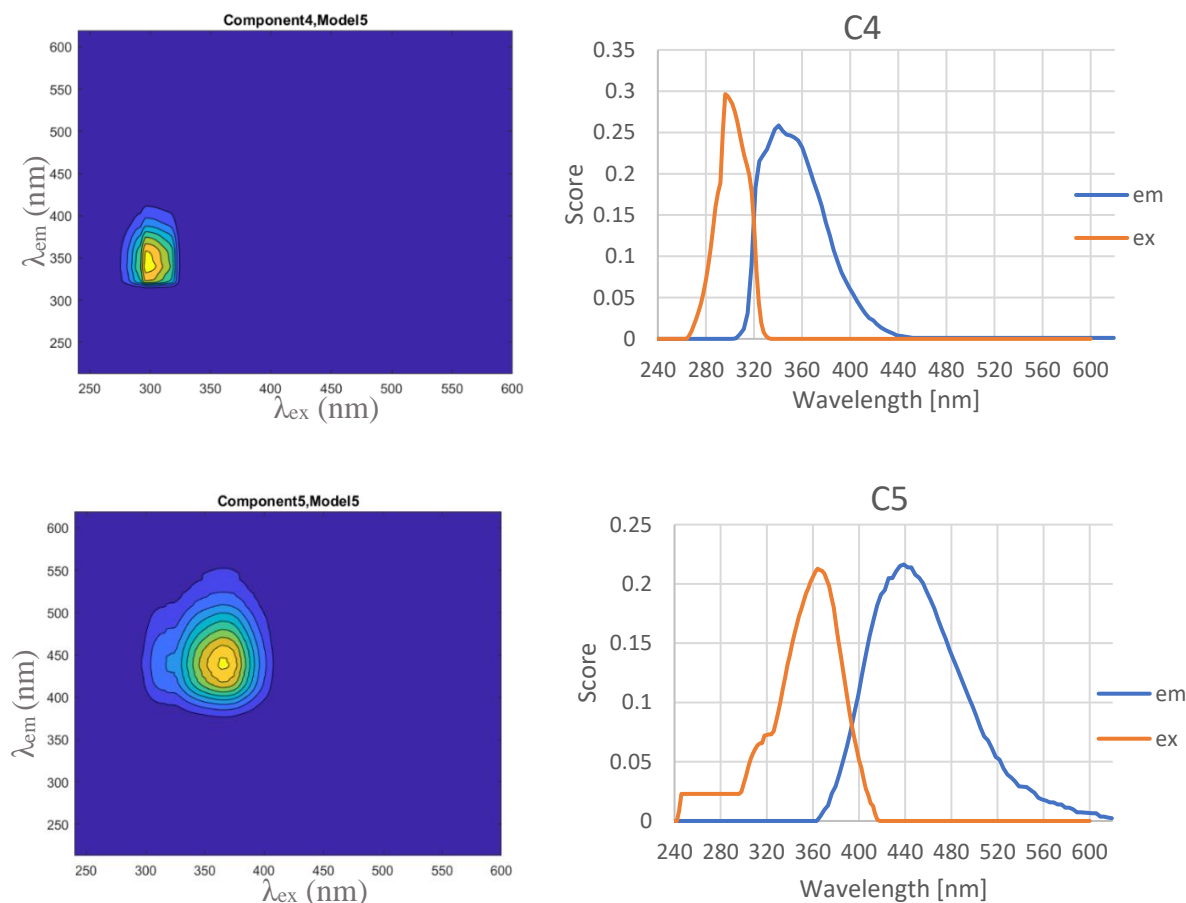


Figure 12. EEMs and plots of emission (λ_{em}) and excitation (λ_{ex}) wavelengths of the fluorescence intensity peaks of components C4 and C5.

Table 17. Peak wavelengths for the five PARAFAC components C1-C5.

Component	λ_{ex} (nm)	λ_{em} (nm)	Peak and character
C1	<240 nm	415.7 nm	A, humic-like
C2	<240 nm	495.2 nm	Humic-like
C3	<240 nm	340.6 nm	T, tryptophan-like
C4	296 nm	340.6 nm	T, tryptophan-like
C5	364 nm	438.8 nm	C, humic-like/fulvic-like

4.3.2 Spatial patterns

The median of the total component score (sum of all five components' scores) was highest at site 8 and lowest at site 5 (Figure 13). The humic-like components C1 and C2 were the components with the highest medians at all ten sites.

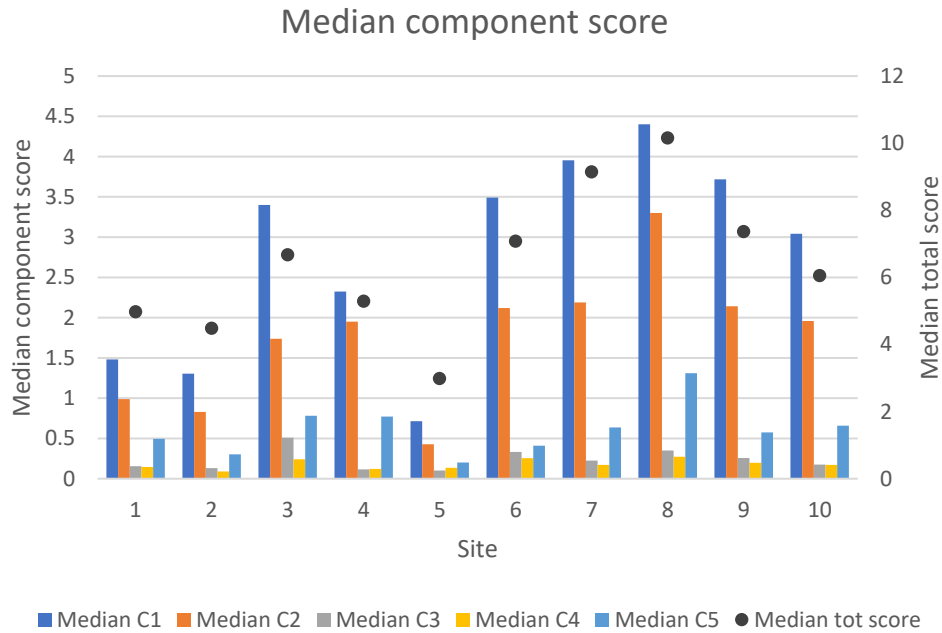


Figure 13. Median values of PARAFAC components C1-C5 for each site 1-10. Median value of the total score (dots) is given by the secondary axis to the right.

None of the PARAFAC components was correlated with catchment area, fraction of arable land or monthly median pCO₂ (Table 18). However, component C2 was nearly significantly correlated with fraction of arable land. All components except C5 were significantly correlated with DOC (Table 19, Figure 14). C5 was instead the only component correlated to one of the fluorescence indices; a positive correlation between median C5 and median HIX. The only significant correlation between components and the water chemistry variables was between C2 and NO₂⁻+NO₃⁻-N ($p = 0.028$, $\tau = -0.592$, $n = 10$). This correlation was not linear (Appendix B.3.1 Figure B12).

Table 18. Correlations between components and catchment area, fraction of arable land in the catchment area and CO₂. Kendall's tau (τ) and significance level (p) are given.

Median	Catchment area (km ²)	Arable land (%)	pCO ₂ (µatm)	Spec. discharge (mm/day)
C1	$p = 0.73$ $\tau = 0.11$	$p = 0.13$ $\tau = -0.39$	$p = 0.77$ $\tau = 0.14$	$p = 0.71$ $\tau = 0.094$
C2	$p = 0.48$ $\tau = 0.2$	$p = 0.058$ $\tau = -0.48$	$p = 0.77$ $\tau = 0.14$	$p = 0.71$ $\tau = 0.094$
C3	$p = 0.60$ $\tau = 0.16$	$p = 0.42$ $\tau = -0.21$	$p = 0.56$ $\tau = 0.24$	$p = 0.85$ $\tau = -0.047$
C4	$p = 0.2$ $\tau = 0.48$	$p = 0.32$ $\tau = -0.25$	$p = 0.56$ $\tau = 0.24$	$p = 0.85$ $\tau = -0.047$
C5	$p = 0.29$ $\tau = -0.29$	$p = 0.65$ $\tau = 0.11$	$p = 0.77$ $\tau = -0.14$	$p = 0.27$ $\tau = 0.28$

Table 19. Correlation between median component scores and median DOC, FI, β/α and HIX. Kendalls tau (τ) and significance level (p) are given. Significant correlations ($p < 0.05$) are in bold.

Median	DOC _s (mg/l)	FI	β/α	HIX
C1	p = 0.0092 $\tau = 0.64$	p = 0.48 $\tau = -0.2$	p = 1 $\tau = 0.022$	p = 0.22 $\tau = 0.33$
C2	p = 0.0022 $\tau = 0.73$	p = 0.29 $\tau = -0.23$	p = 0.86 $\tau = -0.067$	p = 0.11 $\tau = 0.42$
C3	p = 0.047 $\tau = 0.51$	p = 0.60 $\tau = -0.16$	p = 0.22 $\tau = 0.33$	p = 1 $\tau = 0.022$
C4	p = 0.029 $\tau = 0.56$	p = 0.73 $\tau = -0.11$	p = 0.29 $\tau = 0.29$	p = 1 $\tau = -0.022$
C5	p = 0.22 $\tau = 0.33$	p = 0.29 $\tau = 0.29$	p = 0.73 $\tau = -0.11$	p = 0.0092 $\tau = 0.64$

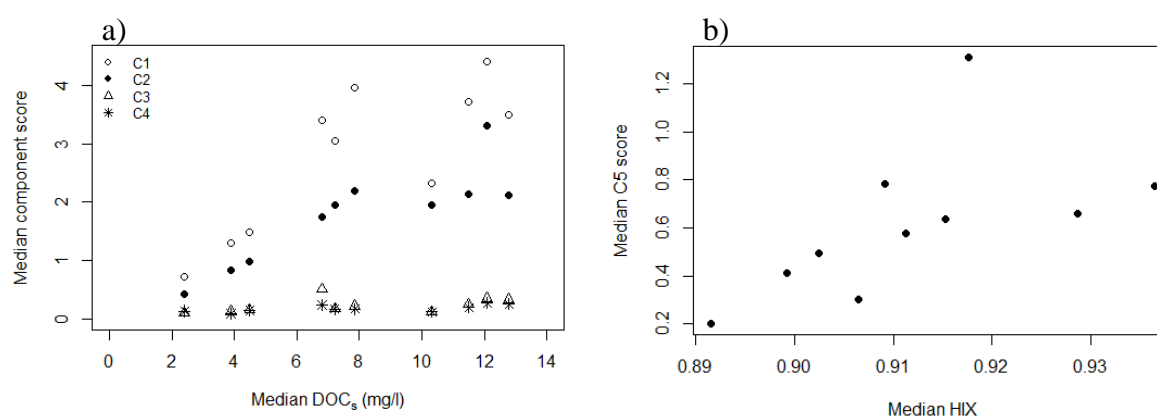


Figure 14. a) Plot of significant correlations on a spatial scale between PARAFAC component score and DOC_s concentration. b) Plot of median C5 score against median HIX.

4.3.3 Temporal patterns

The three humic-like components C1, C2 and C5 were significantly correlated with DOC_s at most of the sites (Figure 15, Appendix B.3.1 Table B3). C3 was only significantly correlated with DOC_s at site 8, and C4 at site 8 and 10. No correlations between components and DOC_s were found at site 4 and 6.

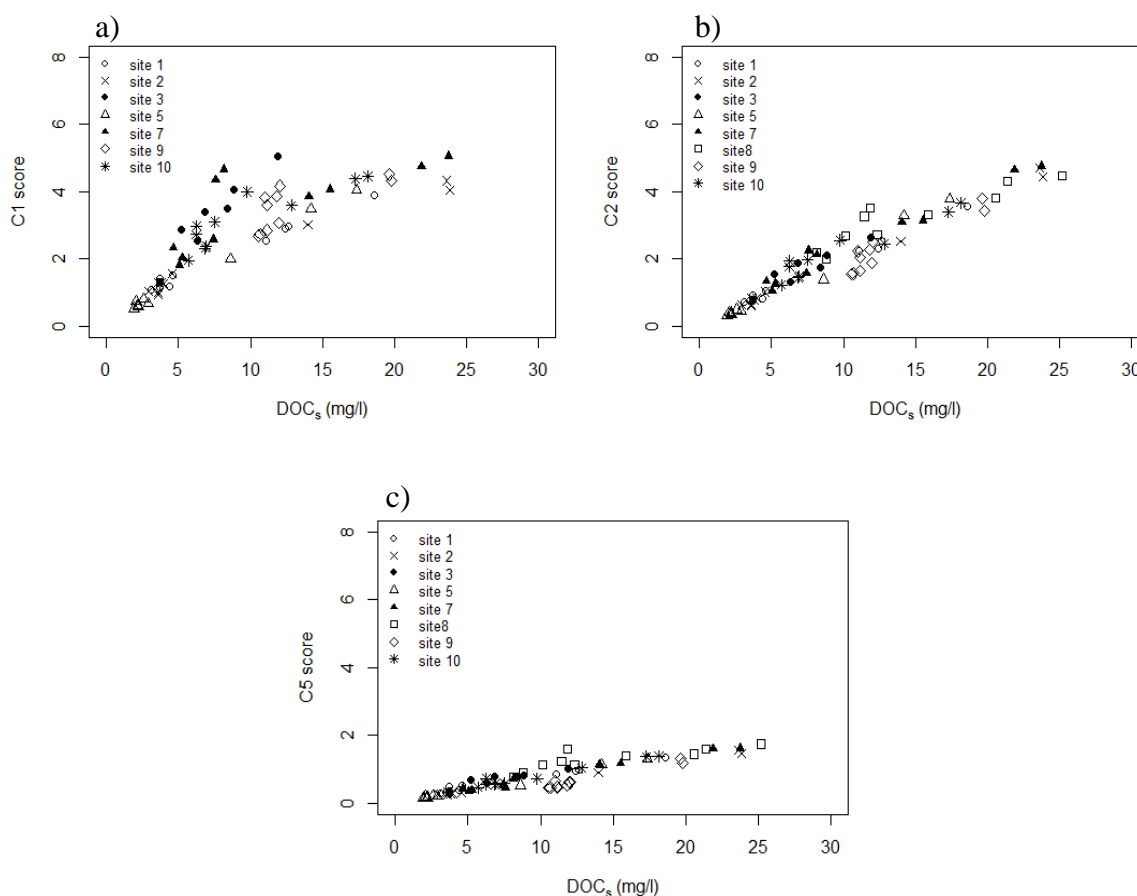


Figure 15. Plots of DOC_s concentration against a) C1 score b) C2 score and c) C5 score for sites where correlations were significant.

At site 1, a significant correlation was found between C1 and CO_2 , as well as for C2 and CO_2 (Table 20). Both correlations were positive. Half of the CO_2 observations had the value of the upper instrumental detection limit, and thus it was not possible to say anything about the linearity (Appendix B.3.1 Figure B13). No significant correlation was found between CO_2 and any of the PARAFAC components at site 5.

Table 20. Correlation between CO_2 and PARAFAC components. Significant correlations are written in bold.

Site	pCO_2 (μatm)				
	C1	C2	C3	C4	C5
1	p = 0.034 tau = 0.65	p = 0.034 tau = 0.65	p = 0.063 tau = - 0.56	p = 0.063 tau = - 0.56	p = 0.063 tau = 0.56
5	p = 1 tau = - 0.067	p = 1 tau = - 0.067	p = 0.14 tau = - 0.6	p = 0.27 tau = - 0.47	p = 0.72 tau = 0.2

Significant correlations between the PARAFAC components and specific discharge were found at some of the sites (Appendix B.3.1 Table B4). C3 and C4 were only correlated with discharge at site 8. Both these correlations were negative and non-linear. The significant correlations for C1, C2 and C5 were all positive (Figure 16).

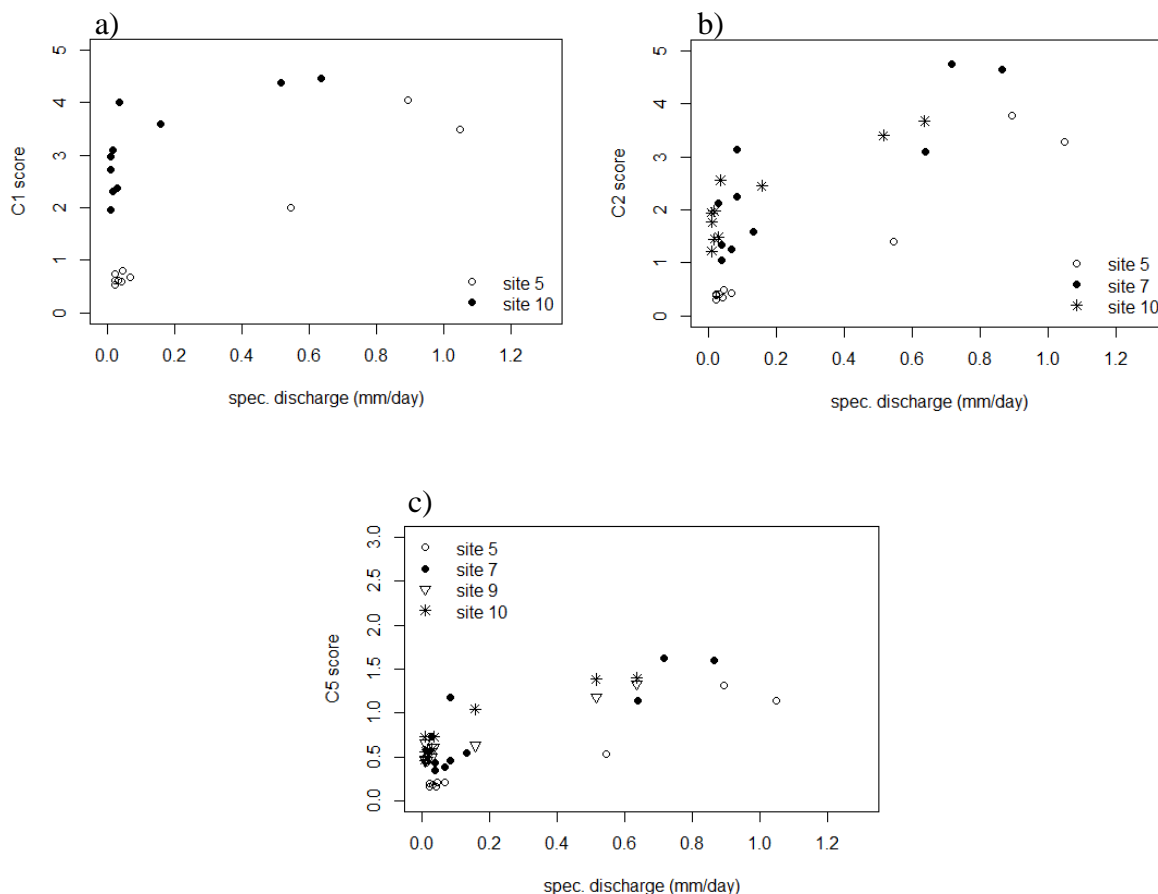


Figure 16. Plots of specific discharge and PARAFAC components a) C1, b) C2 and c) C5 at sites where correlations were significant.

C1 was found to correlate positively with $\text{NH}_4^+\text{-N}$ at site 10, and C1 and $\text{PO}_4^{3-}\text{-P}$ were significantly correlated at site 3 (Table 23). C1 was negatively correlated with $\text{NO}_2^- + \text{NO}_3^- \text{-N}$ at two sites, and positively correlated at one site. At four of the sites, C1 was significantly negatively correlated with EC. C1 and pH were significantly correlated at site 9, and C1 and temperature were significantly correlated at site 5. Dissolved oxygen was negatively correlated to C1 at site 6 and positively at site 2. Plots of significant correlations with C1 can be found in Appendix B.3.2.

C2 and $\text{NH}_4^+\text{-N}$ was significantly correlated at site 10 and C2 and $\text{PO}_4^{3-}\text{-P}$ were significantly correlated at site 8 (Table 24). C2 and $\text{NO}_2^- + \text{NO}_3^- \text{-N}$ was significantly correlated at three sites, where the correlation was positive at one site and negative at two. C2 and EC was significantly correlated at four sites, all correlations were negative. C2 and DO was correlated at three sites. The correlations were positive at all three sites. C2 and temperature was correlated at three sites,

all correlations were negative. A positive correlation between C2 and pH was found at one site, site 9. Plots of significant correlations with C2 can be found in Appendix B.3.3.

No correlation was found between C3 and $\text{NH}_4^+\text{-N}$, nor with C3 and pH, at any site (Table 25). A significant negative non-linear correlation was found between C3 and $\text{NO}_2^- + \text{NO}_3^- \text{-N}$ at site 7, and at site 2 and 8 positive significant correlations were found between C3 and $\text{PO}_4^{3-}\text{-P}$. EC and C3 were positively significantly correlated at site 8. A significant correlation between C3 and DO was found at site 7. At site 7, 8 and 9, positive significant correlations between C3 and temperature were found. Plots of significant correlations with C3 can be found in Appendix B.3.4.

C4 was the component with the fewest significant correlations. No correlations between C4 and $\text{PO}_4^{3-}\text{-P}$, C4 and DO or between C4 and pH were found at any of the sites. A positive correlation between C4 and $\text{NH}_4^+\text{-N}$ was found at site 7 and 10 (Table 26). C4 and $\text{NO}_2^- + \text{NO}_3^- \text{-N}$ were correlated at site 10. EC and temperature were both correlated to C4 at site 8. Plots of significant correlations with C4 are found in Appendix B.3.5.

C5 and $\text{NH}_4^+\text{-N}$ were significantly correlated at site 10. Significant correlations were found between C5 and $\text{NO}_2^- + \text{NO}_3^- \text{-N}$ at three sites, and between C5 and $\text{PO}_4^{3-}\text{-P}$ at three sites (Table 27). Significant correlations between C5 and EC, as well as between C5 and DO, were found at site 2, 5 and 7. Temperature and C5 were correlated at two sites, while no correlation between pH and C5 was found at any of the sites. Plots of significant correlations with C5 are found in Appendix B.3.6.

Table 21. Correlations between C1 and water chemistry variables. Kendall's tau (τ) and significance level (p) are given. Significant correlations ($p < 0.05$) in bold.

Site	NH ₄ ⁺ -N ($\mu\text{g/l}$)		NO ₂ +NO ₃ ⁻ -N ($\mu\text{g/l}$)		PO ₄ ³⁻ -P ($\mu\text{g/l}$)		EC ($\mu\text{S/l}$)		DO (mg/l)		pH		Temp ($^{\circ}\text{C}$)		
C1	1	p = 0.15 τ = - 0.36	p = 0.38 τ = 0.24	p = 0.86 τ = - 0.045	p = 0.22 τ = - 0.33	p = 0.16 τ = 0.38	p = 0.92 τ = - 0.028	p = 0.29 τ = - 0.29							
	2	p = 1 τ = 0	p = 0.37 τ = - 0.23	p = 0.73 τ = - 0.090	p = 0.017 τ = - 0.6	p = 0.0022 τ = 0.73	p = 0.83 τ = - 0.061	p = 0.22 τ = - 0.33							
	3	p = 0.77 τ = 0.14	p = 0.24 τ = 0.43	p = 0.033 τ = 0.68	p = 1 τ = - 0.048	p = 0.14 τ = - 0.52	p = 0.72 τ = - 0.2	p = 0.14 τ = 0.52							
	4	p = 1 τ = 0	p = 1 τ = 0.33	p = 1 τ = 0.33	p = 1 τ = -1	p = 1 τ = -1	N/A	p = 1 τ = 1							
	5	p = 0.86 τ = 0.045	p = 0.047 τ = - 0.51	p = 0.59 τ = - 0.14	p = 0.029 τ = - 0.56	p = 0.073 τ = 0.47	p = 0.60 τ = - 0.14	p = 0.029 τ = - 0.56							
	6	p = 1 τ = - 0.067	p = 0.017 τ = - 0.87	p = 0.13 τ = 0.55	p = 0.47 τ = - 0.33	p = 0.017 τ = - 0.87	p = 0.47 τ = - 0.33	p = 0.27 τ = 0.47							
	7	p = 0.073 τ = 0.45	p = 0.12 τ = 0.42	p = 0.22 τ = 0.33	p = 0.0092 τ = - 0.64	p = 0.29 τ = 0.29	p = 0.26 τ = - 0.33	p = 0.11 τ = - 0.42							
	8	p = 0.38 τ = 0.24	p = 0.86 τ = 0.067	p = 0.60 τ = - 0.16	p = 0.73 τ = 0.11	p = 0.73 τ = - 0.11	p = 0.46 τ = - 0.20	p = 0.86 τ = - 0.067							
	9	p = 0.18 τ = 0.34	p = 0.23 τ = 0.31	p = 0.59 τ = - 0.14	p = 0.0041 τ = - 0.72	p = 0.29 τ = 0.29	p = 0.011 τ = 0.69	p = 0.47 τ = - 0.18							
	10	p = 0.0065 τ = 0.69	p = 0.017 τ = 0.6	p = 0.65 τ = 0.11	p = 1 τ = 0	p = 0.18 τ = 0.43	p = 0.40 τ = 0.29	p = 0.40 τ = - 0.29							
Total no. of sign. corr.	+	-	+	-	+	-	+	-	+	-	+	-	+	-	
	1	0	1	2	1	0	0	4	1	1	1	0	0	1	

Table 22. Correlations between C2 and water chemistry variables. Significant correlations are in bold. Kendall's tau (τ) and significance level (p) are given. Significant correlations ($p < 0.05$) in bold.

	Site	NH ₄ ⁺ -N ($\mu\text{g/l}$)	NO ₂ ⁻ +NO ₃ ⁻ -N ($\mu\text{g/l}$)	PO ₄ ³⁻ -P ($\mu\text{g/l}$)	EC ($\mu\text{S/l}$)	DO (mg/l)	pH	Temp ($^{\circ}\text{C}$)
C2	1	p = 0.151 τ = - 0.36	p = 0.38 τ = 0.24	p = 0.86 τ = - 0.045	p = 0.22 τ = - 0.33	p = 0.16 τ = 0.38	p = 0.92 τ = - 0.028	p = 0.29 τ = - 0.29
	2	p = 1 τ = 0	p = 0.37 τ = - 0.23	p = 1 τ = 0	p = 0.047 τ = - 0.51	p = 0.0022 τ = 0.73	p = 0.66 τ = - 0.12	p = 0.22 τ = - 0.33
	3	p = 1 τ = 0.048	p = 0.38 τ = 0.33	p = 0.068 τ = 0.59	p = 1 τ = 0.048	p = 0.069 τ = - 0.62	p = 1 τ = - 0.067	p = 0.069 τ = 0.62
	4	p = 1 τ = 0	p = 1 τ = 0.33	p = 1 τ = 0.33	p = 1 τ = -1	p = 1 τ = -1	N/A	p = 1 τ = 1
	5	p = 0.86 τ = 0.045	p = 0.017 τ = - 0.6	p = 0.59 τ = - 0.14	p = 0.029 τ = - 0.56	p = 0.029 τ = 0.56	p = 0.60 τ = - 0.14	p = 0.029 τ = - 0.56
	6	p = 0.47 τ = - 0.33	p = 0.14 τ = - 0.6	p = 0.44 τ = 0.28	p = 1 τ = - 0.067	p = 0.14 τ = - 0.6	p = 1 τ = -0.067	p = 0.72 τ = 0.2
	7	p = 0.37 τ = 0.23	p = 0.0092 τ = 0.64	p = 0.073 τ = 0.47	p = 0.0047 τ = - 0.69	p = 0.047 τ = 0.51	p = 0.92 τ = - 0.056	p = 0.0092 τ = - 0.64
	8	p = 0.29 τ = - 0.29	p = 0.11 τ = 0.42	p = 0.017 τ = - 0.6	p = 0.11 τ = - 0.42	p = 0.11 τ = 0.42	p = 0.60 τ = 0.14	p = 0.017 τ = - 0.6
	9	p = 0.18 τ = 0.34	p = 0.23 τ = 0.31	p = 0.59 τ = - 0.14	p = 0.0041 τ = - 0.72	p = 0.29 τ = 0.29	p = 0.011 τ = 0.69	p = 0.47 τ = - 0.18
	10	p = 0.0065 τ = 0.69	p = 0.017 τ = 0.6	p = 0.65 τ = 0.11	p = 1 τ = 0	p = 0.18 τ = 0.43	p = 0.40 τ = 0.29	p = 0.40 τ = - 0.29
Total no. of sign. corr.	+ -	+ -	+ -	+ -	+ -	+ -	+ -	
	1 0	2 1	0 1	0 4	3 0	1 0	0 3	

Table 23. Correlations between C3 and water chemistry variables. Kendall's tau (τ) and significance level (p) are given. Significant correlations ($p < 0.05$) in bold.

Site	NH ₄ ⁺ -N ($\mu\text{g/l}$)		NO ₂ ⁻ +NO ₃ ⁻ -N ($\mu\text{g/l}$)		PO ₄ ³⁻ -P ($\mu\text{g/l}$)		EC ($\mu\text{S/l}$)		DO (mg/l)		pH		Temp ($^{\circ}\text{C}$)			
	C3	1	p = 0.28 $\tau = 0.27$	p = 0.86 $\tau = 0.067$	p = 0.28 $\tau = 0.27$	p = 0.48 $\tau = 0.2$	p = 0.38 $\tau = - 0.24$	p = 0.35 $\tau = 0.25$	p = 0.38 $\tau = 0.24$	2	p = 1 $\tau = 0$	p = 0.47 $\tau = 0.18$	p = 0.048 $\tau = 0.49$	p = 0.22 $\tau = 0.33$	p = 0.48 $\tau = - 0.2$	p = 1 $\tau = 0$
	3	p = 1 $\tau = 0.048$	p = 0.14 $\tau = 0.52$	p = 0.068 $\tau = 0.59$	p = 1 $\tau = 0.048$	p = 0.56 $\tau = - 0.24$	p = 1 $\tau = - 0.067$	p = 0.56 $\tau = 0.24$	4	p = 1 $\tau = 0$	p = 1 $\tau = 0.33$	p = 1 $\tau = 0.33$	p = 1 $\tau = - 1$	p = 1 $\tau = - 1$	N/A	p = 1 $\tau = 1$
	5	p = 0.59 $\tau = 0.14$	p = 1 $\tau = 0.022$	p = 0.11 $\tau = 0.41$	p = 0.48 $\tau = - 0.2$	p = 0.60 $\tau = - 0.16$	p = 0.17 $\tau = 0.37$	p = 0.22 $\tau = 0.33$	6	p = 0.14 $\tau = - 0.6$	p = 0.47 $\tau = - 0.33$	p = 1 $\tau = 0$	p = 0.72 $\tau = 0.2$	p = 0.47 $\tau = - 0.33$	p = 0.72 $\tau = 0.2$	p = 0.056 $\tau = 0.73$
	7	p = 0.37 $\tau = 0.23$	p = 0.029 $\tau = - 0.56$	p = 0.073 $\tau = - 0.47$	p = 0.22 $\tau = 0.33$	p = 0.00095 $\tau = - 0.78$	p = 1 $\tau = 0$	p = 0.0092 $\tau = 0.64$	8	p = 0.48 $\tau = 0.2$	p = 0.11 $\tau = - 0.42$	p = 0.047 $\tau = 0.51$	p = 0.017 $\tau = 0.6$	p = 0.11 $\tau = - 0.42$	p = 0.60 $\tau = - 0.14$	p = 0.017 $\tau = 0.6$
	9	p = 0.18 $\tau = - 0.34$	p = 0.052 $\tau = - 0.50$	p = 0.11 $\tau = - 0.41$	p = 0.59 $\tau = 0.14$	p = 0.16 $\tau = - 0.38$	p = 0.53 $\tau = 0.17$	p = 0.0071 $\tau = 0.67$	10	p = 0.59 $\tau = 0.14$	p = 0.86 $\tau = 0.067$	p = 0.24 $\tau = - 0.30$	p = 0.72 $\tau = - 0.14$	p = 0.40 $\tau = 0.29$	p = 1 $\tau = 0$	p = 1 $\tau = 0$
Total no. of sign. corr.		+ -	+ -	+ -	+ -	+ -	+ -	+ -	+ -	+ -	+ -	+ -	+ -	+ -		
		0 0	0 1	2 0	1 0	0 1	0 0	3 0								

Table 24. Correlations between C4 and water chemistry variables. Kendall's tau (τ) and significance level (p) are given. Significant correlations ($p < 0.05$) in bold.

Site	NH ₄ ⁺ -N ($\mu\text{g/l}$)		NO ₂ ⁻ +NO ₃ ⁻ -N ($\mu\text{g/l}$)		PO ₄ ³⁻ -P ($\mu\text{g/l}$)		EC ($\mu\text{S/l}$)		DO (mg/l)		pH		Temp ($^{\circ}\text{C}$)			
	C4	1	p = 0.86 τ = 0.045	p = 0.29 τ = 0.29	p = 0.86 τ = 0.045	p = 0.22 τ = 0.33	p = 1 τ = - 0.022	p = 0.46 τ = 0.20	p = 1 τ = 0.022	2	p = 0.37 τ = 0.23	p = 1 τ = 0	p = 0.37 τ = 0.23	p = 0.60 τ = 0.16	p = 0.86 τ = 0.067	p = 0.83 τ = - 0.061
	3	p = 1 τ = - 0.048	p = 0.56 τ = 0.24	p = 0.36 τ = 0.29	p = 0.38 τ = 0.33	p = 0.77 τ = - 0.14	p = 0.47 τ = 0.33	p = 0.38 τ = 0.33	4	p = 1 τ = 0	p = 1 τ = 0.33	p = 1 τ = 0.33	p = 1 τ = -1	p = 1 τ = -1	N/A	p = 1 τ = 1
	5	p = 0.28 τ = 0.27	p = 0.73 τ = - 0.11	p = 0.28 τ = 0.27	p = 0.60 τ = - 0.16	p = 1 τ = - 0.022	p = 0.25 τ = 0.31	p = 0.73 τ = 0.11	6	p = 0.14 τ = - 0.6	p = 0.47 τ = - 0.33	p = 1 τ = 0	p = 0.72 τ = 0.2	p = 0.47 τ = - 0.33	p = 0.72 τ = 0.2	p = 0.056 τ = 0.73
	7	p = 0.048 τ = 0.49	p = 0.60 τ = - 0.16	p = 0.86 τ = - 0.067	p = 1 τ = 0.022	p = 0.16 τ = - 0.38	p = 1 τ = 0	p = 0.38 τ = 0.24	8	p = 0.22 τ = 0.33	p = 0.073 τ = - 0.47	p = 0.073 τ = 0.47	p = 0.0092 τ = 0.64	p = 0.073 τ = - 0.47	p = 0.46 τ = - 0.20	p = 0.029 τ = 0.56
	9	p = 0.79 τ = - 0.068	p = 0.64 τ = - 0.12	p = 0.15 τ = - 0.36	p = 0.21 τ = - 0.32	p = 1 τ = - 0.022	p = 0.058 τ = 0.51	p = 0.21 τ = 0.32	10	p = 0.029 τ = 0.55	p = 0.029 τ = 0.56	p = 0.93 τ = 0.023	p = 0.90 τ = 0.071	p = 0.28 τ = 0.36	p = 0.90 τ = 0.071	p = 0.55 τ = - 0.21
Total no. of sign. corr.		+ -	+ -	+ -	+ -	+ -	+ -	+ -	+ -	+ -	+ -	+ -	+ -	+ -	+ -	+ -
		2 0	1 0	0 0	1 0	0 0	0 0	0 0	0 0	0 0	0 0	1 0	1 0	1 0	1 0	1 0

Table 25. Correlations between C5 and water chemistry variables. Kendall's tau (τ) and significance level (p) are given. Significant correlations ($p < 0.05$) in bold.

	Site	NH ₄ ⁺ -N ($\mu\text{g/l}$)		NO ₂ ⁻ +NO ₃ ⁻ -N ($\mu\text{g/l}$)		PO ₄ ³⁻ -P ($\mu\text{g/l}$)		EC ($\mu\text{S/l}$)		DO (mg/l)		pH		Temp ($^{\circ}\text{C}$)	
C5	1	p = 0.11 τ = - 0.41		p = 0.29 τ = 0.29		p = 0.72 τ = - 0.090		p = 0.29 τ = - 0.29		p = 0.11 τ = 0.42		p = 0.92 τ = 0.028		p = 0.22 τ = - 0.33	
	2	p = 0.59 τ = - 0.14		p = 0.72 τ = - 0.090		p = 0.59 τ = - 0.14		p = 0.029 τ = - 0.56		p = 0.00095 τ = 0.78		p = 0.38 τ = - 0.24		p = 0.073 τ = - 0.47	
	3	p = 0.77 τ = 0.14		p = 0.24 τ = 0.43		p = 0.033 τ = 0.68		p = 1 τ = - 0.048		p = 0.14 τ = - 0.52		p = 0.72 τ = - 0.2		p = 0.14 τ = 0.52	
	4	p = 1 τ = 0		p = 1 τ = 0.33		p = 1 τ = 0.33		p = 1 τ = - 1		p = 1 τ = - 1		N/A		p = 1 τ = 1	
	5	p = 0.72 τ = - 0.090		p = 0.0092 τ = - 0.64		p = 0.28 τ = - 0.27		p = 0.047 τ = - 0.51		p = 0.047 τ = 0.51		p = 0.25 τ = - 0.31		p = 0.0047 τ = - 0.69	
	6	p = 0.47 τ = - 0.33		p = 0.14 τ = - 0.6		p = 0.44 τ = 0.28		p = 1 τ = - 0.067		p = 0.14 τ = - 0.6		p = 1 τ = - 0.067		p = 0.72 τ = 0.2	
	7	p = 0.37 τ = 0.23		p = 0.0092 τ = 0.64		p = 0.029 τ = 0.56		p = 0.017 τ = - 0.6		p = 0.047 τ = 0.51		p = 0.61 τ = - 0.17		p = 0.0092 τ = - 0.64	
	8	p = 0.73 τ = - 0.11		p = 0.38 τ = 0.24		p = 0.047 τ = - 0.51		p = 0.38 τ = - 0.24		p = 0.38 τ = 0.24		p = 0.92 τ = - 0.028		p = 0.11 τ = - 0.42	
	9	p = 0.24 τ = 0.30		p = 0.052 τ = 0.50		p = 0.47 τ = 0.18		p = 0.11 τ = - 0.41		p = 0.38 τ = 0.24		p = 0.14 τ = 0.40		p = 0.072 τ = - 0.45	
	10	p = 0.011 τ = 0.64		p = 0.0022 τ = 0.73		p = 0.18 τ = 0.34		p = 0.72 τ = 0.14		p = 0.061 τ = 0.57		p = 0.18 τ = 0.43		p = 0.061 τ = - 0.57	
Total no. of sign. corr.		+	-	+	-	+	-	+	-	+	-	+	-	+	-
		1	0	2	1	2	1	0	3	3	0	0	0	0	2

5 DISCUSSION

5.1 IDENTIFICATION OF PARAFAC COMPONENTS

The PARAFAC components found were identified as peak A (component C1), shoulder of peak A (C2), peak T₁ (C3), peak T₂ (C4) and peak C (C5). Components C1, C2 and C5 have been related to humic-like FDOM, while C3 and C4 have been related to protein-like FDOM associated with the fluorescence of tryptophan. Peak A and C are common in freshwaters and have both been related to humic-like organic matter from degraded terrestrial matter, with high aromaticity and molecular weight (Baker et al., 2008; Hudson et al., 2007; Stubbins et al., 2014). Peak A has though been suggested to be more processed and degraded than peak C, and thus less degradable by biotic processes (i.e. less bioavailable) and light (i.e. less photolabile) (Stubbins et al., 2014).

Tryptophan-like fluorescence is often found in anthropologically influenced waters, and is associated with autochthonous DOM and microbial and algal activity. Both agriculture as well as treated wastewater effluents have been related to high tryptophan-like fluorescence. Peak T have been found to be highly bioavailable, but less photolabile than peak A and peak C (Stubbins et al., 2014).

5.2 SPATIAL PATTERNS

No correlation was found between median DOC concentration and the total catchment area, nor with the fraction of arable land in the catchment. There are several aspects thought to affect the DOC amount in a stream and its catchment, like land use, hydrology and in-stream processes. DOM concentration is generally higher in the top layers of the soil than in the deeper layers, and the DOM quality is shifting from terrestrial and aromatic to more microbial with the depth (Gabor et al., 2014). The influence of water transported in deeper soil layers is higher in larger catchment areas (Klaminder et al., 2011). With DOM concentrations being lower in deeper soil layers, it could be expected that streams with larger catchments would contain less DOM. However, in a previous study of 136 Swedish streams, no correlation between DOC concentration and catchment area could be found (Winterdahl et al., 2014). Of the DOC quality parameters (fluorescence indices and PARAFAC components), FI was correlated with both catchment area as well as the fraction of arable land in the catchment. The positive correlation between FI and the fraction of arable land indicated that a larger fraction of arable land is related to more microbially derived DOM. This result was expected, as previous studies have found agricultural land to shift the DOM character from plant-derived to more microbially derived DOM (Graeber et al., 2015). Wilson and Xenopoulos (2009) found the fraction of arable land in the riparian zone being positively correlated with FI. In the same study, a correlation between β/α and the fraction of arable land was also found. That was, however, not seen in this work. The correlation between FI and catchment area was negative, indicating that a larger catchment area is linked to more terrestrial and aromatic dissolved organic matter. As previously mentioned, larger catchments are more influenced of water travelling in deeper soil layers, where the DOM concentration is low and of a more microbial character. The negative correlation found between FI and catchment area was thus not expected. It is possible that the correlation is a spurious correlation, caused by the correlation between catchment area and the fraction of arable land in the catchment. The residuals of the linear regression model between FI and the fraction of arable land was not correlated with the catchment area. This is indicating that the correlation between catchment area and FI is a spurious correlation.

Of all ten sites, site 5 had the lowest DOC median value. Site 5 differs from natural stream conditions by both being influenced by agriculture and by being located downstream a small water treatment plant. Depending on the efficiency of the water treatment plant, the treated water released to the stream might either dilute or increase the concentration of nutrients and DOC in the stream water. It is possible that the low DOC concentrations at site 5 were an effect of this.

FI and temperature were significantly correlated on a spatial scale. The median temperature could be seen, not considering site 4 and 6, to increase from site 1 to 10. This is possibly an effect of the time difference between the collection of the samples. On each sampling occasion, the sampling started around 8 – 9 am at site 1 and were finished at site 10 around 1 pm. This would naturally give lower temperatures at sites 1-5 and higher at sites 7-10. Out of all ten sites, the lowest median and the highest median temperature were found at site 4 and 6, respectively. This was expected since the time series were incomplete at these sites and samples were collected during either autumn or summer.

No correlations were found on a spatial scale between DOC concentration and any of the nutrients. Correlations were however found between nutrient concentration and some of the DOM quality parameters. It was hypothesized that correlations would be found between DOM quality and nutrient concentration, since high nutrient amounts should enhance the microbial and algal production of DOM. Both FI and β/α were positively correlated with $\text{NH}_4^+\text{-N}$ as well as to $\text{PO}_4^{3-}\text{-P}$ concentration, indicating that more microbial and freshly produced DOM was related to higher nutrient concentrations. The correlations between FI and the nutrients were slightly less strong than those between β/α and the nutrients. Wilson and Xenopoulos (2009) found β/α to be correlated with total dissolved nitrogen, but not with total dissolved phosphorus. The expected correlation between PARAFAC components related to microbial DOM and nutrient concentrations could not be seen on a spatial scale. Instead, the humic-like component C2 was found to be correlated with $\text{NO}_2^- + \text{NO}_3^- \text{-N}$.

Intensified agricultural management has been related to increased concentrations of dissolved inorganic nitrogen (DIN), which in turn has been correlated with microbial-like DOM (Graeber et al., 2015). However, a more complex interaction between several factors associated with agricultural management was thought to explain and control the correlation, rather than a direct effect of the amount of DIN available. Changed hydrology due to drainage of the land, the use of fertilisers and the intense cultivation were all suggested as possible factors changing the DOM character (Graeber et al., 2015). The effects of agriculture on the soil DOM composition were also emphasised by (Wilson and Xenopoulos, 2009) as a possible factor behind the found correlation between nitrogen and enhanced autochthonous production in agricultural streams. Agriculture is thought to affect the soil DOM composition, with a shift to more DOM of low molecular weight and low degree of humification (Wilson and Xenopoulos, 2009). Here, it is also possible that the storage of the samples has had a greater impact on the protein-like, freshly produced compounds than on the humic-like ones, changing the ratio between the freshly produced and the humified matter, and hence the fluorescence indices. This could explain why the expected correlations between microbial DOM components, i.e. C3 and C4, and nutrients and catchment characteristics could not be found. The storage effect is further discussed in section 5.4.1.

5.3 TEMPORAL PATTERNS

5.3.1 DOC

For the sites with observations on all sampling events, DOC concentrations could be seen to increase during the latter part of the sampling period, from sampling event 7. This coincides with a change in specific discharge, temperature and shorter storage time. It is possible that all these aspects explain the increasing DOC concentration. At site 3, the pattern was different from the other sites. The highest DOC concentration was measured at sampling event 6, and after that slightly decreasing. Sampling event 6 was the first sampling at site 3 after rewetting of the stream. High DOC concentrations following draughts have been reported in previous studies, and in peat lands this has been suggested to be caused by microbial processes in soil and effects on the solubility of the DOC (Ritson et al., 2017). Previous studies have suggested that storm events, high flow and wet soil conditions are increasing the release and transport of aromatic and terrestrial DOM to agricultural streams (Eckard et al., 2017; Wilson and Xenopoulos, 2009). Wilson and Xenopoulos (2009) are implying that even short periods of soil moisture conditions can influence the DOM quality in agricultural lands, due to the land being artificially drained. It is possible that the high concentration of DOC at sampling event 6 was caused by a flush of the soil, transporting allochthonous DOC to the stream. The slightly decreasing DOC concentrations measured for the following sampling dates might then be explained by lower DOC concentration in the incoming water, due to the large amount of DOC already being transported to the stream. Site 3 was the site with the smallest catchment area and the highest amount of arable land, 91 %. Due to the large fraction of agricultural land, the amount of soil DOC is possibly not very high. Moreover, the hydrological response in the stream is thought to be rapid, due to the small catchment area and drainage of the soil. Another possibility is that in-stream processes were resumed after the rewetting of the stream, and that DOC is mainly autochthonous. The slightly decreasing concentrations after sample event 6 could then be a dilution effect due to increased runoff of water with low DOC concentration to the stream, or by a decreasing microbial activity caused by lower temperatures. The temporal pattern of FI at site 3 is indicating that a mix of these theories are true, with a slightly higher input of terrestrial DOM at sampling event 6, followed by a shift towards more microbially derived DOC the following dates.

The humic-like components C1, C2 and C5 were significantly correlated with DOC at most of the sites, and all correlations were positive. The tryptophan-like components C3 and C4, however, were only significantly correlated with DOC at one, and two sites, respectively. At site 8, both C3 and C4 were negatively correlated with DOC, and at site 10, C4 was positively correlated with DOC. This is indicating that the humic-like components influence the DOC concentration to a greater extent than the tryptophan-like components do. However, different compounds may have different ability and efficiency to fluoresce. It has been reported that correlations between peak T fluorescence and DOC concentration could not be found, due to the high fluorescence efficiency of peak T (Baker et al., 2008). This might be the reason for the lack of correlations found in this study. Peak C, on the other hand, have been reported to correlate with DOC concentration (Baker et al., 2008).

FI and DOC were negatively correlated at six of the ten sites. Two of the sites where no significant correlations were found were site 4 and 6. These two sites had fewer observations than the other sites, which might explain the lack of correlations. The other two sites where no correlation between FI and DOC could be found were site 9 and 10. These two sites were

located close to each other, which could indicate that they are affected by similar physical factors. Site 9 and 10 had similar fraction of arable land in the catchment area, but differed in the size of the catchment area, with site 9 having a catchment area 3.5 times larger than site 10. The correlations between DOC concentration and the three indices implied that the increasing DOC concentrations at the end of the sampling period were caused by an increasing amount of older, more degraded terrestrial matter. This was supported by the results from correlations with specific discharge, temperature and EC, suggesting that increased discharge from shallow soil layers was the driving factor behind the shift in DOM quality, see sections 5.3.2.

5.3.2 Specific discharge and EC

The results from correlations between fluorescence indices and specific discharge indicated that higher specific discharge was linked to more terrestrial, older and more humified organic matter. The discharge was thus found to influence the quality of the DOM in streams. The same pattern could be seen between the correlations between EC and the indices. FI and EC were positively correlated at three sites (1, 5 and 8), β/α and EC at one site (8), and HIX and EC were negatively correlated at two sites (2 and 8). This is indicating that more microbial, freshly produced and less humified DOM is related to higher EC. This might be an effect of changes in the runoff and discharge, rather than a direct relation between the DOM composition and EC. EC is a measure of the amount of dissolved substances and ions in the water and is affected by both the amount and the charge of the ions (Naiman and Bilby, 1998). A higher EC corresponds to a higher ability of the water to carry an electrical current, due to a higher amount of charged particles solved in the water. The major part of these ions is transported to streams by groundwater. Rain and storm events can have a dilutional effect on EC, due to rain and surface runoff having a lower concentration of solved ions than groundwater (Naiman and Bilby, 1998). Hence, variations in EC can be an indication of the influence of groundwater inflow versus surface runoff to stream water. The correlations found between the indices and EC are thought to be an effect of this. Increasing runoff from the upper soil layers and the soil surface could cause a dilutional effect on EC, as well as on autochthonous DOM, and adding of more allochthonous terrestrial DOM.

Significant correlations between specific discharge and C1, C2 and C5 were found at two, three and four sites, respectively. All correlations were positive, which align with the theory that the three humic-like components are allochthonous and terrestrially derived. C3 and C4 were only correlated with discharge at site 8. Both these correlations were negative and non-linear, implying lower protein-like FDOM scores with higher specific discharge. This might indicate either a dilution effect due to increased runoff from the upper soil layers with low amount of microbial DOM, or a change in the autochthonous production of DOM due to a shift of seasons.

Similar results, supporting the idea of the increasing runoff driving the variation in components scores, were found for the relation between the components and EC. C3 and C4 were positively correlated to EC at site 8, implying that the C3 and C4 scores are higher when the input of groundwater is larger than that of surface runoff. Negative correlations were found between EC and C1 and C2 at site 2, 5, 7 and 9, and between EC and C5 at site 2, 5 and 7.

5.3.3 Temperature

Positive correlations between β/α and temperature were found at the same five sites as negative correlations between HIX and temperature were found, sites 2, 5, 7, 8 and 9. Correlations between FI and temperature were only found at site 7 and 8. These correlations were positive.

These results are suggesting that a higher temperature is related to more microbial, freshly produced and less humified DOM. This might be a true correlation, with temperature enhancing the microbial and algal activity. However, since a decrease in temperature occurred closely in time with increasing discharge due to increasing and more intense rain events, it is difficult to tell these two factors' influence on the DOM quality apart. The specific discharge was found to be correlated with the indices at several sites, and suggested to increase the fraction of terrestrially derived DOM with increasing discharge.

Just like the correlations between fluorescence indices and temperature indicated, the correlations between the PARAFAC components and temperature are also indicating that higher temperature increases the protein-like FDOM, and decreases the influence of humic-like FDOM. As previously discussed, this relation might be a direct effect of temperature, but might also partly be explained by changes in discharge. Baker et al. (2003) found, during summer, high intensities of tryptophan-like fluorescence related to untreated wastewater during the summer months. It was suggested that the high peak values were an effect of the low baseflow and hence low dilutional effect. In this study, high peaks in tryptophan-like fluorescence were measured at site 7 and 8 at sampling events 3 and 2, respectively. Since the two sites are located in the same area and the peaks appeared closely in time, the high tryptophan peaks are likely caused by the same factors or originated from the same source.

5.3.4 Nutrients

No overall consistent pattern could be seen in the correlations between nutrient concentration and DOC concentration, nor with DOM quality parameters. Six of the ten sites had significant correlations between DOC and at least one of the nutrient variables ($\text{NH}_4^+\text{-N}$, $\text{NO}_2^-+\text{NO}_3^-\text{-N}$, $\text{PO}_4^{3-}\text{-P}$), but the sign of the correlation coefficient was not consistent among sites. The four sites where no correlations were found were site 2, 4, 6 and 9, of which site 4 had insufficient amount of data, and site 6 had less observations than the other sites. Regarding the fluorescence indices, the expected results of higher nutrient concentration being related to more microbial and freshly produced DOM, were only found at a few sites. At some sites, the opposite result was found instead. HIX and $\text{NO}_2^-+\text{NO}_3^-\text{-N}$ were positively correlated at three sites, which was not expected, and is thought to be an effect of the discharge. The correlations found between nutrient concentration and the PARAFAC components related to microbial activity, i.e. C3 and C4, were few. All but one of the correlations were however positive. For the correlations between humic-like components and nutrient concentrations, the sign of the correlation coefficient was not consistent among sites. However, within the sites, the sign of the significant correlations was consistent. For example, the three humic-like components were consistently positively correlated to $\text{NH}_4^+\text{-N}$ and $\text{NO}_2^-+\text{NO}_3^-\text{-N}$ at site 10, while the correlations were negative at site 5. Previous studies have found nitrogen, but not phosphorus, to influence the DOM quality (Graeber et al., 2015; Wilson and Xenopoulos, 2009). The importance and the complexity of the interplay between nutrient concentrations and agriculture management factors previously mentioned, and their influence on DOM quality, might be an explanation to the contradictory results and lack of consistency. It is possible that the effect of $\text{NH}_4^+\text{-N}$ and $\text{NO}_2^-+\text{NO}_3^-\text{-N}$ on DOM quality is obscured due to other changing factors during the sampling period. It is also possible that a substantial amount of protein-like FDOM has been degraded in the samples during storage. With a longer sampling period and shorter storage time, it is possible that the increasing amount of protein-like FDOM components would have been correlated with increasing inorganic nitrogen concentrations.

DOC and $\text{NO}_2^- + \text{NO}_3^- - \text{N}$ concentrations were positively correlated at site 7 and 10, and negatively at site 5. Site 5 was the site with the highest $\text{NO}_2^- + \text{NO}_3^- - \text{N}$ median, and unlike site 7 and 10 the temporal trend of $\text{NO}_2^- + \text{NO}_3^- - \text{N}$ concentration was negative, with a decrease at sampling event 8. Eckard et al (2017) suggested that a decrease in nitrate concentrations coinciding with increasing discharge is an indication of reduced influence of groundwater, since groundwater in agricultural landscapes have high nitrate concentrations. The difference in the sign of correlation coefficient might thus be caused by differences in hydrological character between catchments.

Significant correlations of opposite signs were also found between DOC and $\text{PO}_4^{3-} - \text{P}$ at two sites: positive at site 3, and negative at site 8. Site 8 was the site with highest median $\text{PO}_4^{3-} - \text{P}$ of all ten sites. The $\text{PO}_4^{3-} - \text{P}$ concentration was relatively stable and high during the first half of the sampling period and decreased steadily from sampling event 7 and onwards. This might be a dilutional effect due to increased runoff. The result of the DOM quality analysis is supporting this theory, showing a slight shift towards more terrestrially derived DOM. As for site 3, the temporal variation of $\text{PO}_4^{3-} - \text{P}$ concentrations was similar to the temporal DOC concentration pattern explained in section 5.3.1. Thus, $\text{PO}_4^{3-} - \text{P}$ might have been transported to the stream following the flush and rewetting of the soil. The addition of $\text{PO}_4^{3-} - \text{P}$ might have enhanced the microbial activity in the stream and autochthonous production, and could explain the variation in DOC concentration.

5.3.5 CO_2

No correlation was found between any of the indices and CO_2 on a spatial scale. On a temporal scale, however, negative correlations were found between FI and CO_2 and between β/α and CO_2 , for site 1. At the same site, a positive correlation was found between HIX and CO_2 . These correlations are indicating that a larger amount of old, terrestrially derived and humified DOM is related to a higher CO_2 concentration. This is in line with findings in previous studies, but could also be an effect of changes in the discharge pattern. Bodmer et al. (2016) found pCO_2 to be positively correlated to the molecular size of DOM and a PARAFAC component related to terrestrially derived DOC with high molecular weight. This was explained by the so-called priming effect, and previous findings of larger DOC compounds being degraded to a greater extent than DOC of lower molecular weight. The priming effect is the phenomena where an input of more bioavailable DOM increases the degradation of less bioavailable DOM (Guenet et al., 2010). The effect of the priming effect is that DOM with low bioavailability may contribute significantly to the CO_2 production in stream water. However, the priming effect has also been suggested to mainly occur in soils, and not in aquatic environments (Catalán et al., 2015).

The correlation on a temporal scale between CO_2 and the indices could only be checked at two sites, and therefore it is not possible to verify the results on a larger scale. At site 5, a positive significant correlation could be seen for β/α and CO_2 , but no correlations were found with the other two indices. It is also possible that a different result would have been obtained if samples had been stored for a shorter time, since the most bioavailable DOM might have been degraded rapidly.

The combination of the correlations with decreasing FI and β/α , and increasing HIX, was the same found between the indices and DOC concentration, as well as with the specific discharge. It is thus possible that the increasing pCO_2 is caused by increasing DOC concentrations, or by

increased specific discharge. The specific discharge might contribute to the CO₂ concentration by the transport of DOM or CO₂ from soil respiration. In the related MSc thesis project, pCO₂ was found to be significantly correlated with specific discharge (Osterman, 2018).

In line with the result of correlations between fluorescence indices and CO₂, increasing CO₂ concentrations were found to be related with two of the humic-like PARAFAC components, C1 and C2. C1 and C2 are both related to peak A fluorescence, associated with highly degraded DOM of terrestrial origin, with low bioavailability. This is aligning with the findings in Bodmer et al. (2016), where a PARAFAC component of similar fluorescence characteristics as C2 in this study, was found to be positively correlated with pCO₂. As previously discussed, the priming effect might be a reason for this positive correlation.

5.4 SOURCES OF ERROR

5.4.1 Storage effect

The water samples, on which fluorescence and DOC was measured, had been stored in the dark at 4 °C. Since the samples were stored unfiltered, it is possible that microbial processes might have proceeded during the time of storage. Both degradation and transformation of the DOM compounds might have occurred, and different compounds have likely been affected differently.

It is possible that the difference in DOC concentration between the two data sets of DOC concentrations (DOC_s and DOC_{ns}) were caused by degradation in the samples during storage, but this could not be proved statistically. Although the two sets were measured on the same kind of analyser, the instrumental bias appeared to differ between machines such that DOC_{ns} concentrations were consistently higher than DOC_s. This, together with possible errors and differences in the pre-treatment of samples, could be another explanation for the differences.

To check the differences between the two sets statistically, the Kruskal-Wallis test was used. The Kruskal-Wallis test should ideally be applied to groups of data of the same distribution. The data was thus log-transformed in order to make the groups more normally distributed. The normal distribution was checked with Shapiro-Wilks test, and two groups were found to still not be normally distributed after log-transformation. If the groups are of different distribution, the Kruskal-Wallis test and following post-hoc test is instead a test of whether the groups are of the same distribution or not (Helsel and Hirsch, 2002). However, this is often not taken into account, and the Kruskal-Wallis test is widely used as a test to compare group medians. In this study, since values were log-transformed and the variation between and within groups was quite low, it was considered adequate to use the Kruskal-Wallis test as a test of group medians being identical or not.

A reanalysis of DOC, TOC and fluorescence was planned to take place in January 2018, in order to get an idea of the effect of the storage. However, this could not be carried out, since problems arose with the TOC analyser and due to the limited amount of time.

Storage of unfiltered samples at 10 °C has been shown to affect the scores of PARAFAC components (Bieroza and Heathwaite, 2016). Increasing scores of tryptophan-like components could be seen after 1 hour of storage, while 24 hours of storage resulted in a lower increase or even a decrease of the initial scores. Components related to terrestrially derived organic matter were less affected than tryptophan-like components (Bieroza and Heathwaite, 2016). In this

study, samples were stored at a lower temperature, but for a longer time. It is likely that storage has had an impact on the PARAFAC component scores, and that different components have been affected differently. The significance of the effect is however not known.

Kothawala et al (2012), found that degradation of peak C was greater than peak A degradation in an incubation experiment of filtered lake water. The samples were stored for 3.5 years in the dark at 20°C. The fluorescence indices were found not to be significantly altered (Kothawala et al., 2012). Peacock et al (2015) suggested that storage in the dark at 4 °C reduced the degradation rate of DOC remarkably, compared to storage at 20 °C. Additionally, it was shown that aromatic compounds were more resistant to degradation. The DOC decay rate was exponential, with a higher rate of degradation in the beginning of the storage period (Peacock et al., 2015).

In this study, the two components related to peak A fluorescence were found to have the highest PARAFAC score in most of the samples. It is possible that the FDOM pool in the stream mainly consisted of peak A related DOM, but it might also be a result of a larger storage effect on the more bioavailable compounds related to peak C and peak T fluorescence. Tryptophan-like components, being the most bioavailable compounds, might have been consumed shortly after sampling.

5.4.2 Sampling period

The summer of 2017 in Uppsala was dry, with few rain events and low groundwater levels. Towards the end of the sampling period, in October, the rain events increased in numbers and intensity. With the coming of autumn, the temperatures also dropped. During that same time, this project was initiated and the time between sampling and analysis, i.e. the storage time, was therefore shorter than for the samples collected during July-September. The coincidence of the changes in weather conditions and storage time made it difficult to distinguish the driving factor behind changes in variables.

Site 3, 4 and 6 had less observations than the other sites ($n = 7$, $n = 3$, $n = 6$, respectively). At site 3, observations were missing in the middle of the sampling period, while at site 4 and 6 data were missing at the start respectively the end of the sampling period. This meant that the change in weather conditions and storage time was not recorded at site 4 and 6, since samples were collected either before or after the change. At site 3, however, samples were collected both at the beginning and the end of the sampling period. Correlations on a temporal scale could not be computed adequately for site 4, due to the insufficient amount of observations.

5.4.3 CO₂ data

The upper limit of the CO₂ sensor was 10,000 ppm, which initially was thought to be enough. However, this limit was met numerous times during the sampling period and thus the exact CO₂ concentrations could not be measured during some periods. Additionally, problems with the sensor and the battery due to lower temperatures and higher flows towards the end of the sampling period, resulted in the data series for CO₂ being shorter than for the water samples.

5.4.4 Specific discharge

Data of specific discharge was not site specific. Site 7 and 8 were located close to the station Stabby, and site 9 and 10 to the Sävjaån station. Site 1 - 6 were not located near any of the three stations. For these sites, data was used from the Vattholma station, since it was located upstream from the sites. Because of this, it is possible that the specific discharge data is more accurate

for sites 7-10 than sites 1-6. This was not optimal and might, especially, give deceptive results for correlations on a spatial scale. If discharge data would have been available for each specific site, more accurate, and potentially different, results would have been obtained.

5.4.5 Fluorescence and PARAFAC

Although combined fluorescence and PARAFAC analysis is a powerful tool to analyse DOM quality, it is a rather complex and not fully explored area of research. It is not yet possible to determine exact compounds causing a specific fluorescence signal, and hence PARAFAC components can only be related to different types of DOM. The fluorescence signal can also be reduced (i.e. quenched), or shifted to longer or shorter wavelengths, due to physicochemical factors like pH, binding of metals, the degree of degradation of the DOM, and in presence of other light absorbing substances (Coble et al., 2014). For protein-like FDOM, the intensity and location of the fluorescence signal in the EEM is also affected of whether the compound appears as a free amino acid or is bound in protein-structure (Coble et al., 2014).

Apart from the 5-component PARAFAC model that was chosen and considered to best describe the fluorescence data, a 7-component model was found as well, whose components all aligned with commonly reported fluorescence peaks. The 7-component model was however not split-half validated, and thus could not be said to be stable. With more water samples as input data to the PARAFAC analysis, it is possible that the 7-component model could have been validated and considered the best model.

6 CONCLUSIONS

The results indicated that the variables affecting the DOM quality and/or quantity were the fraction of arable land in the catchment and the magnitude and flow paths of the runoff. The fraction of arable land in the catchment could not be found to affect the DOM quantity, but was found to be positively correlated with FI. This suggested that a higher fraction of arable land in the catchment is related to a higher amount of DOM of microbial or algal origin. Contradictory to what was hypothesized, no overall consistent pattern could be found in the correlations between nutrient concentration and the DOM quality parameters, nor between nutrient concentration and DOM quantity. The results instead indicated that discharge magnitude and runoff flow paths might have affected both DOM quality and quantity, as well as the nutrient concentrations. Further studies are needed to get a better understanding of the impact of each of these variables, as well as the effect of the interplay between the variables, on the DOM quality and quantity.

The scarce set of pCO₂ data made analysis of correlations between pCO₂ and DOM quality and quantity difficult, and brought uncertainties to the results. No spatial correlation could be found between pCO₂ and DOM quality, nor between pCO₂ and DOM quantity, in the streams. Temporal correlations could be studied at two sites, at which no correlation between DOM quantity and pCO₂ could be found at either of the sites. However, two PARAFAC components associated with terrestrial and highly decomposed FDOM were found to correlate with pCO₂ at one site.

REFERENCES

- Baker, A., Inverarity, R., Charlton, M., Richmond, S., 2003. Detecting river pollution using fluorescence spectrophotometry: case studies from the Ouseburn, NE England. *Environ. Pollut.* 124, 57–70. [https://doi.org/10.1016/S0269-7491\(02\)00408-6](https://doi.org/10.1016/S0269-7491(02)00408-6)
- Baker, A., Tipping, E., Thacker, S.A., Gondar, D., 2008. Relating dissolved organic matter fluorescence and functional properties. *Chemosphere* 73, 1765–1772. <https://doi.org/10.1016/j.chemosphere.2008.09.018>
- Battin, T.J., Luysaert, S., Kaplan, L.A., Aufdenkampe, A.K., Richter, A., Tranvik, L.J., 2009. The boundless carbon cycle. *Nat. Geosci.* 2, 598–600. <https://doi.org/10.1038/ngeo618>
- Bieroza, M.Z., Heathwaite, A.L., 2016. Unravelling organic matter and nutrient biogeochemistry in groundwater-fed rivers under baseflow conditions: Uncertainty in in situ high-frequency analysis. *Sci. Total Environ.* 572, 1520–1533. <https://doi.org/10.1016/j.scitotenv.2016.02.046>
- Bodmer, P., Heinz, M., Pusch, M., Singer, G., Premke, K., 2016. Carbon dynamics and their link to dissolved organic matter quality across contrasting stream ecosystems. *Sci. Total Environ.* 553, 574–586. <https://doi.org/10.1016/j.scitotenv.2016.02.095>
- Catalán, N., Kellerman, A.M., Peter, H., Carmona, F., Tranvik, L.J., 2015. Absence of a priming effect on dissolved organic carbon degradation in lake water: Absence of priming in lake water. *Limnol. Oceanogr.* 60, 159–168. <https://doi.org/10.1002/lno.10016>
- Coble, P., Lead, J., Baker, A., Reynolds, D., Spencer, R.G.M., (2014). *Aquatic Organic Matter Fluorescence*, Cambridge University Press.
- Cole, J.J., Prairie, Y.T., Caraco, N.F., McDowell, W.H., Tranvik, L.J., Striegl, R.G., Duarte, C.M., Kortelainen, P., Downing, J.A., Middelburg, J.J., Melack, J., 2007. Plumbing the Global Carbon Cycle: Integrating Inland Waters into the Terrestrial Carbon Budget. *Ecosystems* 10, 171–184.
- D’Amario, S.C., Xenopoulos, M.A., 2015. Linking dissolved carbon dioxide to dissolved organic matter quality in streams. *Biogeochemistry* 126, 99–114. <https://doi.org/10.1007/s10533-015-0143-y>
- Duarte, C.M., Prairie, Y.T., 2005. Prevalence of Heterotrophy and Atmospheric CO₂ Emissions from Aquatic Ecosystems. *Ecosystems* 8, 862–870. <https://doi.org/10.1007/s10021-005-0177-4>
- Eckard, R.S., Pellerin, B.A., Bergamaschi, B.A., Bachand, P.A.M., Bachand, S.M., Spencer, R.G.M., Hernes, P.J., 2017. Dissolved Organic Matter Compositional Change and Biolability During Two Storm Runoff Events in a Small Agricultural Watershed: DOM Change Following Agricultural Storms. *J. Geophys. Res. Biogeosciences* 122, 2634–2650. <https://doi.org/10.1002/2017JG003935>
- Eriksson, J., Dahlin, S., Nilsson, I., Simonsson, M. (2011). *Marklära*. Lund: Studentlitteratur AB.
- Fellman, J.B., Hood, E., Spencer, R.G.M., 2010. Fluorescence spectroscopy opens new windows into dissolved organic matter dynamics in freshwater ecosystems: A review. *Limnol. Oceanogr.* 55, 2452–2462. <https://doi.org/10.4319/lo.2010.55.6.2452>
- Gabor, R.S., Eilers, K., McKnight, D.M., Fierer, N., Anderson, S.P., 2014. From the litter layer to the saprolite: Chemical changes in water-soluble soil organic matter and their correlation to microbial community composition. *Soil Biol. Biochem.* 68, 166–176. <https://doi.org/10.1016/j.soilbio.2013.09.029>
- Giraudox, P. (2017). *Package 'pgirmess'*. Available: <https://cran.r-project.org/web/packages/pgirmess/pgirmess.pdf> Read: 2018-03-07

- Graeber, D., Boëchat, I.G., Encina-Montoya, F., Esse, C., Gelbrecht, J., Goyenola, G., Gücker, B., Heinz, M., Kronvang, B., Meerhoff, M., Nimptsch, J., Pusch, M.T., Silva, R.C.S., von Schiller, D., Zwirnmann, E., 2015. Global effects of agriculture on fluvial dissolved organic matter. *Sci. Rep.* 5. <https://doi.org/10.1038/srep16328>
- Guenet, B., Danger, M., Abbadie, L., Lacroix, G., 2010. Priming effect: bridging the gap between terrestrial and aquatic ecology. *Ecology* 91, 2850–2861. <https://doi.org/10.1890/09-1968.1>
- Hansen, A.M., Kraus, T.E.C., Pellerin, B.A., Fleck, J.A., Downing, B.D., Bergamaschi, B.A., 2016. Optical properties of dissolved organic matter (DOM): Effects of biological and photolytic degradation: DOM optical properties following degradation. *Limnol. Oceanogr.* 61, 1015–1032. <https://doi.org/10.1002/lno.10270>
- Helsel, D.R., Hirsch, R.M., 2002. *Statistical Methods in Water Resources* 524.
- Hotchkiss, E.R., Hall Jr, R.O., Sponseller, R.A., Butman, D., Klaminder, J., Laudon, H., Rosvall, M., Karlsson, J., 2015. Sources of and processes controlling CO₂ emissions change with the size of streams and rivers. *Nat. Geosci.* 8, 696–699. <https://doi.org/10.1038/ngeo2507>
- Hudson, N., Baker, A., Reynolds, D., 2007. Fluorescence analysis of dissolved organic matter in natural, waste and polluted waters—a review. *River Res. Appl.* 23, 631–649. <https://doi.org/10.1002/rra.1005>
- Kaiser, K., Kalbitz, K., 2012. Cycling downwards – dissolved organic matter in soils. *Soil Biol. Biochem.* 52, 29–32. <https://doi.org/10.1016/j.soilbio.2012.04.002>
- Karlsson, J., Byström, P., Ask, J., Ask, P., Persson, L., Jansson, M., 2009. Light limitation of nutrient-poor lake ecosystems. *Nature* 460, 506–509. <https://doi.org/10.1038/nature08179>
- Klaminder, J., Grip, H., Mörth, C.-M., Laudon, H., 2011. Carbon mineralization and pyrite oxidation in groundwater: Importance for silicate weathering in boreal forest soils and stream base-flow chemistry. *Appl. Geochem.* 26, 319–325. <https://doi.org/10.1016/j.apgeochem.2010.12.005>
- Kothawala, D.N., von Wachenfeldt, E., Koehler, B., Tranvik, L.J., 2012. Selective loss and preservation of lake water dissolved organic matter fluorescence during long-term dark incubations. *Sci. Total Environ.* 433, 238–246. <https://doi.org/10.1016/j.scitotenv.2012.06.029>
- Lehmann, J., Kleber, M., 2015. The contentious nature of soil organic matter. *Nature.* <https://doi.org/10.1038/nature16069>
- Naiman, R.J., Bilby, R.E., 1998. *River ecology and management : lessons from the Pacific coastal ecoregion*. New York: Springer.
- Niederer, C., Schwarzenbach, R.P., Goss, K.-U., 2007. Elucidating Differences in the Sorption Properties of 10 Humic and Fulvic Acids for Polar and Nonpolar Organic Chemicals. *Environ. Sci. Technol.* 41, 6711–6717. <https://doi.org/10.1021/es0709932>
- Ohno, T., 2002. Fluorescence Inner-Filtering Correction for Determining the Humification Index of Dissolved Organic Matter. *Environ. Sci. Technol.* 36, 742–746. <https://doi.org/10.1021/es0155276>
- Osterman, M. (2018). *Carbon dioxide in agricultural streams – magnitude and patterns of an understudied atmospheric carbon source*. Uppsala University.
- Pan, B., Ning, P., Xing, B., 2008. Part V - Sorption of pharmaceuticals and personal care products. <https://doi.org/10.1007/s11356-008-0052-x>
- Peacock, M., Freeman, C., Gauci, V., Lebron, I., Evans, C.D., 2015. Investigations of freezing and cold storage for the analysis of peatland dissolved organic carbon (DOC) and

- absorbance properties. *Environ. Sci. Process. Impacts* 17, 1290–1301. <https://doi.org/10.1039/C5EM00126A>
- Ritson, J.P., Brazier, R.E., Graham, N.J.D., Freeman, C., Templeton, M.R., Clark, J.M., 2017. The effect of drought on dissolved organic carbon (DOC) release from peatland soil and vegetation sources. *Biogeosciences* 14, 2891–2902. <https://doi.org/10.5194/bg-14-2891-2017>
- Siegel and Castellán. (1988). *Non parametric statistics for the behavioural sciences*. MacGraw Hill Int., New York. pp 213-214. Available: <http://giraudoux.pagesperso-orange.fr/SiegelCastellan1988.pdf> Read: 2018-03-07
- SMHI (2018). *Vattenwebb Mätningar*. Available: <http://vattenwebb.smhi.se/station/>
- Stedmon, C.A., Markager, S., Bro, R., 2003. Tracing dissolved organic matter in aquatic environments using a new approach to fluorescence spectroscopy. *Mar. Chem.* 82, 239–254. [https://doi.org/10.1016/S0304-4203\(03\)00072-0](https://doi.org/10.1016/S0304-4203(03)00072-0)
- Stedmon, C. A. & Bro, R. (2008). Characterizing dissolved organic matter fluorescence with parallel factor analysis: a tutorial, *Limnology and Oceanography, Methods* 6
- Stubbins, A., Lapierre, J.-F., Berggren, M., Prairie, Y.T., Dittmar, T., del Giorgio, P.A., 2014. What's in an EEM? Molecular Signatures Associated with Dissolved Organic Fluorescence in Boreal Canada. *Environ. Sci. Technol.* 48, 10598–10606. <https://doi.org/10.1021/es502086e>
- Thacker, S.A., Tipping, E., Baker, A., Gondar, D., 2005. Development and application of functional assays for freshwater dissolved organic matter. *Water Res.* 39, 4559–4573. <https://doi.org/10.1016/j.watres.2005.08.020>
- Tranvik, L.J., Downing, J.A., Cotner, J.B., Loiselle, S.A., Striegl, R.G., Ballatore, T.J., Dillon, P., Finlay, K., Fortino, K., Knoll, L.B., Kortelainen, P.L., Kutser, T., Larsen, S., Laurion, I., Leech, D.M., McCallister, S.L., McKnight, D.M., Melack, J.M., Overholt, E., Porter, J.A., Prairie, Y., Renwick, W.H., Roland, F., Sherman, B.S., Schindler, D.W., Sobek, S., Tremblay, A., Vanni, M.J., Verschoor, A.M., von Wachenfeldt, E., Weyhenmeyer, G.A., 2009. Lakes and reservoirs as regulators of carbon cycling and climate. *Limnol. Oceanogr.* 54, 2298–2314. https://doi.org/10.4319/lo.2009.54.6_part_2.2298
- Wilson, H.F., Xenopoulos, M.A., 2009. Effects of agricultural land use on the composition of fluvial dissolved organic matter. *Nat. Geosci.* 2, 37–41. <https://doi.org/10.1038/ngeo391>
- Winterdahl, M., Erlandsson, M., Futter, M.N., Weyhenmeyer, G.A., Bishop, K., 2014. Intra-annual variability of organic carbon concentrations in running waters: Drivers along a climatic gradient. *Glob. Biogeochem. Cycles* 28, 451–464. <https://doi.org/10.1002/2013GB004770>
- Winterdahl, M., Wallin, M.B., Karlsen, R.H., Laudon, H., Öquist, M., Lyon, S.W., 2016. Decoupling of carbon dioxide and dissolved organic carbon in boreal headwater streams. *J. Geophys. Res. Biogeosciences* 121, 2630–2651. <https://doi.org/10.1002/2016JG003420>

APPENDIX A: TIME SERIES AND BOXPLOTS

A.1 DOC TIME SERIES

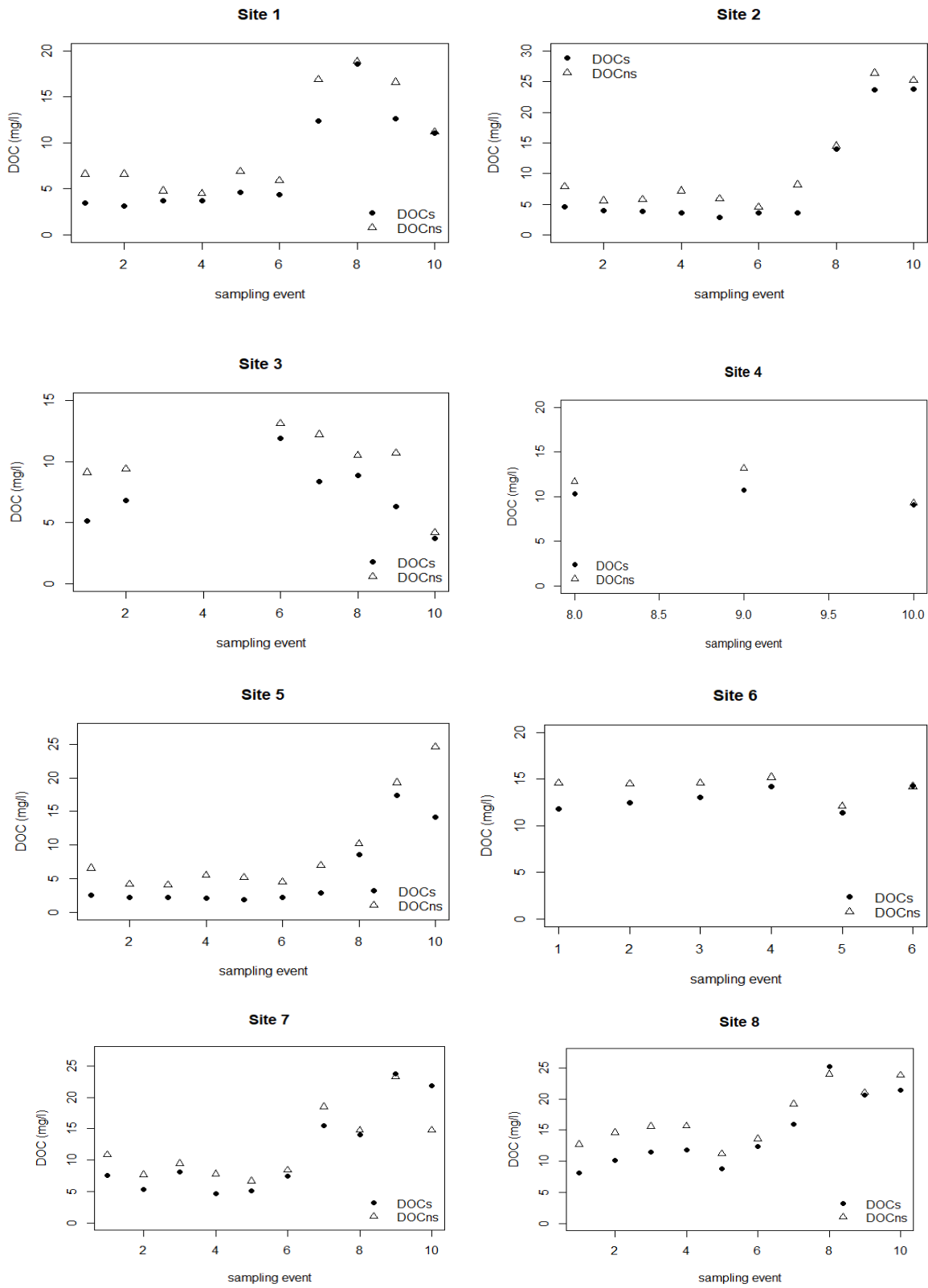


Figure A1. DOC_s and DOC_{ns} concentrations for site 1-8 at sampling event 1-10.

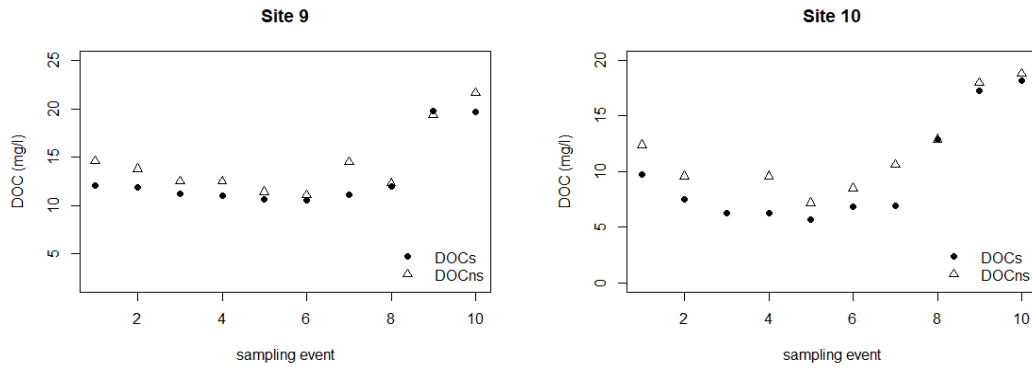


Figure A2. DOC_s and DOC_{ns} concentrations at site 9 and 10 at sampling event 1-10.

A.2 NUTRIENTS

A.2.1 Boxplots

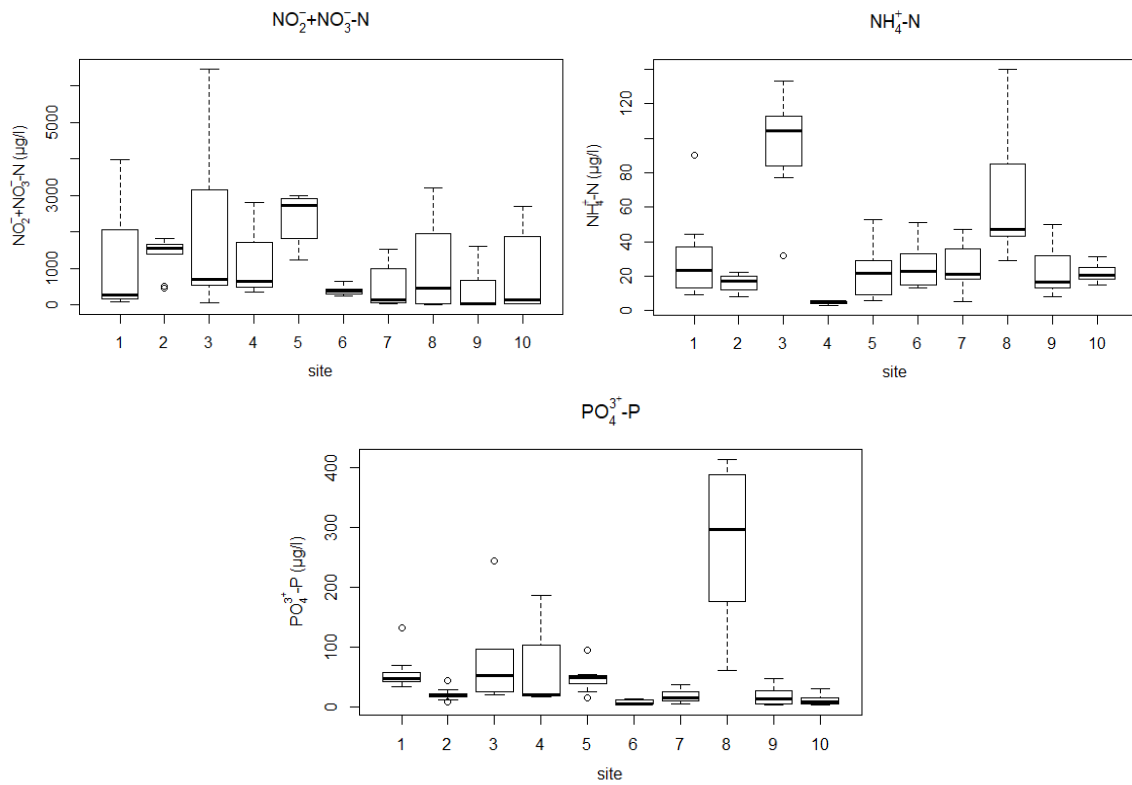


Figure A3. Boxplots of nutrient concentrations at the ten sites.

A.2.2 $\text{NH}_4^+\text{-N}$ time series

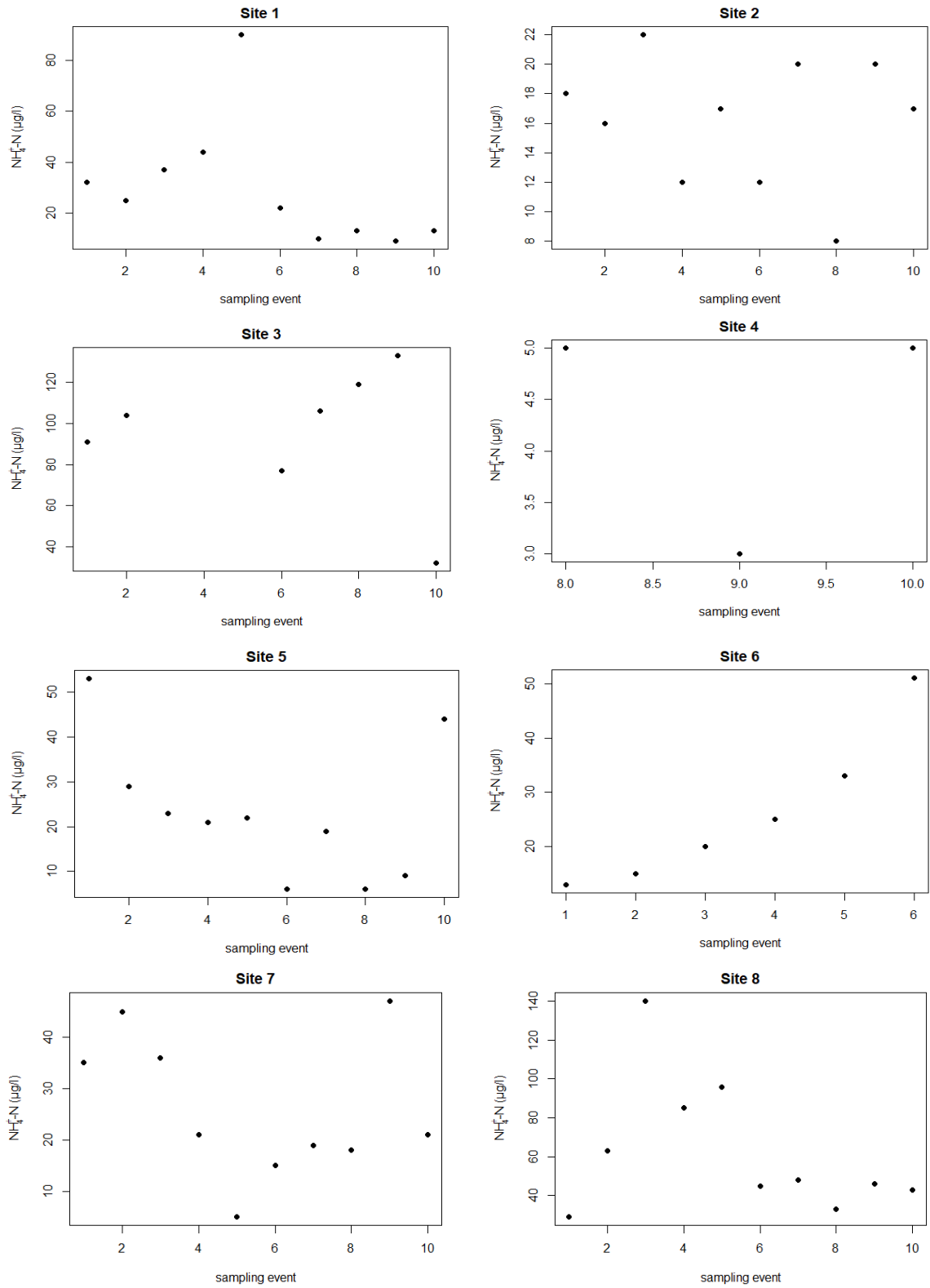


Figure A 4. $\text{NH}_4^+\text{-N}$ concentrations at site 1-8 over time.

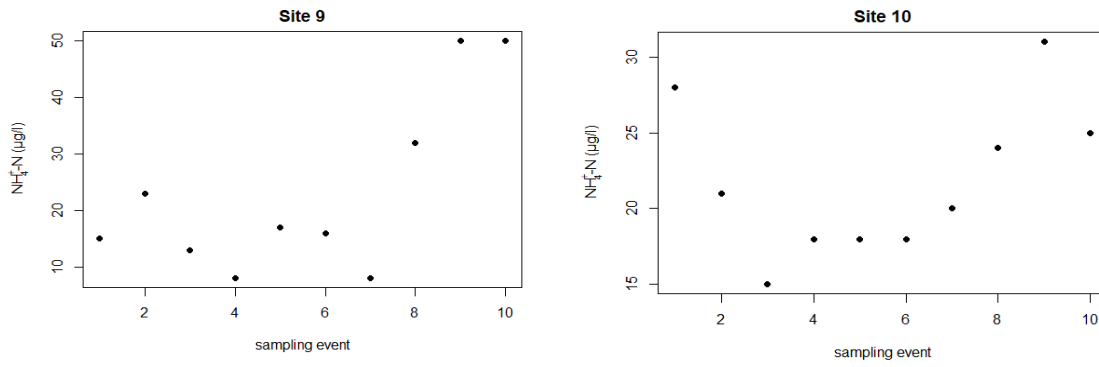


Figure A5. $\text{NH}_4^+\text{-N}$ concentrations at site 9 and 10 over time.

A.2.3 $\text{NO}_2^- + \text{NO}_3^- \text{-N}$ time series

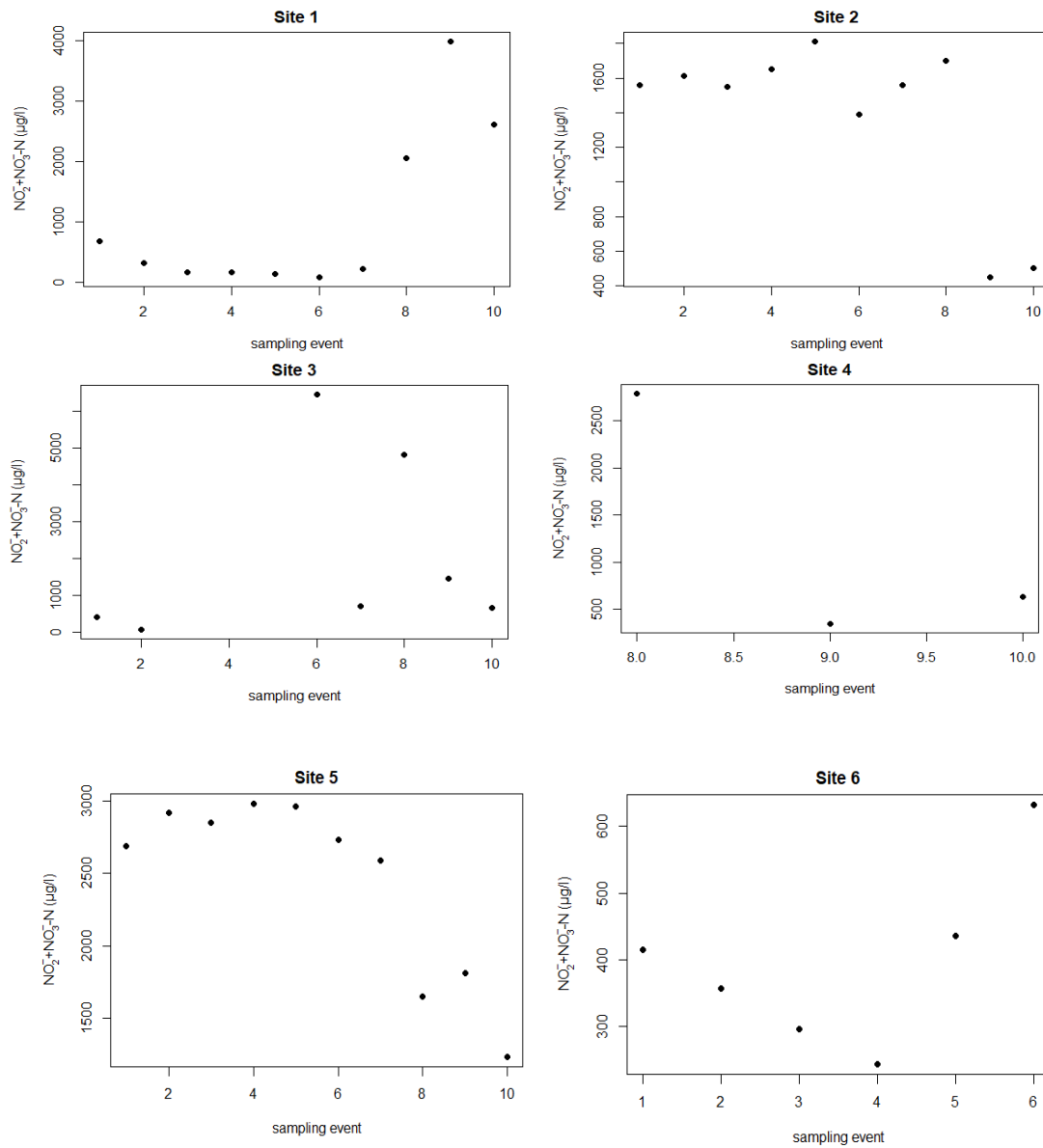


Figure A6. $\text{NO}_2^- + \text{NO}_3^- \text{-N}$ concentrations at site 1-6 over time.

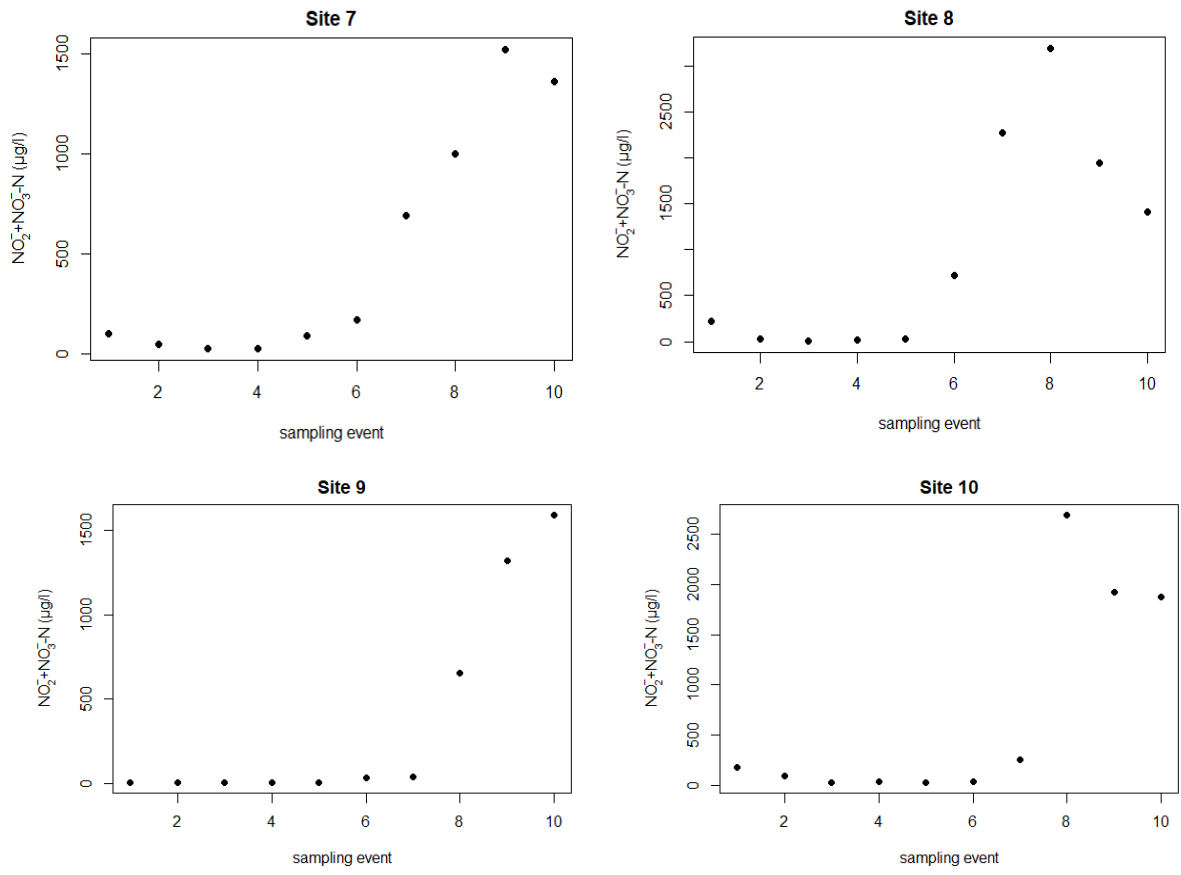


Figure A 7. $\text{NO}_2^- + \text{NO}_3^- \text{N}$ concentrations at site 7-10 over time.

A.2.4 PO₄³⁻-P time series

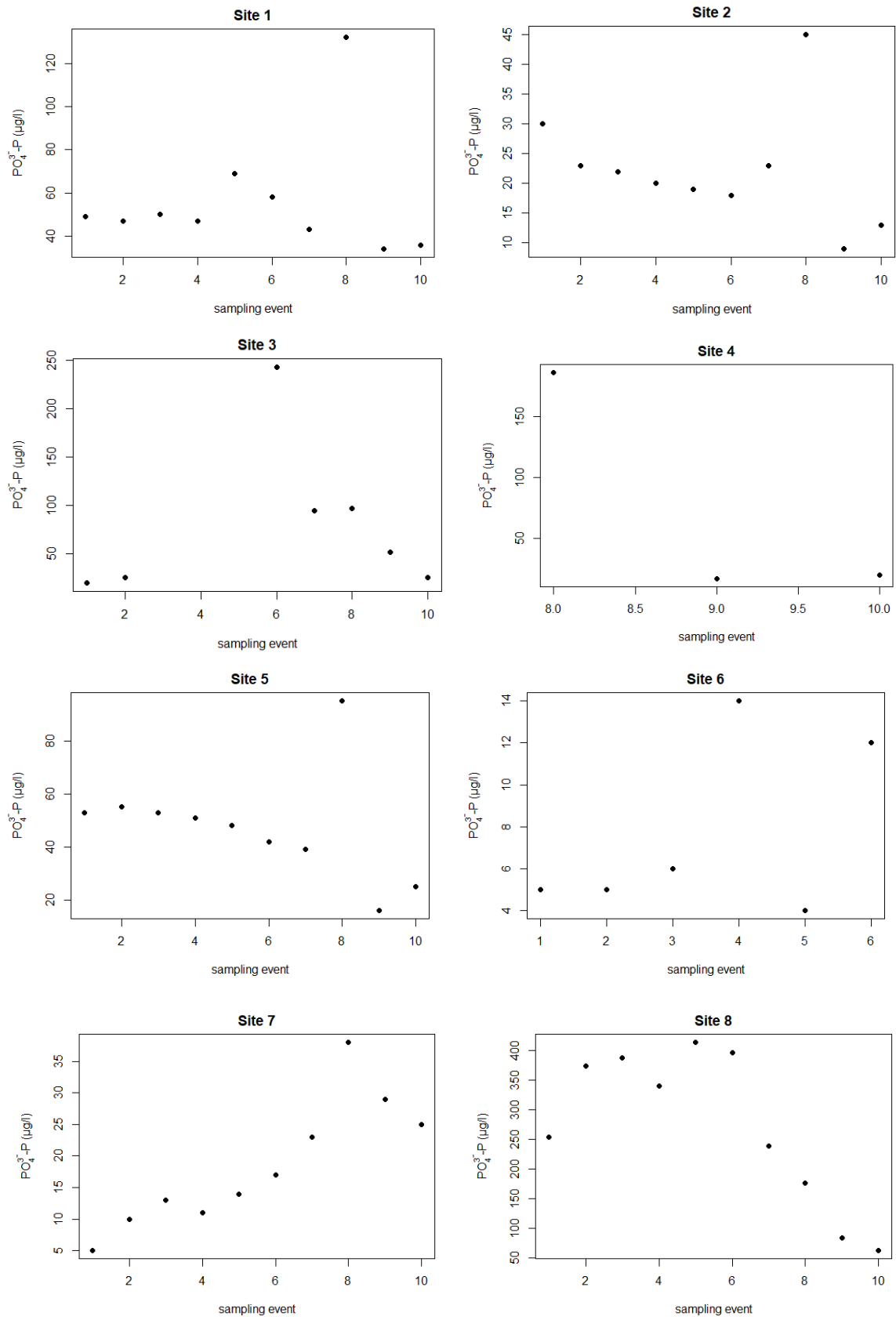


Figure A8. PO₄³⁻-P concentrations at site 1-8 over time.

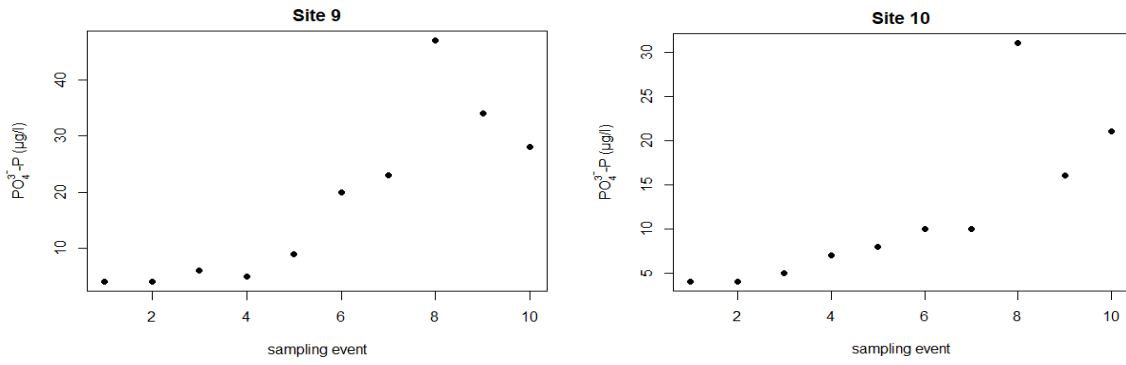


Figure A9. $PO_4^{3-}\text{-P}$ concentrations at site 9 and 10 over time.

A.3 FLUORESCENCE INDICES

A.3.1 FI time series

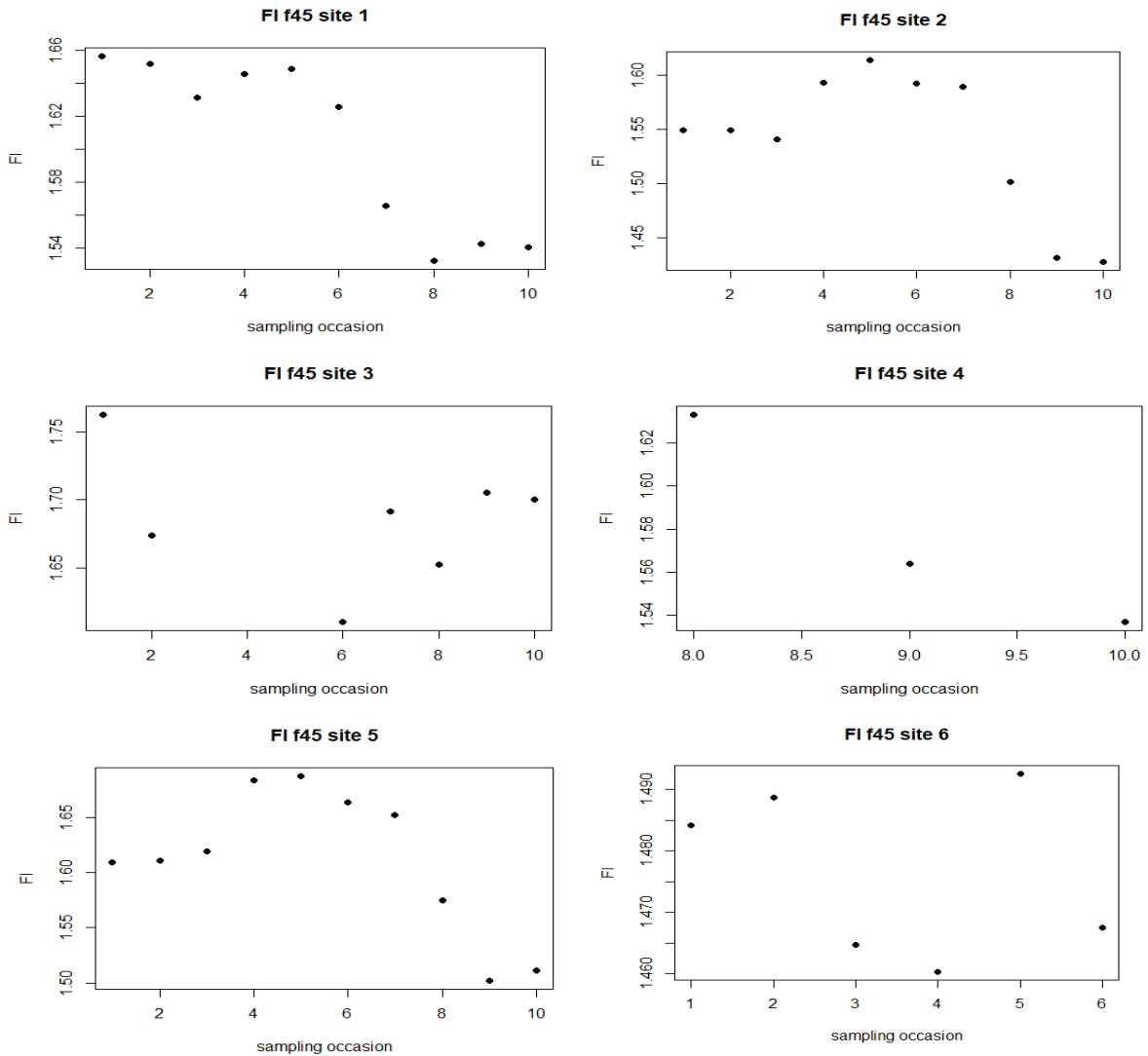


Figure A10. FI at site 1-6 over time.

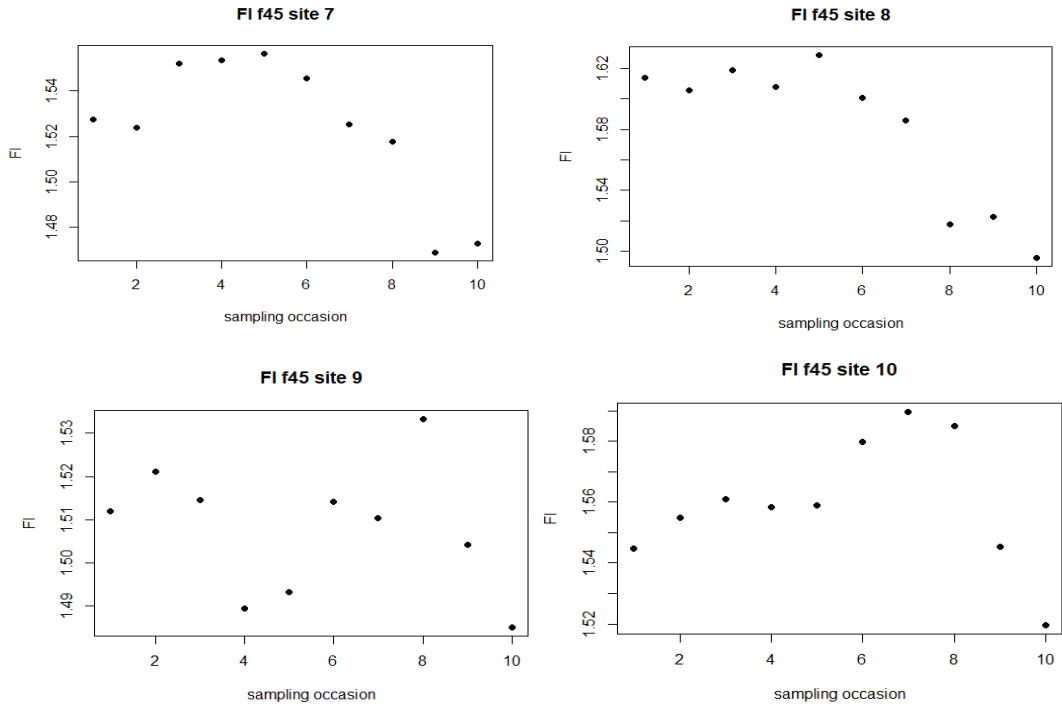


Figure A11. FI at site 7-10 over time.

A.3.2 β/α time series

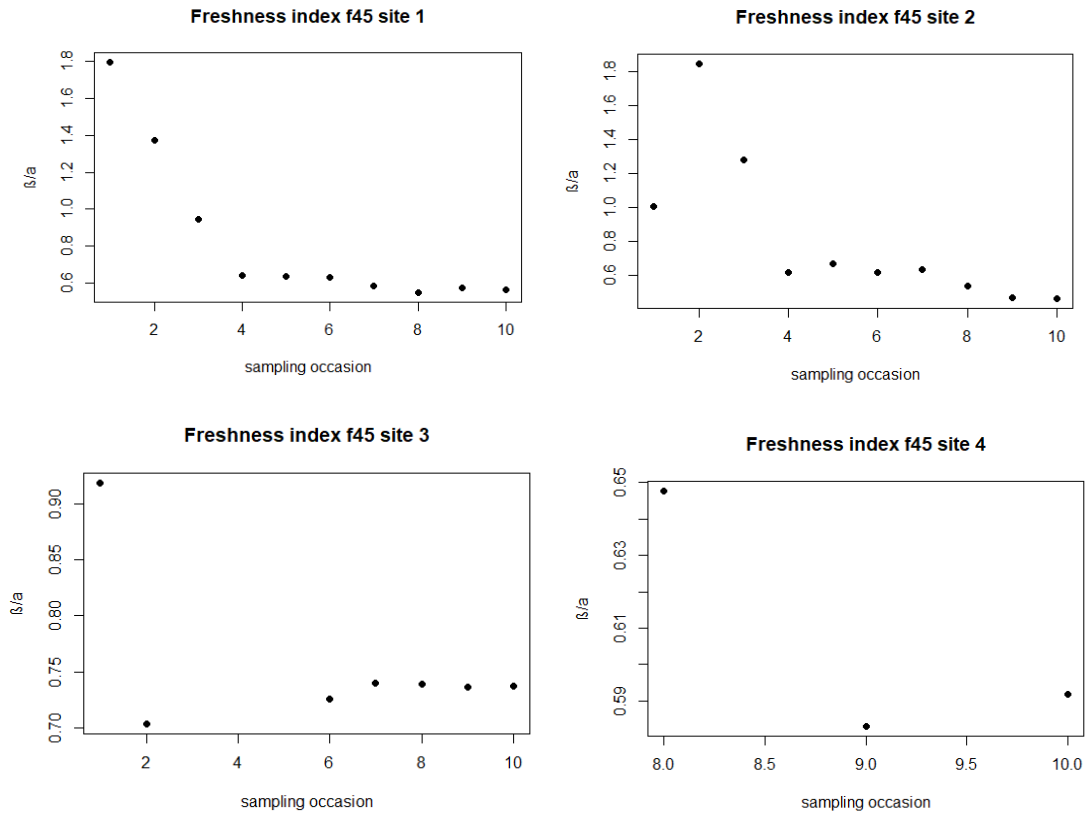


Figure A12. Freshness index at site 1-4 over time.

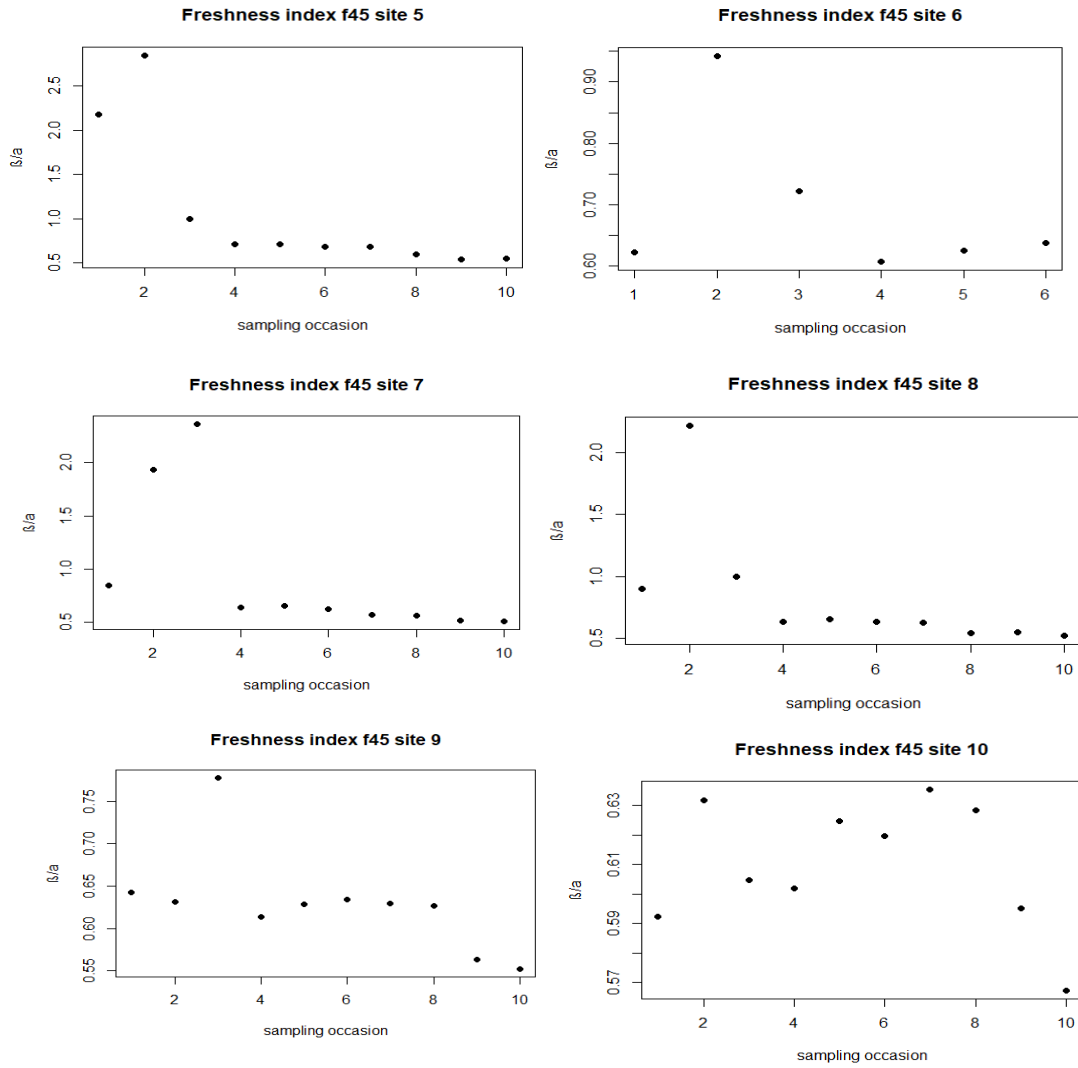


Figure A13. Freshness index and site 5-10 over time.

A.3.3 HIX time series

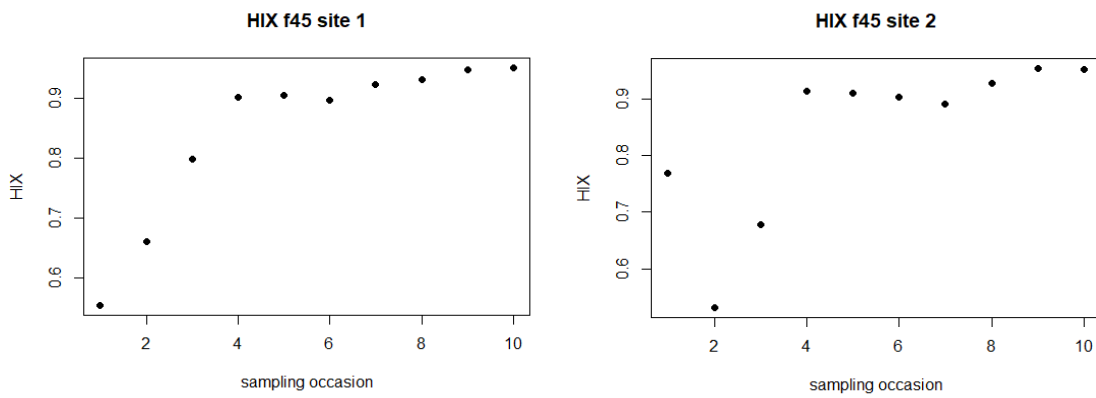


Figure A14. HIX at site 1 and 2 over time.

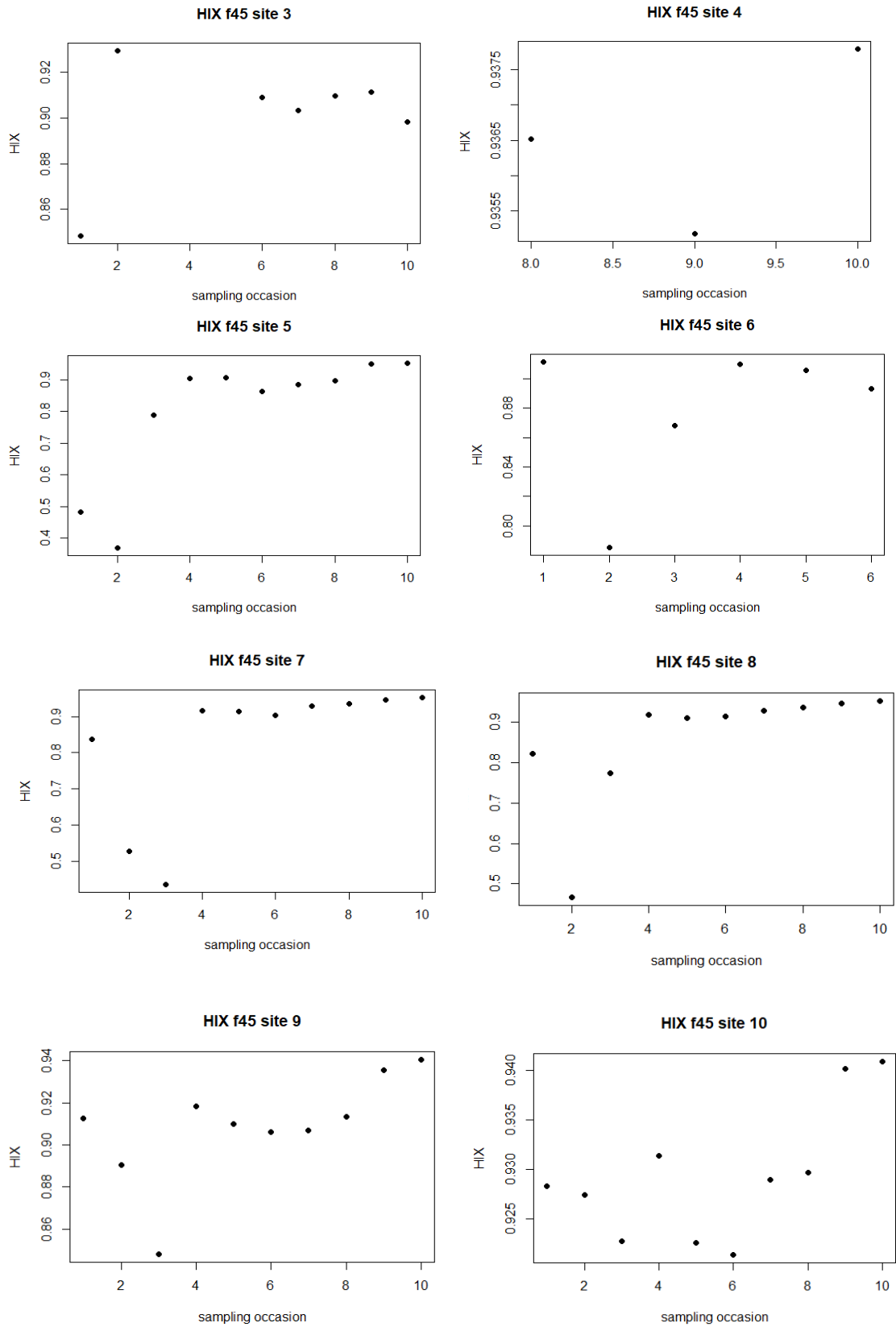


Figure A15. HIX at site 3-10 over time.

A.4 PARAFAC COMPONENTS

A.4.1 C1 time series

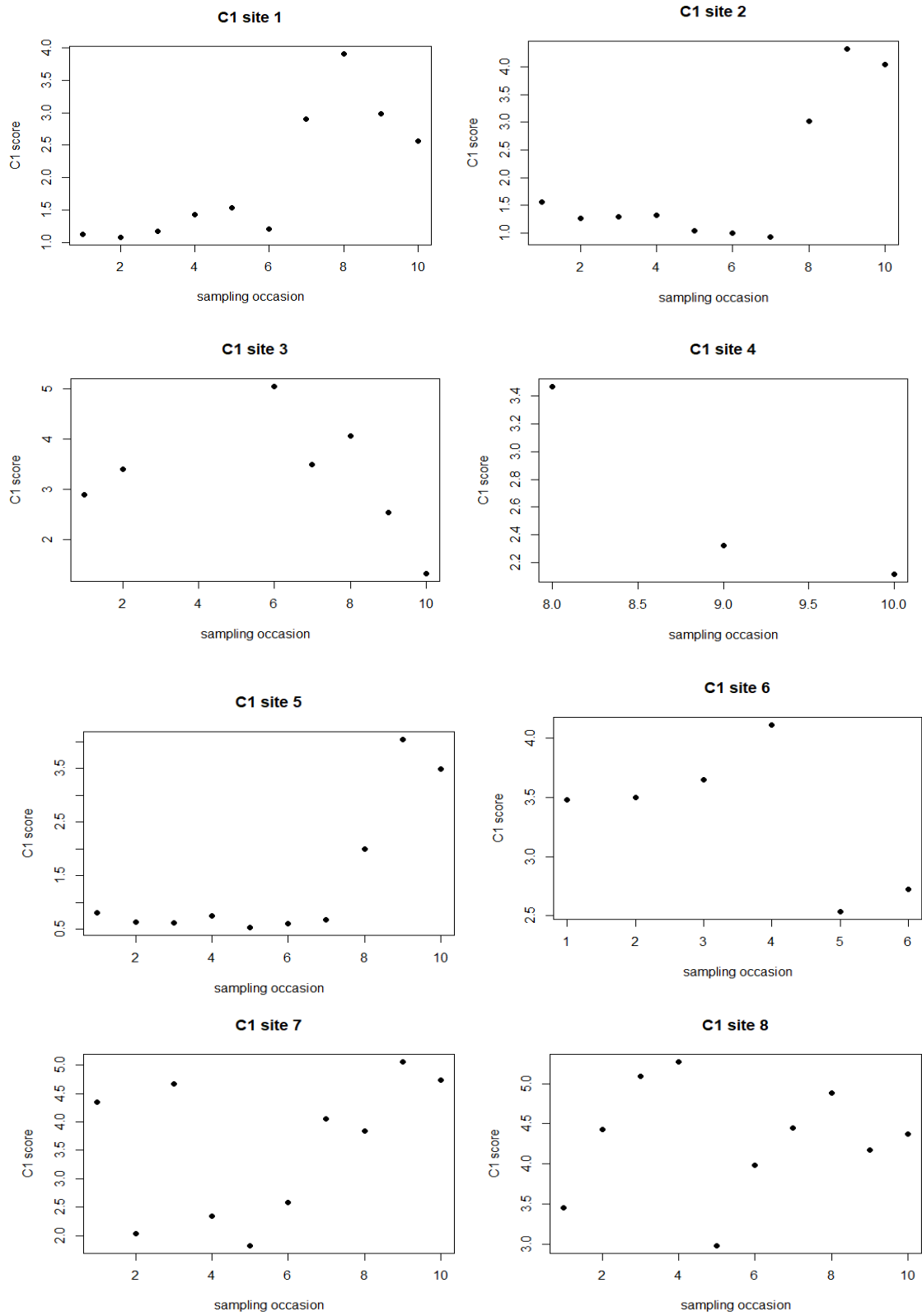


Figure A16. C1 score at site 1-8 over time.

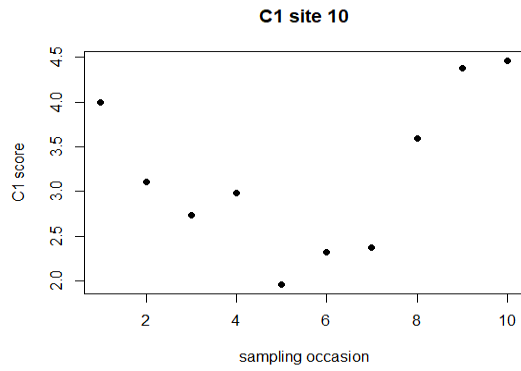
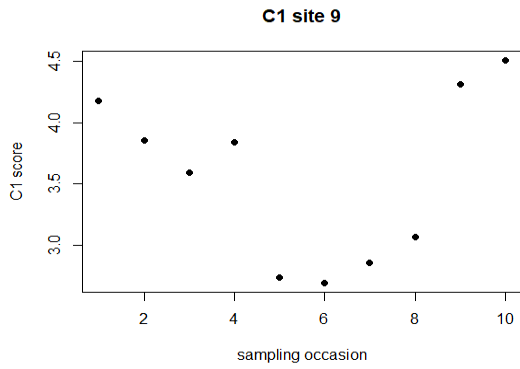


Figure A17. C1 score at site 9 and 10 over time.

A.4.2 C2 time series

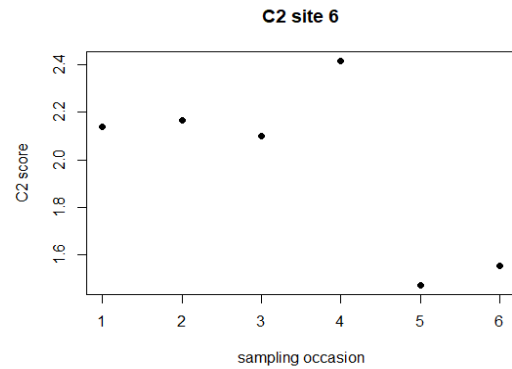
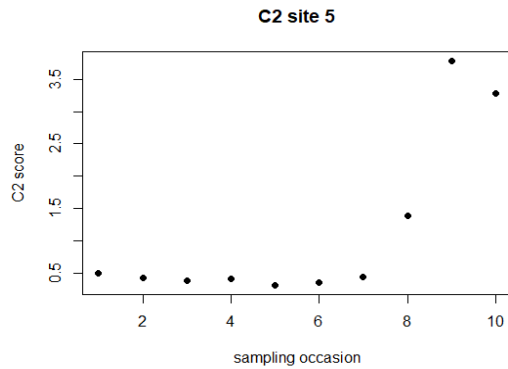
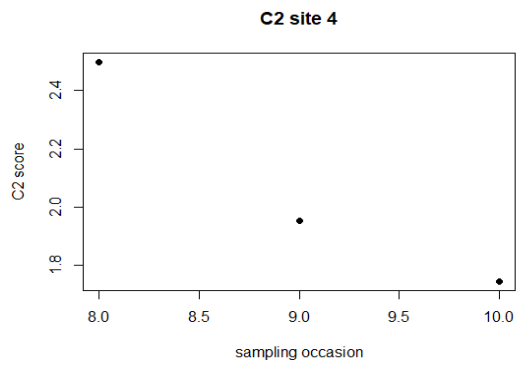
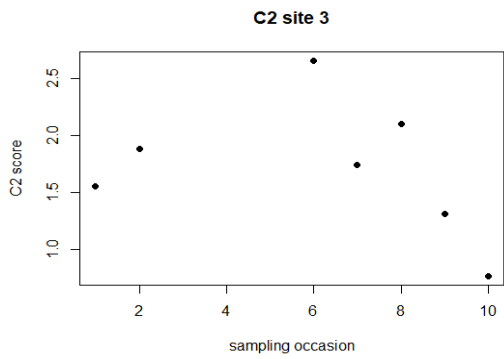
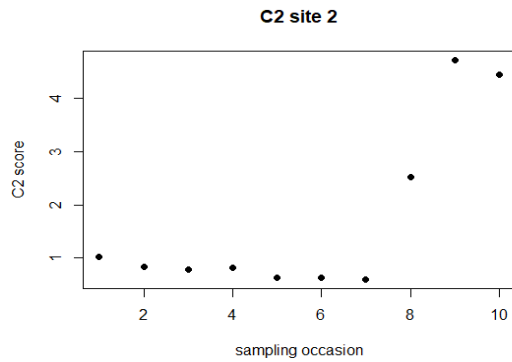
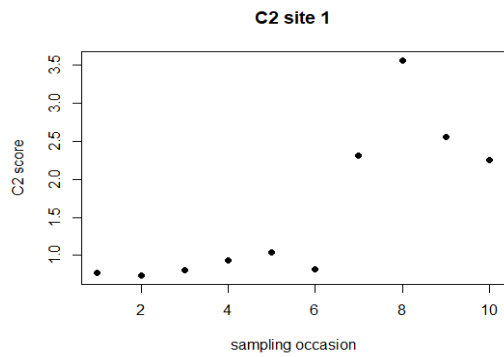


Figure A18. C2 score at site 1-6 over time.

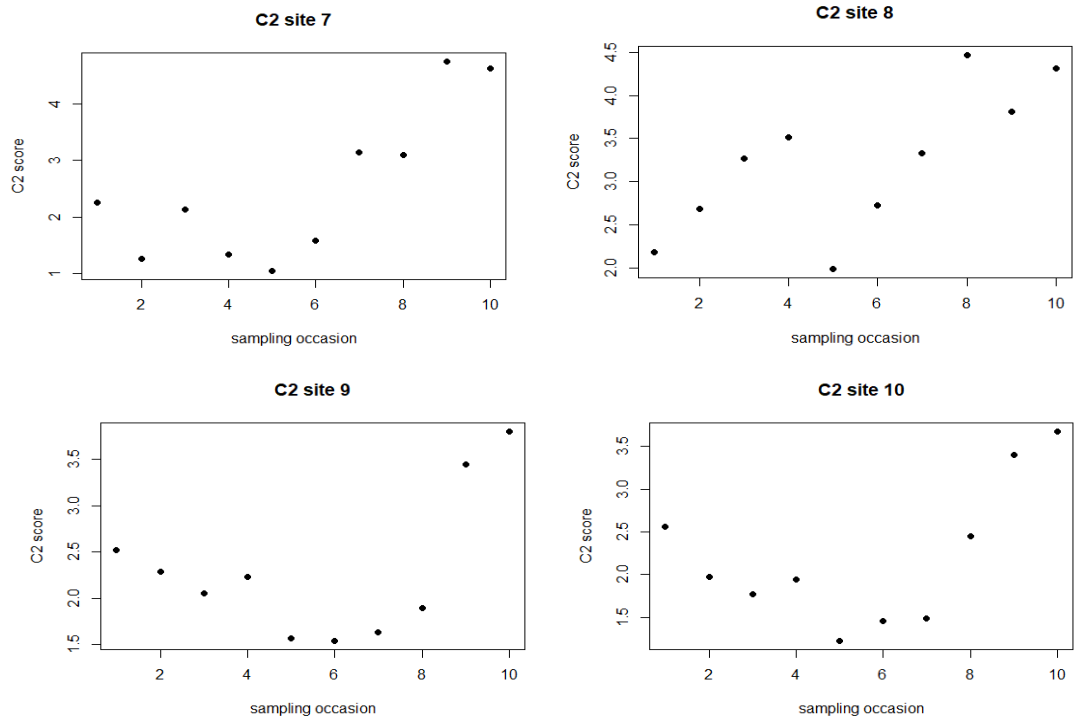


Figure A19. C2 score at site 7-10 over time.

A.4.3 C3 time series

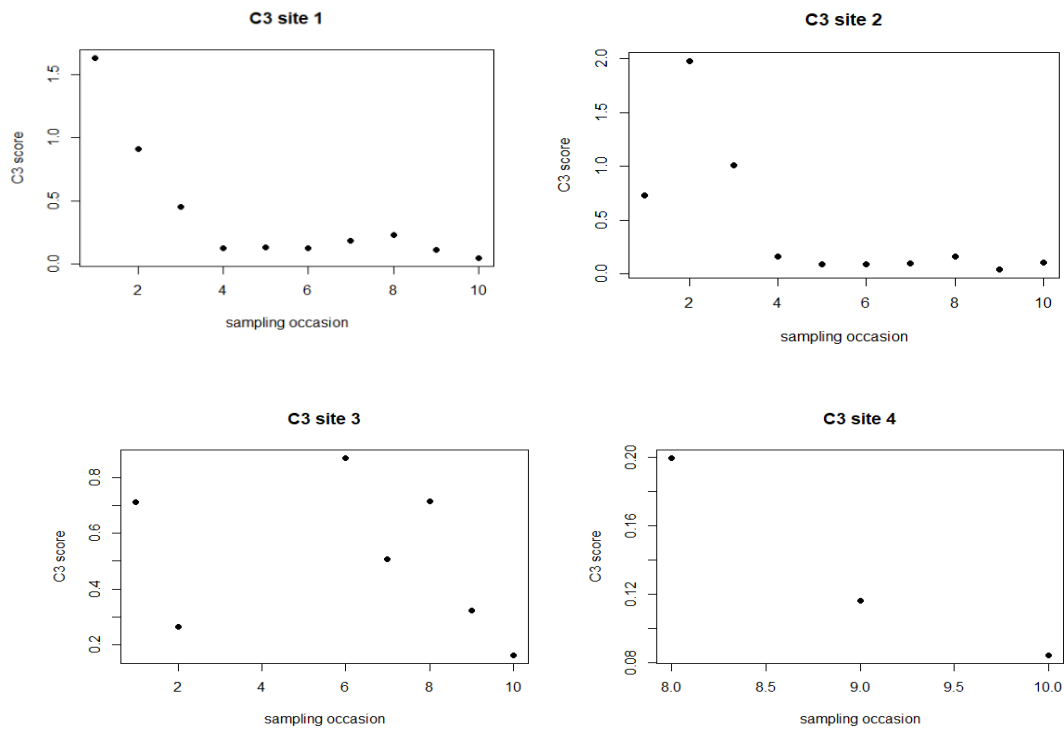


Figure A20. C3 score at site 1-4 over time.

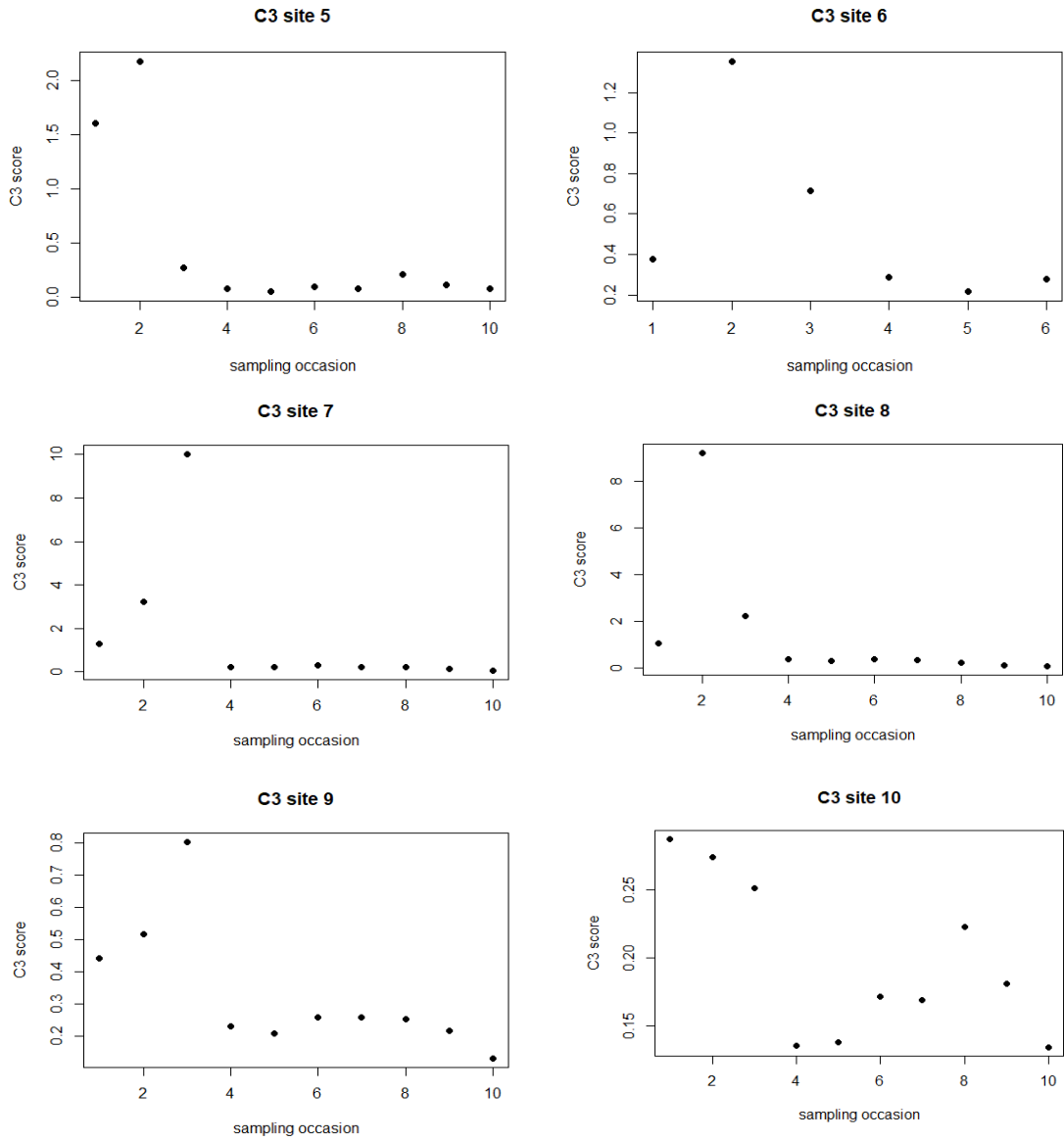


Figure A21. C3 score at site 5-10 over time.

A.4.4 C4 time series

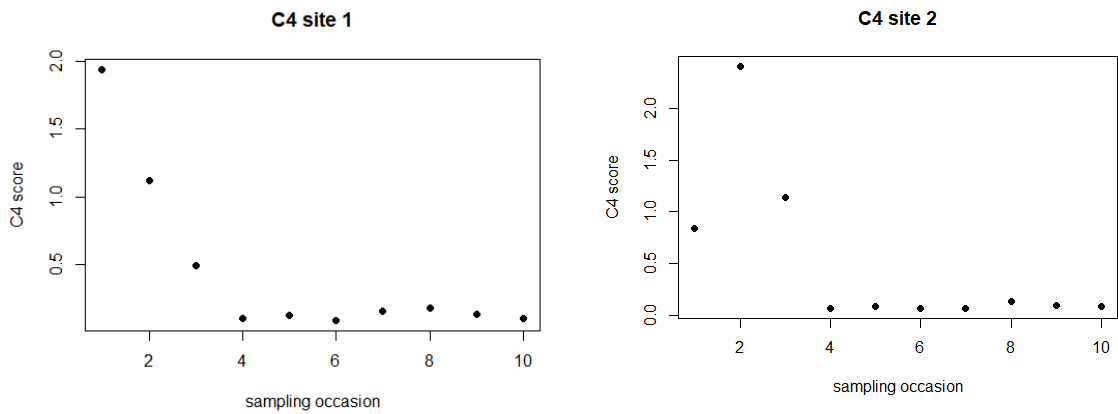


Figure A22. C4 score at site 1 and 2 over time.

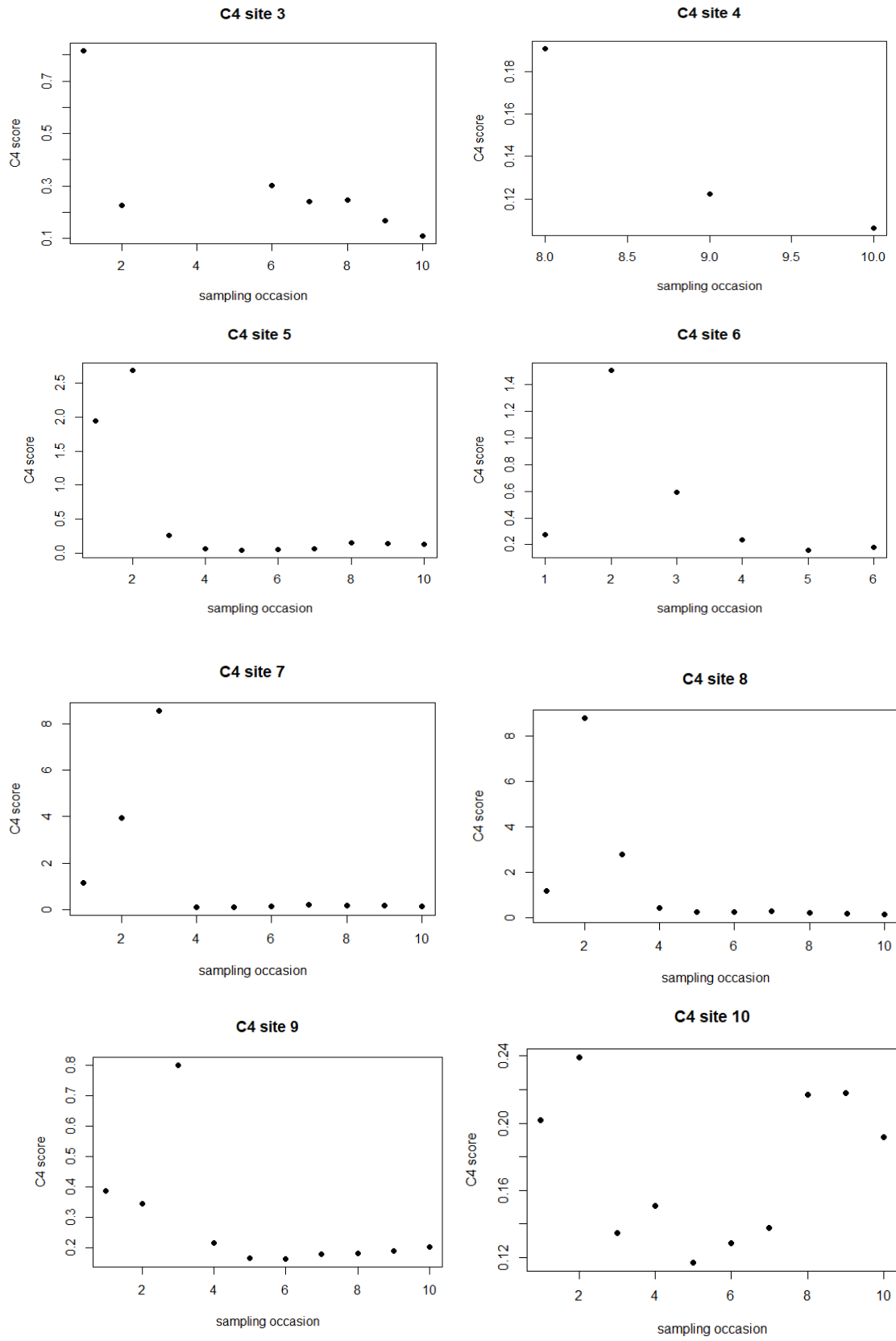


Figure A23. C4 score at site 3-10 over time.

A.4.5 C5 time series

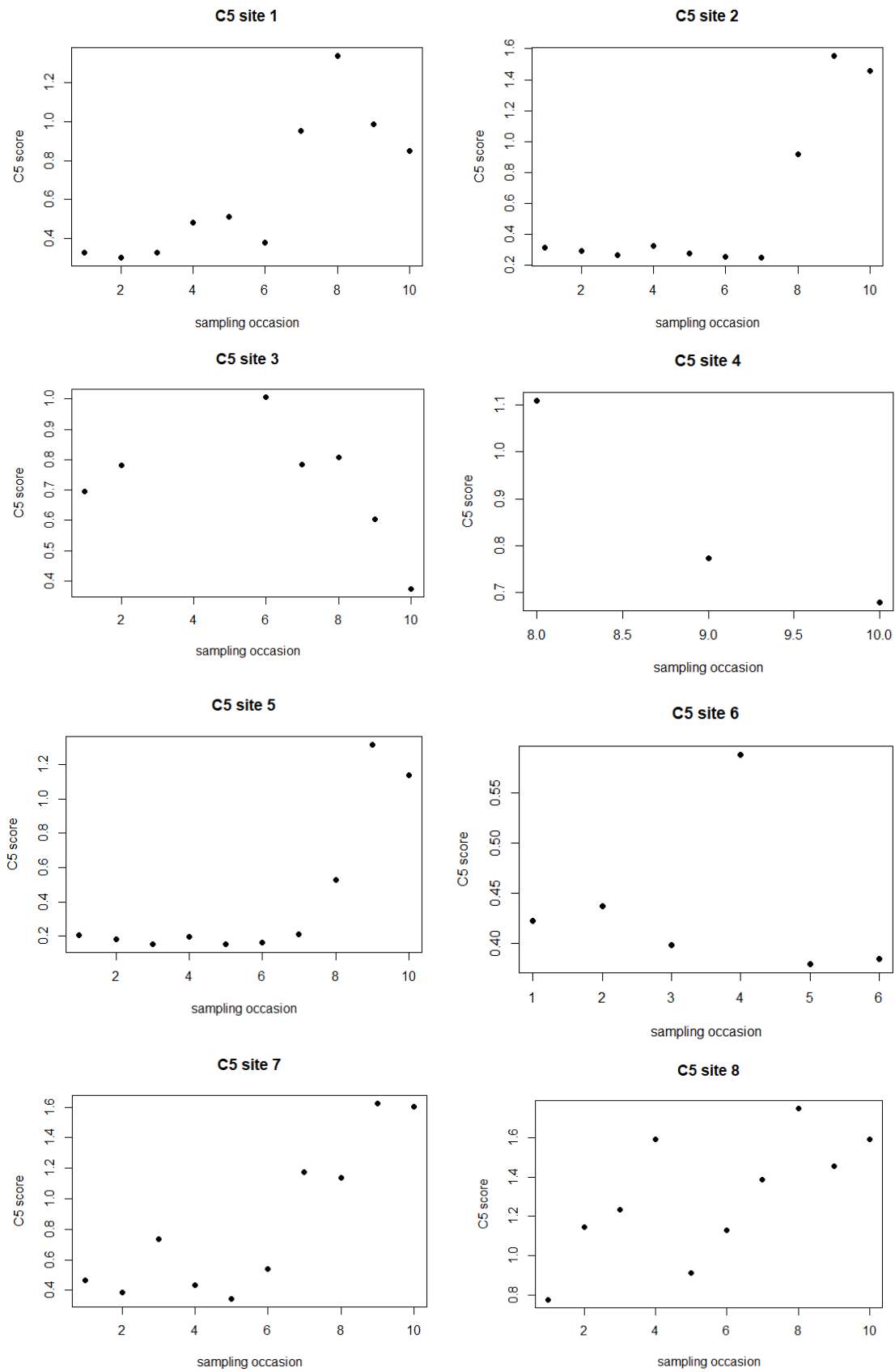


Figure A24. C5 score at site 1-8 over time.

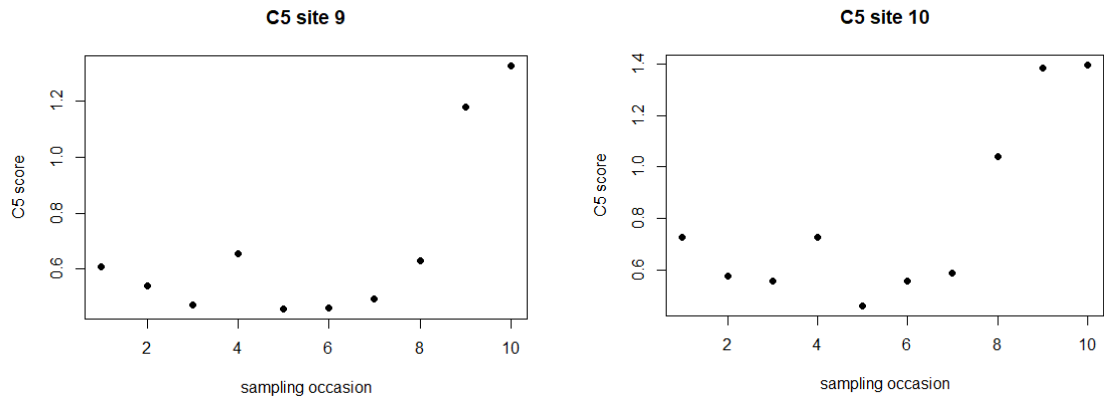


Figure A25. C5 score at site 9 and 10 over time.

APPENDIX B: SIGNIFICANT CORRELATIONS

B.1 DOC: TEMPORAL CORRELATIONS

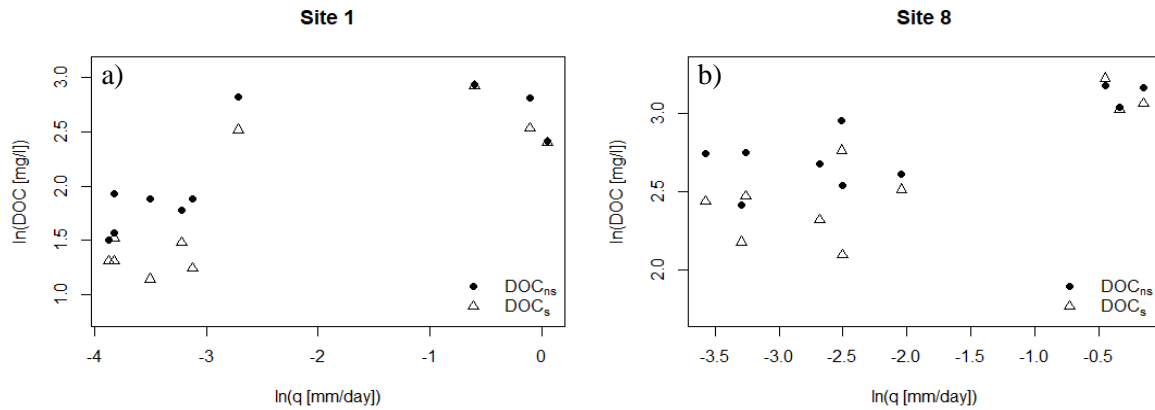


Figure B1. Log-log plot of DOC concentration against specific discharge at a) site 1 and b) site 8.

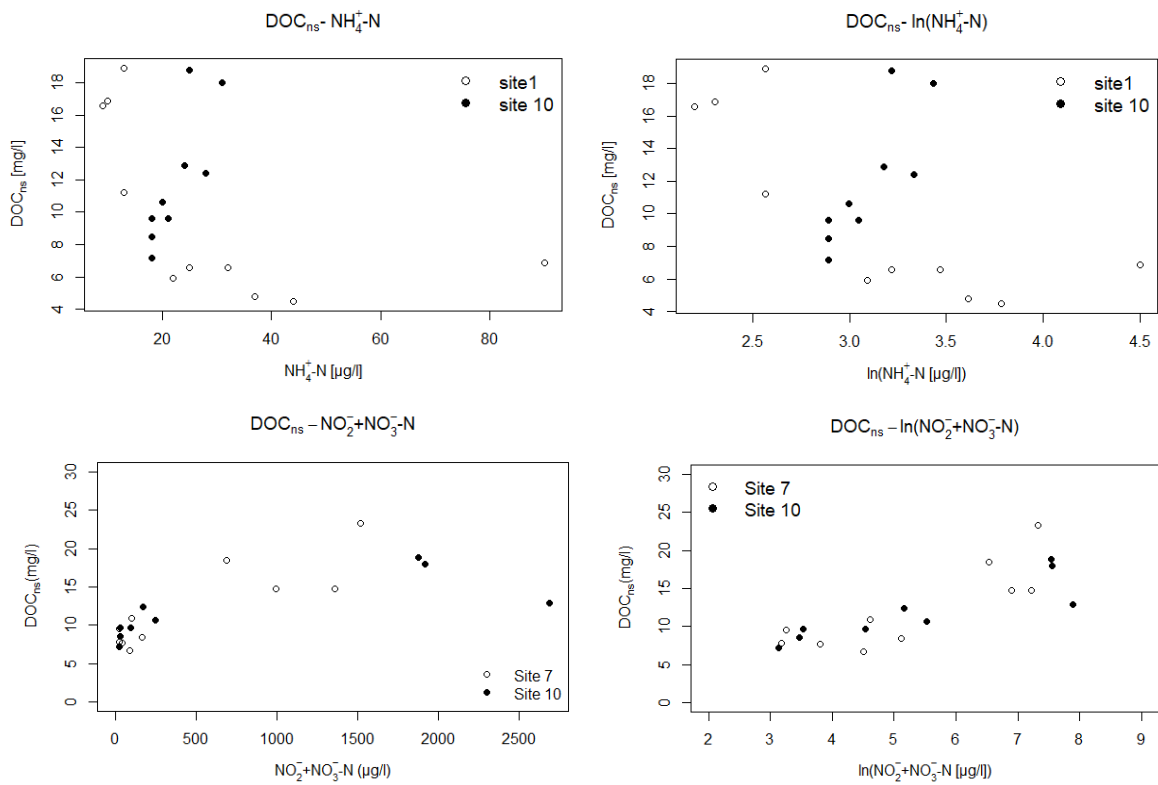


Figure B2. Plots of significant correlations between DOCns concentration and nutrient concentrations.

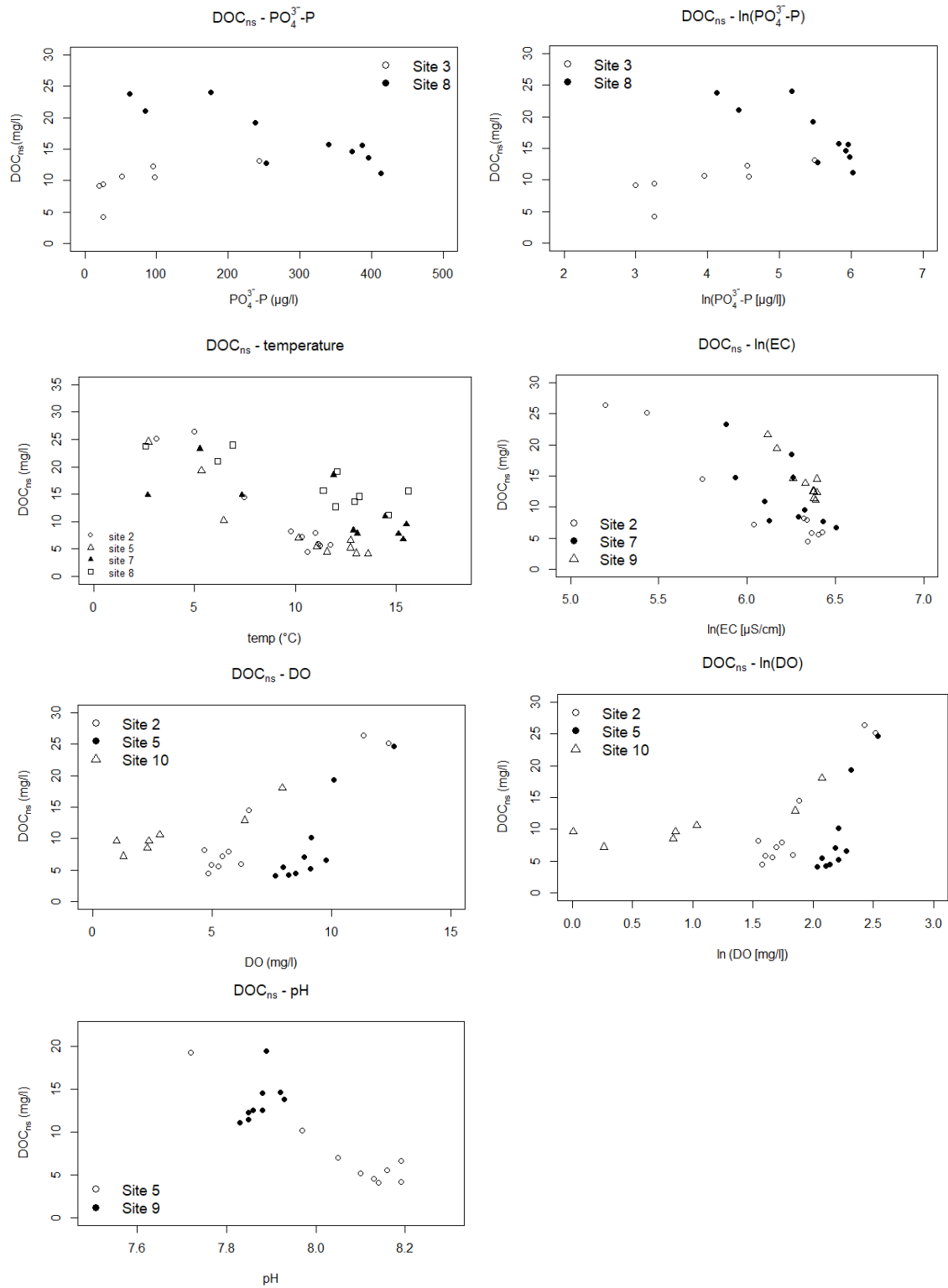


Figure B3. Plots of significant correlations between DOC_{ns} concentration and water chemistry variables.

B.2 FLUORESCENCE INDICES

B.2.1 Spatial correlations

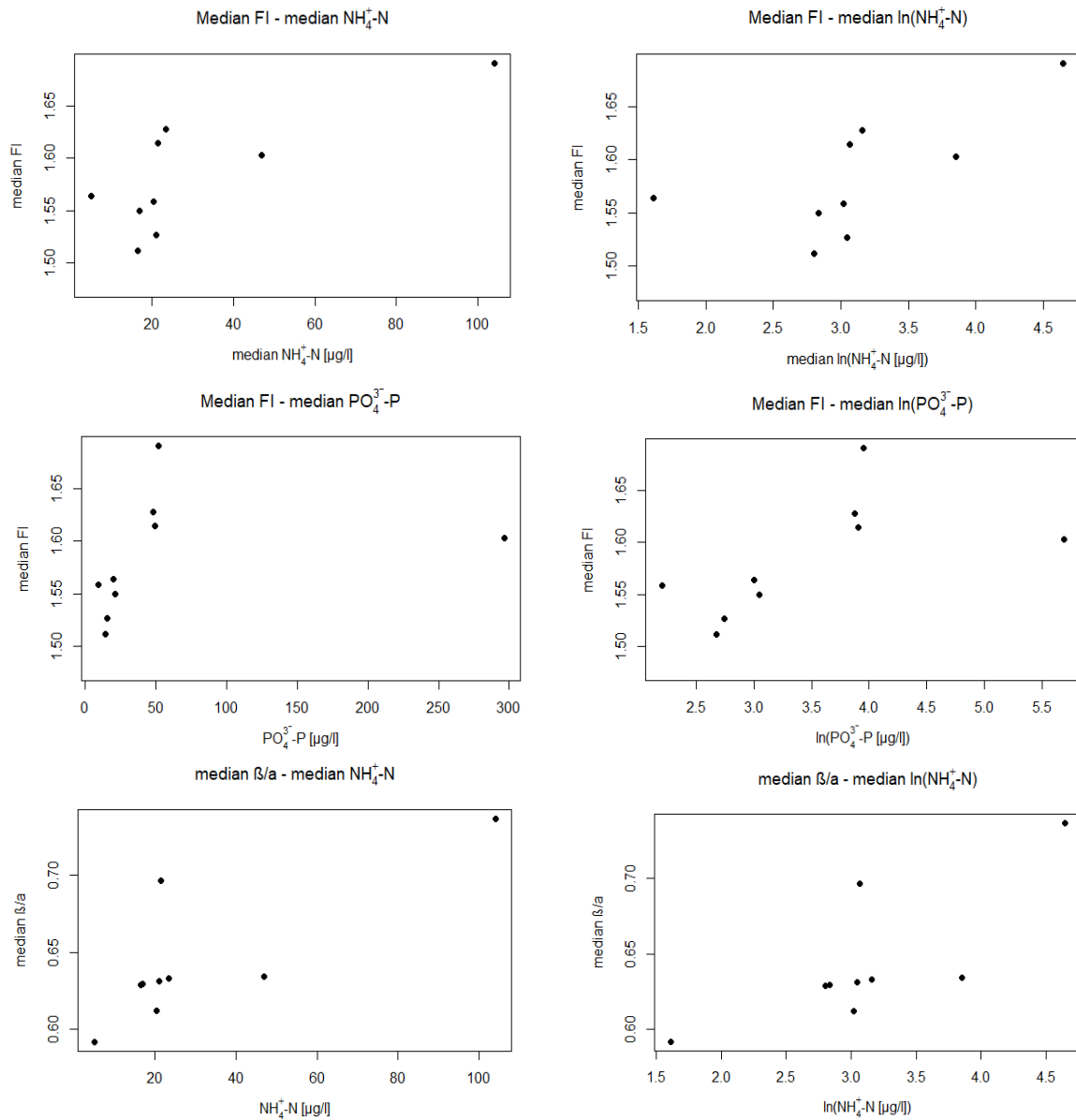


Figure B4. Plots of significant correlations between fluorescence indices and water chemistry variables on a spatial scale.

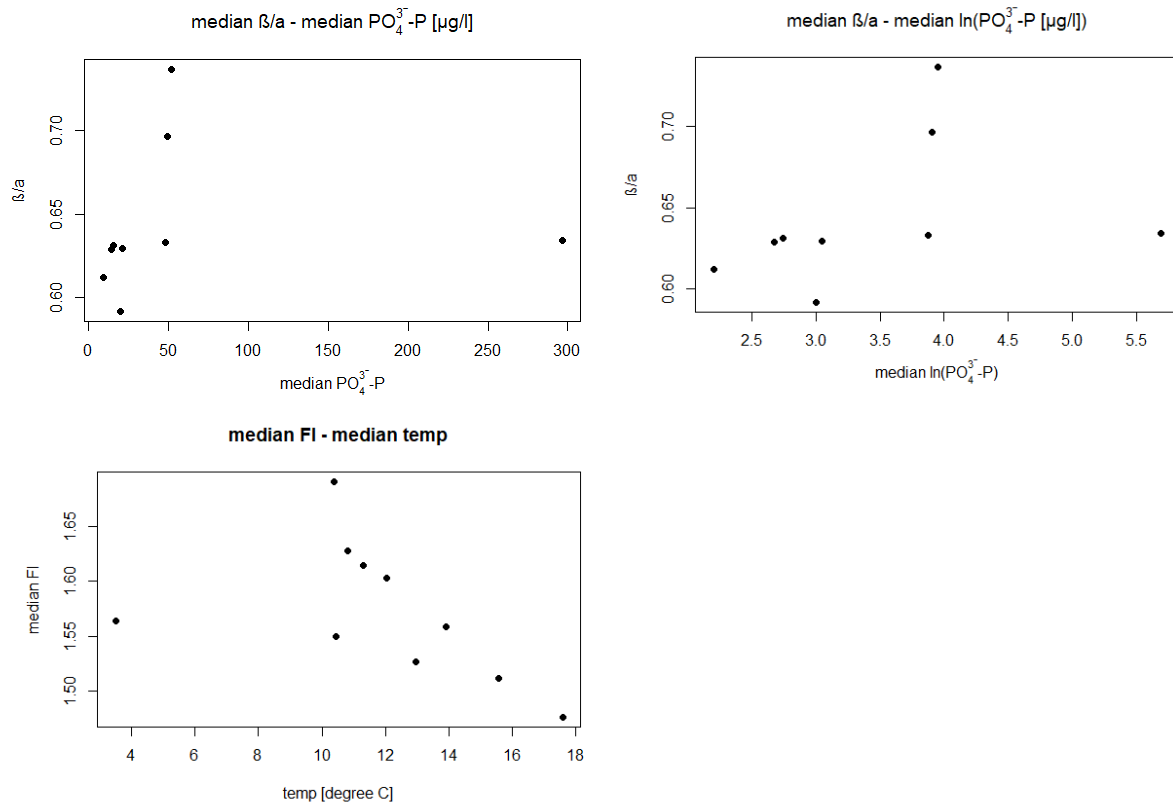


Figure B5. Plots of significant correlations between fluorescence indices and water chemistry variables on a spatial scale.

B.2.2 FI: Temporal correlations

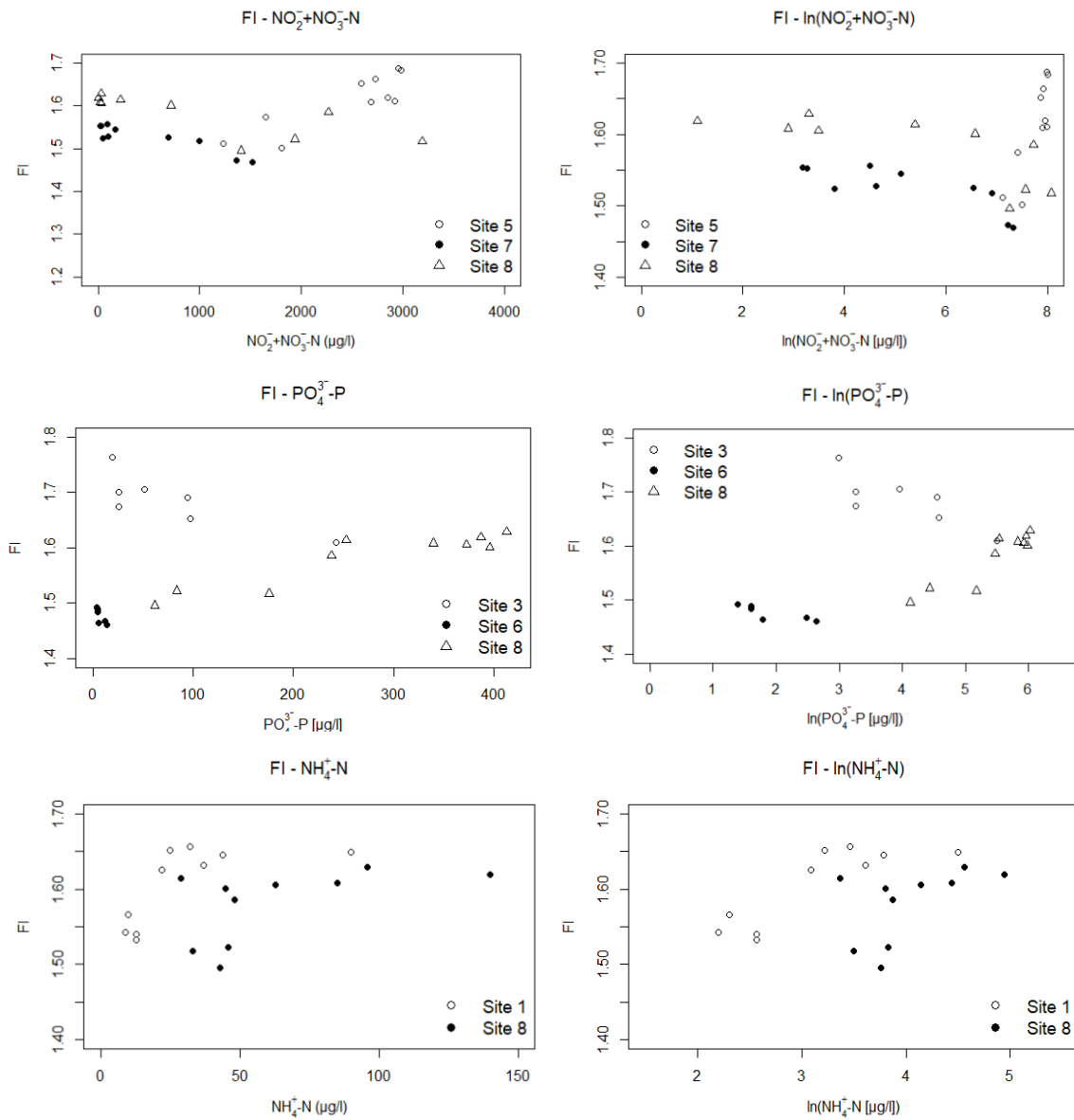


Figure B6. Plots of significant correlations between FI and nutrient concentrations.

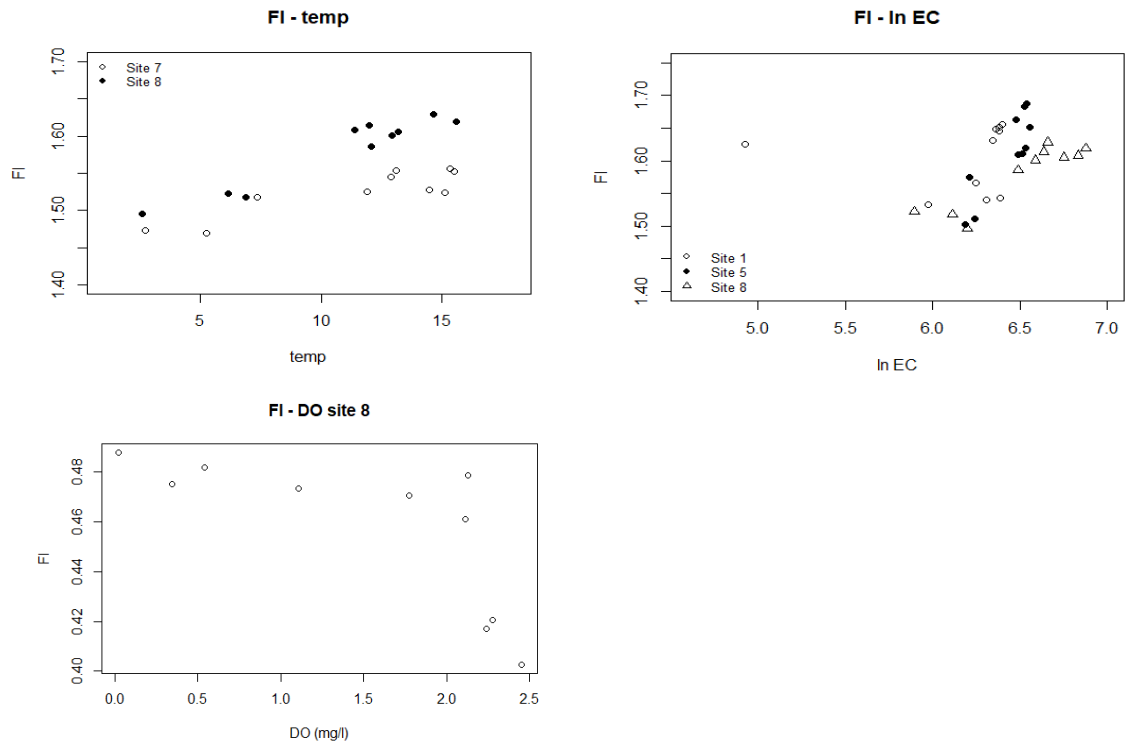


Figure B7. Plots of significant correlations between FI and water chemistry variables.

B.2.3 β/α : Temporal correlations

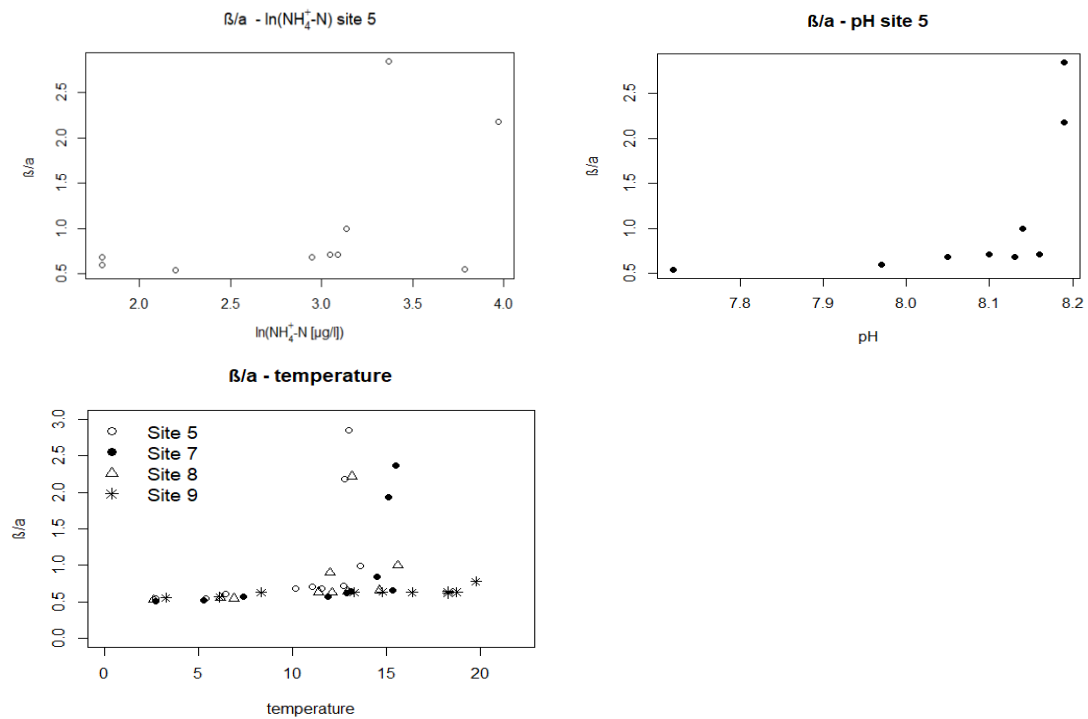


Figure B8. Plots of significant correlations between β/α and water chemistry variables on a temporal scale.

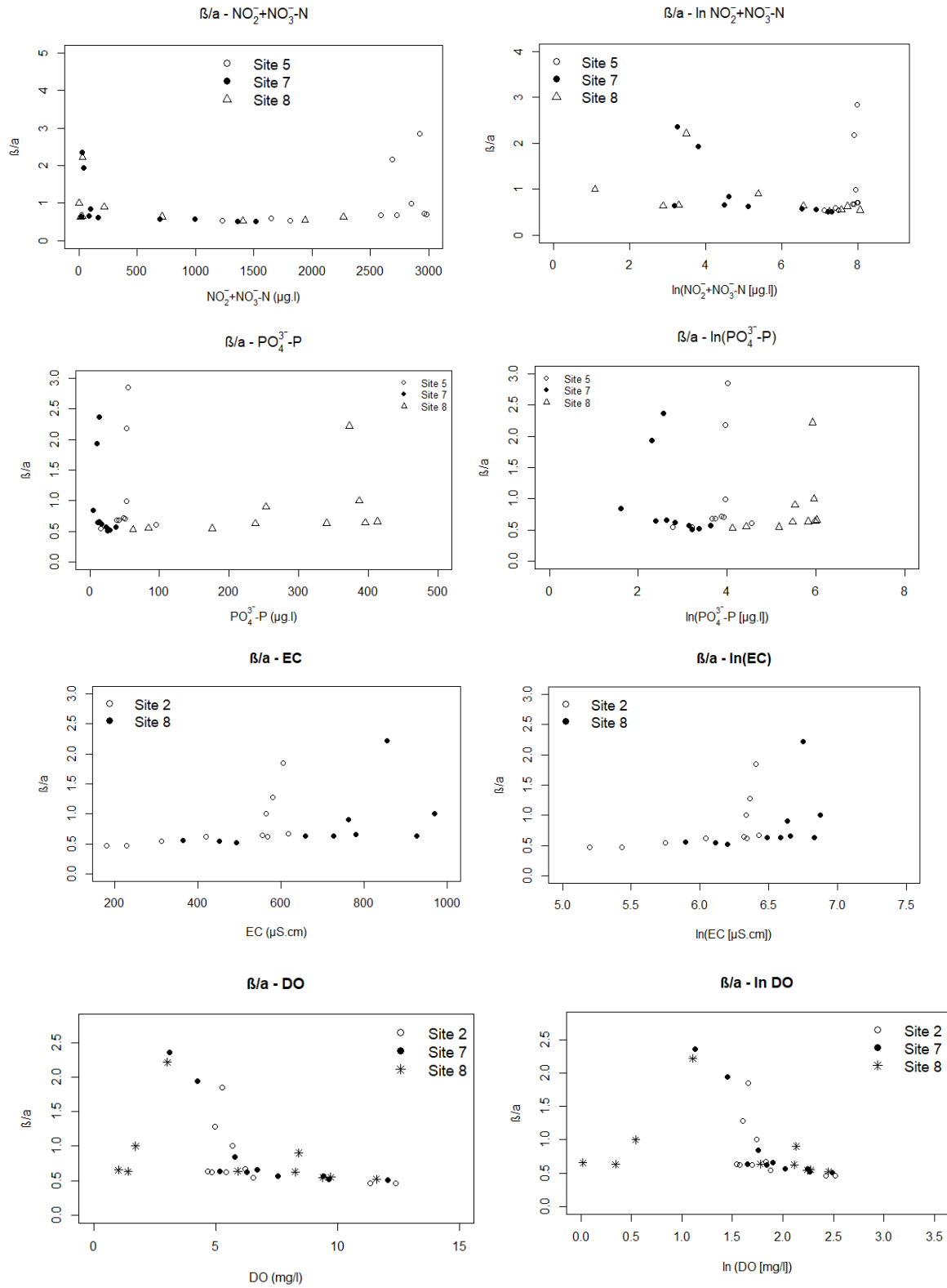


Figure B9. Plots of significant correlations between β/α and water chemistry variables on a temporal scale.

B.2.4 HIX: Temporal correlations

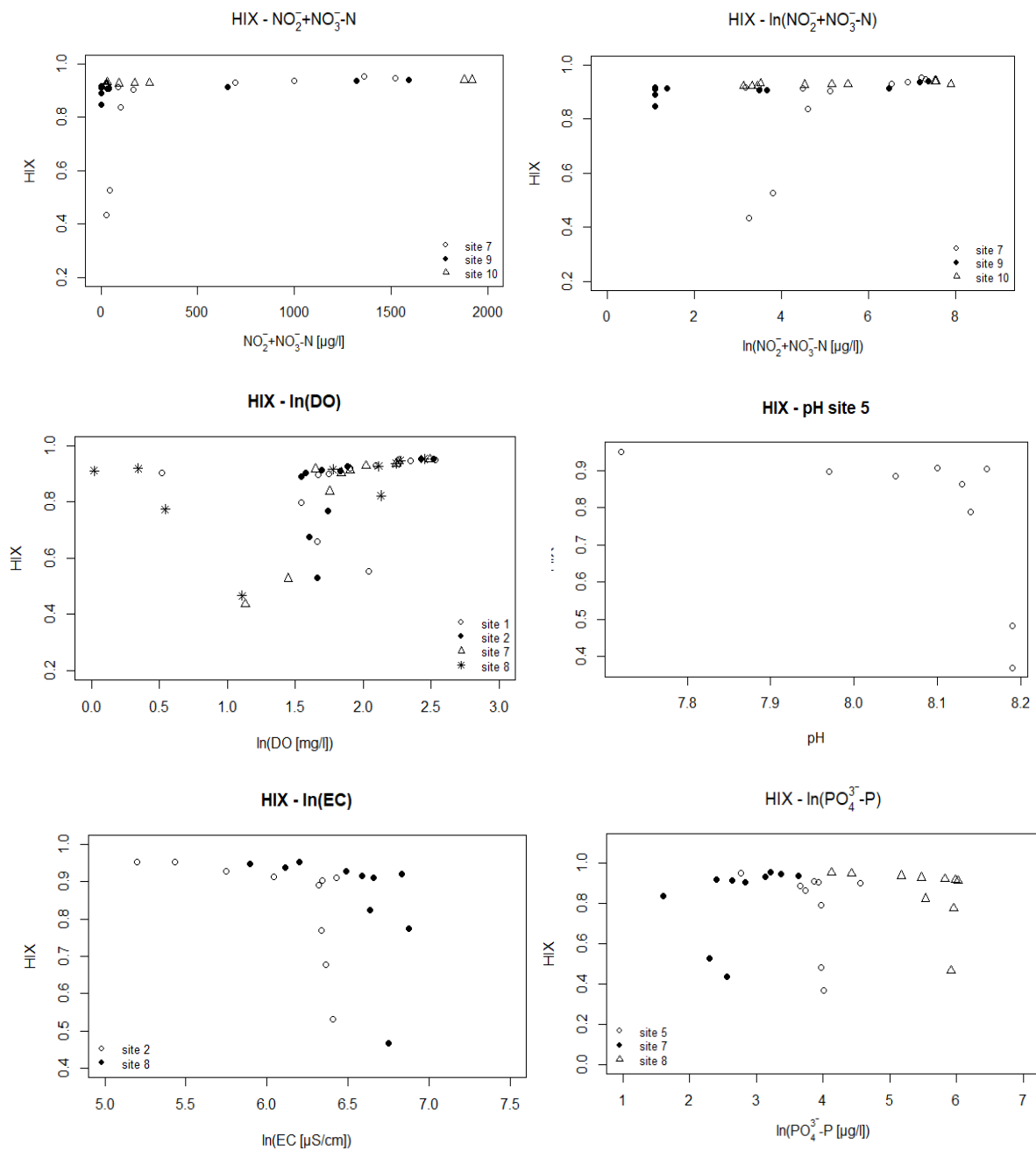


Figure B10. Plots of significant correlations between HIX and water chemistry variables on a temporal scale.

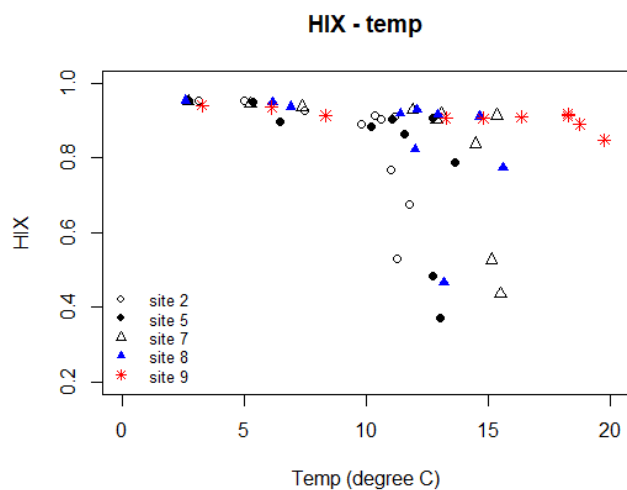


Figure B11. Plot of significant correlations between β/a and temperature on a temporal scale.

B.3 PARAFAC COMPONENTS

B.3.1 Spatial and Temporal correlations

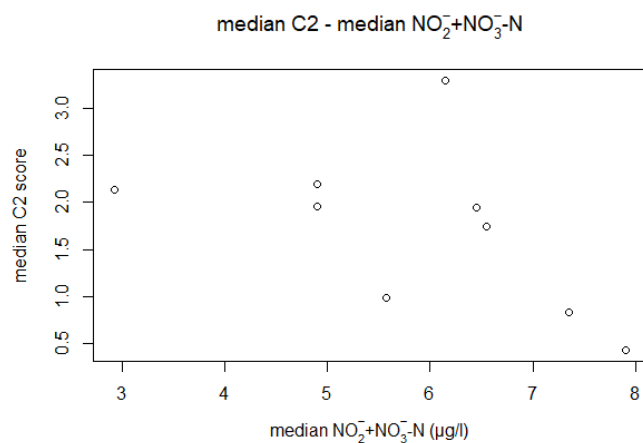


Figure B12. Plot of significant correlation between PARAFAC component C2 and $NO_2^- + NO_3^-$ -N concentration on a spatial scale.

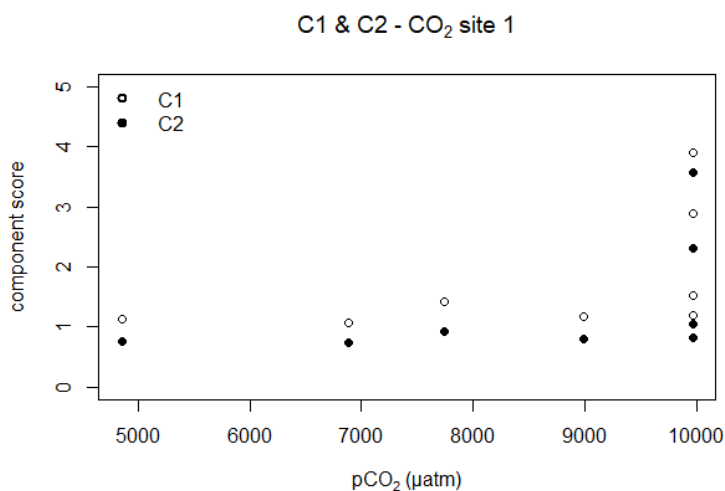


Figure B13. Plot of significant correlations between CO₂ and the PARAFAC components C1 and C2 at site 1.

Table B1. Spatial correlations between components.

Median	C1	C2	C3	C4	C5
C1		p<0.001 τ = 0.911	p<0.05 τ = 0.6	p<0.01 τ = 0.644	p<0.05 τ = 0.511
C2	p<0.001 τ = 0.911		p<0.05 τ = 0.511	p<0.05 τ = 0.556	p = 0.1083 τ = 0.422
C3	p<0.05 τ = 0.6	p<0.05 τ = 0.511		p<0.001 τ = 0.778	p = 0.1557 τ = 0.378
C4	p<0.01 τ = 0.644	p<0.05 τ = 0.556	p<0.001 τ = 0.778		p = 0.2164 τ = 0.333
C5	p<0.05 τ = 0.511	p = 0.1083 τ = 0.422	p = 0.1557 τ = 0.378	p = 0.2164 τ = 0.333	

Table B2. Spatial correlations between PARAFAC components and water chemistry variables.

Median	NH4	NO3+2	PO4	EC	DO (mg/l)	pH	Temp.
C1	p = 0.6122 $\tau = 0.167$	p = 0.0747 $\tau = - 0.479$	p = 0.9195 $\tau = - 0.056$	p = 1 $\tau = 0.022$	p = 1 $\tau = - 0.022$	p = 0.7275 $\tau = 0.111$	p = 0.3807 $\tau = 0.244$
C2	p = 0.9195 $\tau = 0.056$	p < 0.05 $\tau = - 0.592$	p = 0.6122 $\tau = - 0.167$	p = 0.8618 $\tau = - 0.067$	p = 1 $\tau = - 0.022$	p = 0.4843 $\tau = 0.2$	p = 0.3807 $\tau = 0.244$
C3	p = 0.1802 $\tau = 0.389$	p = 0.173 $\tau = - 0.366$	p = 0.9195 $\tau = 0.056$	p = 0.3807 $\tau = 0.244$	p = 0.3807 $\tau = - 0.244$	p = 0.2912 $\tau = - 0.289$	p = 0.2912 $\tau = 0.289$
C4	p = 0.1802 $\tau = 0.389$	p = 0.173 $\tau = - 0.366$	p = 0.612 $\tau = 0.167$	p = 0.4843 $\tau = 0.2$	p = 0.4843 $\tau = - 0.2$	p = 0.8618 $\tau = - 0.067$	p = 0.1083 $\tau = 0.422$
C5	p = 0.7614 $\tau = 0.111$	p = 0.6002 $\tau = - 0.141$	p = 0.7614 $\tau = 0.111$	p = 0.3807 $\tau = 0.244$	p = 0.7275 $\tau = 0.111$	p = 1 $\tau = - 0.022$	p = 0.6007 $\tau = - 0.156$

Table B3. Correlation (Kendall's tau) between DOC measured in stored samples and PARAFAC components at each site. Kendall's tau (τ), significance level (p) and number of observations (n) are given. Significant correlations ($p < 0.05$) are in bold.

Site	n	DOC _s (mg/l)				
		C1	C2	C3	C4	C5
1	10	p < 0.00003 $\tau = 0.91$	p < 0.00003 $\tau = 0.91$	p = 0.22 $\tau = -0.33$	p = 0.73 $\tau = -0.11$	p = 0.00012 $\tau = 0.87$
2	10	p = 0.0091 $\tau = 0.64$	p = 0.0022 $\tau = 0.73$	p = 0.86 $\tau = 0.067$	p = 0.38 $\tau = 0.24$	p = 0.017 $\tau = 0.6$
3	7	p = 0.0028 $\tau = 0.91$	p = 0.011 $\tau = 0.81$	p = 0.069 $\tau = 0.62$	p = 0.14 $\tau = 0.52$	p = 0.0028 $\tau = 0.91$
4	3	p = 1 $\tau = 0.33$	p = 1 $\tau = 0.33$	p = 1 $\tau = 0.33$	p = 1 $\tau = 0.33$	p = 1 $\tau = 0.33$
5	10	p = 0.0047 $\tau = 0.69$	p = 0.0009 $\tau = 0.78$	p = 0.86 $\tau = 0.067$	p = 0.48 $\tau = 0.2$	p = 0.00036 $\tau = 0.82$
6	6	p = 0.27 $\tau = 0.47$	p = 0.72 $\tau = 0.2$	p = 1 $\tau = -0.067$	p = 1 $\tau = -0.67$	p = 0.72 $\tau = 0.2$
7	10	p = 0.0022 $\tau = 0.73$	p = 0.00012 $\tau = 0.87$	p = 0.38 $\tau = -0.24$	p = 0.60 $\tau = 0.16$	p = 0.00012 $\tau = 0.87$
8	10	p = 0.29 $\tau = 0.29$	p = 0.00036 $\tau = 0.82$	p = 0.029 $\tau = -0.56$	p = 0.017 $\tau = -0.6$	p = 0.0022 $\tau = 0.73$
9	10	p = 0.0022 $\tau = 0.73$	p = 0.0022 $\tau = 0.73$	p = 0.73 $\tau = -0.11$	p = 0.22 $\tau = 0.33$	p = 0.017 $\tau = 0.6$
10	10	p = 0.0009 $\tau = 0.78$	p = 0.0009 $\tau = 0.78$	p = 0.86 $\tau = 0.067$	p = 0.029 $\tau = 0.56$	p = 0.00036 $\tau = 0.82$

Table B4. Correlation between specific discharge and PARAFAC component score.

Specific discharge (mm/day)					
Site	C1	C2	C3	C4	C5
1	p = 0.15 $\tau = 0.36$	p = 0.15 $\tau = 0.36$	p = 0.37 $\tau = -0.22$	p = 1 $\tau = 0$	p = 0.11 $\tau = 0.40$
2	p = 0.21 $\tau = 0.31$	p = 0.11 $\tau = 0.40$	p = 0.28 $\tau = -0.27$	p = 1 $\tau = 0$	p = 0.21 $\tau = 0.31$
3	p = 0.24 $\tau = -0.43$	p = 0.14 $\tau = -0.52$	p = 0.38 $\tau = -0.33$	p = 0.24 $\tau = -0.43$	p = 0.24 $\tau = -0.43$
4	p = 0.33 $\tau = -1$	p = 0.33 $\tau = -1$			
5	p = 0.020 $\tau = 0.58$	p = 0.0071 $\tau = 0.67$	p = 0.86 $\tau = -0.045$	p = 0.72 $\tau = 0.090$	p = 0.0041 $\tau = 0.72$
6	p = 0.25 $\tau = -0.41$	p = 0.70 $\tau = -0.14$	p = 0.70 $\tau = 0.14$	p = 0.70 $\tau = 0.14$	p = 0.70 $\tau = -0.14$
7	p = 0.11 $\tau = 0.42$	p = 0.029 $\tau = 0.56$	p = 0.073 $\tau = -0.47$	p = 0.60 $\tau = -0.16$	p = 0.029 $\tau = 0.56$
8	p = 0.73 $\tau = -0.11$	p = 0.11 $\tau = 0.42$	p = 0.047 $\tau = -0.51$	p = 0.0091 $\tau = -0.64$	p = 0.38 $\tau = 0.24$
9	p = 0.073 $\tau = 0.47$	p = 0.073 $\tau = 0.47$	p = 0.29 $\tau = -0.29$	p = 0.86 $\tau = 0.067$	p = 0.017 $\tau = 0.6$
10	p = 0.0091 $\tau = 0.64$	p = 0.0091 $\tau = 0.64$	p = 0.73 $\tau = 0.11$	p = 0.11 $\tau = 0.42$	p = 0.00095 $\tau = 0.78$

B.3.2 C1: Temporal correlations

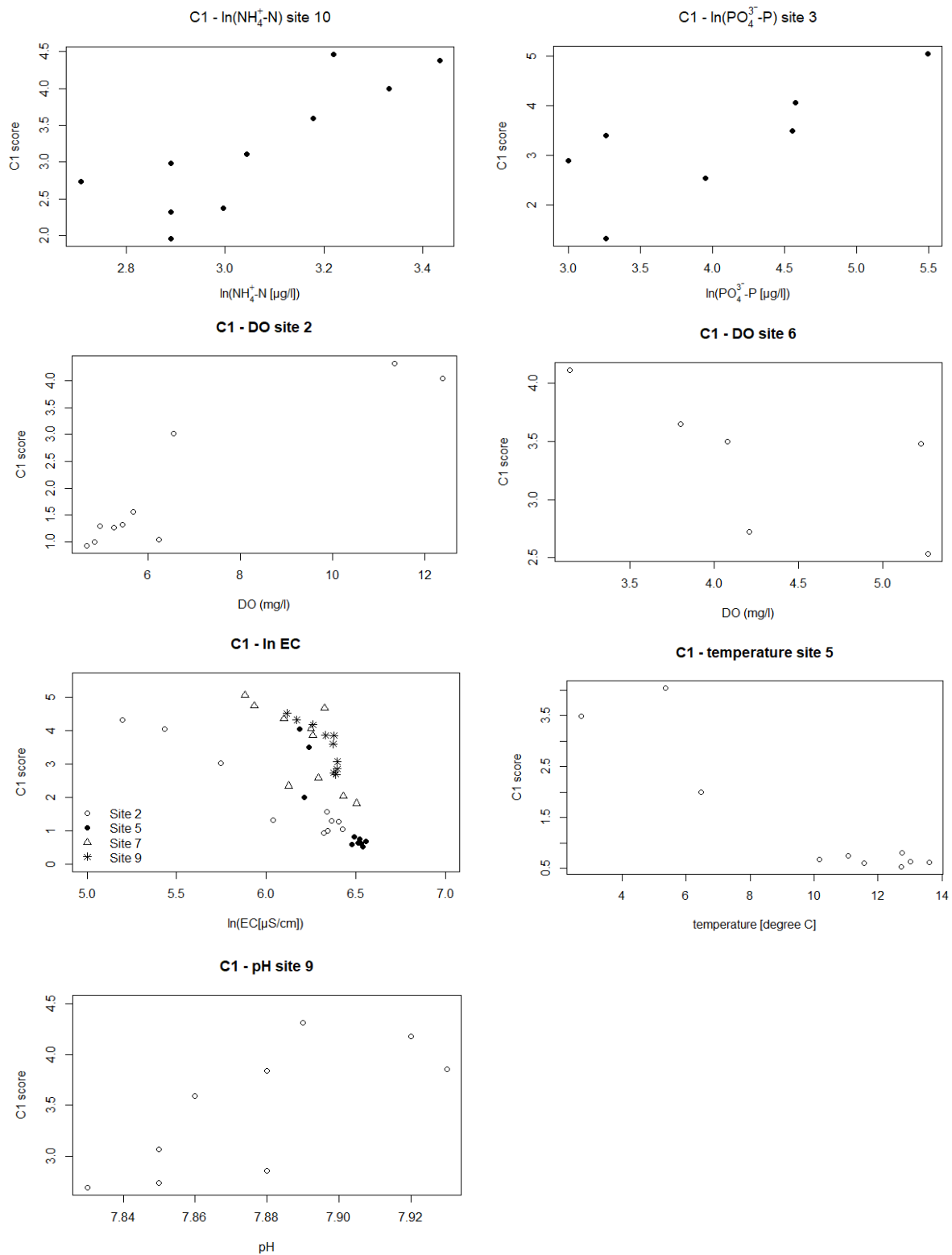


Figure B14. Plots of significant correlations between C1 score and water chemistry variables on a temporal scale.

B.3.3 C2: Temporal correlations

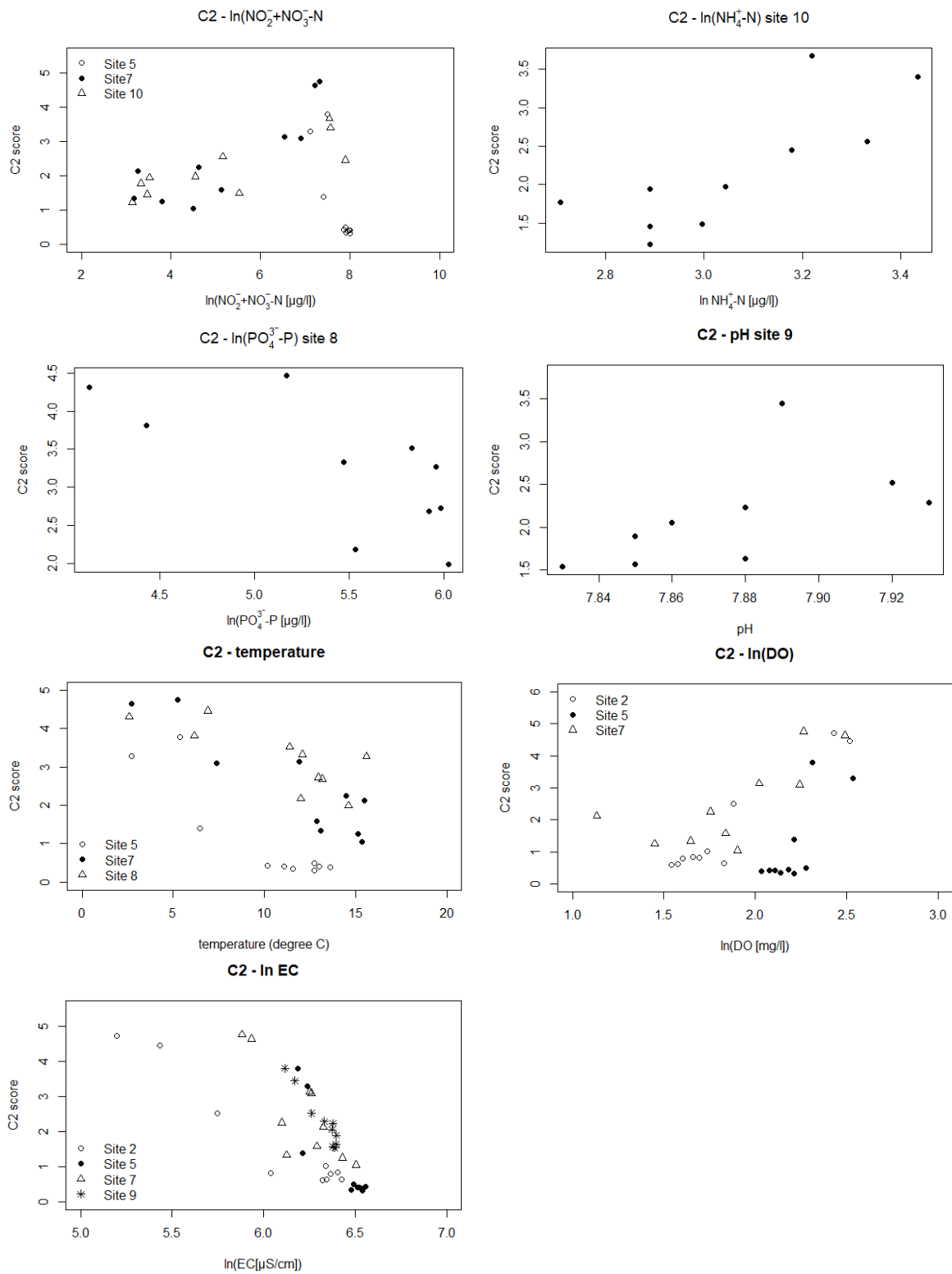


Figure B15. Plots of significant correlations between C2 score and water chemistry variables on a temporal scale.

B.3.4 C3: Temporal correlations

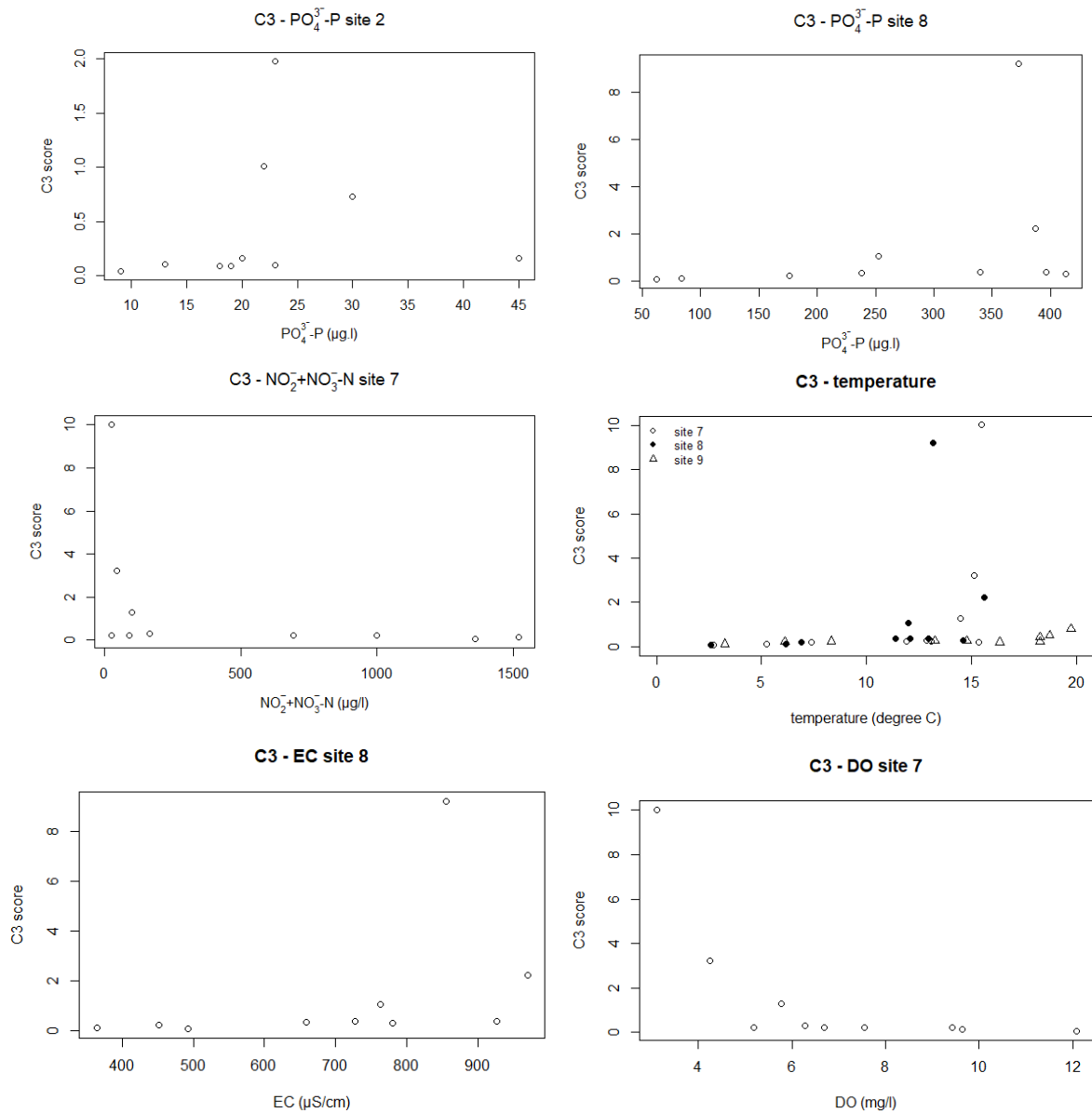


Figure B16. Plots of significant correlations between C3 score and water chemistry variables on a temporal scale.

B.3.5 C4: Temporal correlations

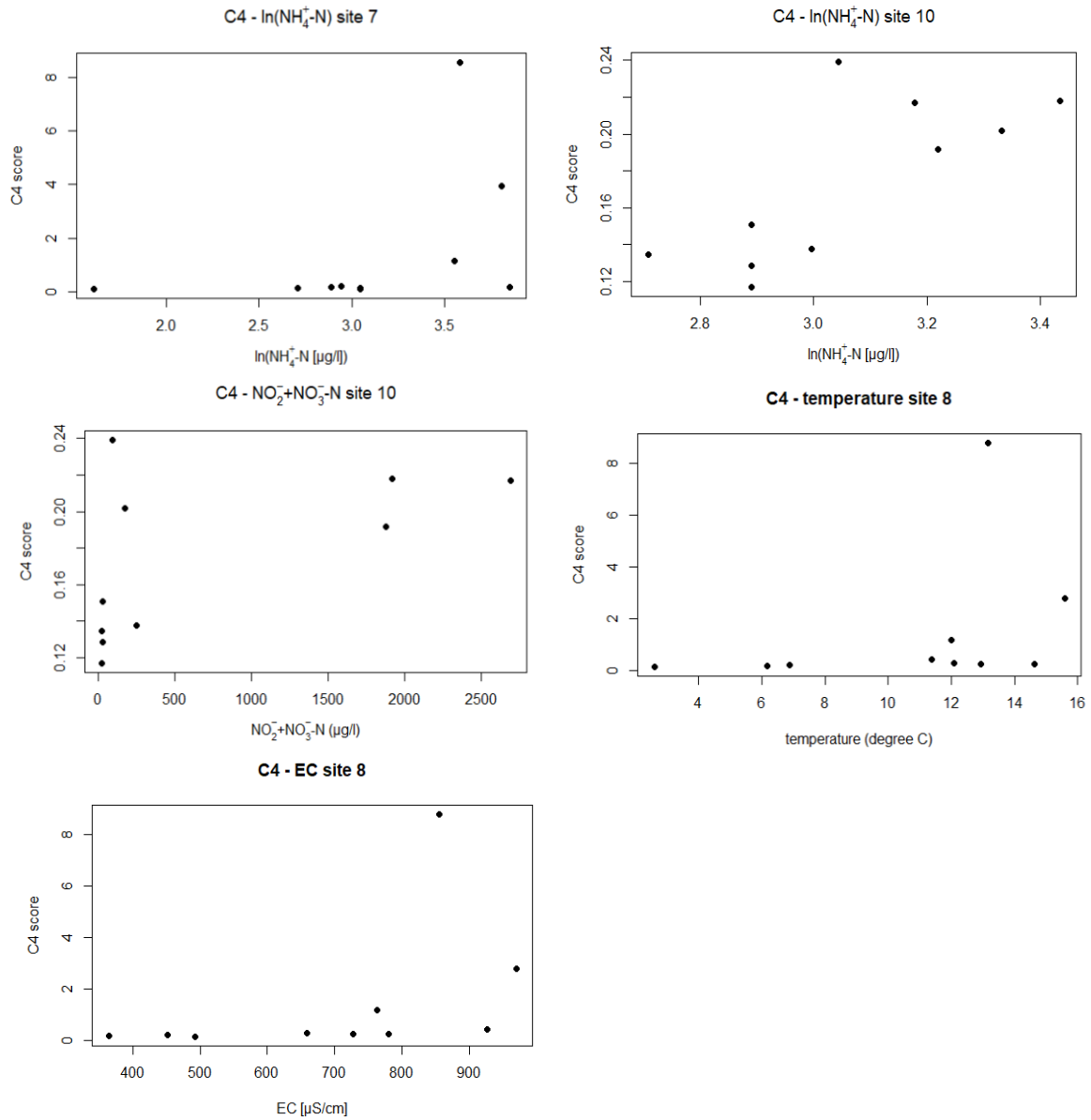


Figure B17. Plots of significant correlations between C4 score and water chemistry variables on a temporal scale.

B.3.6 C5: Temporal correlations

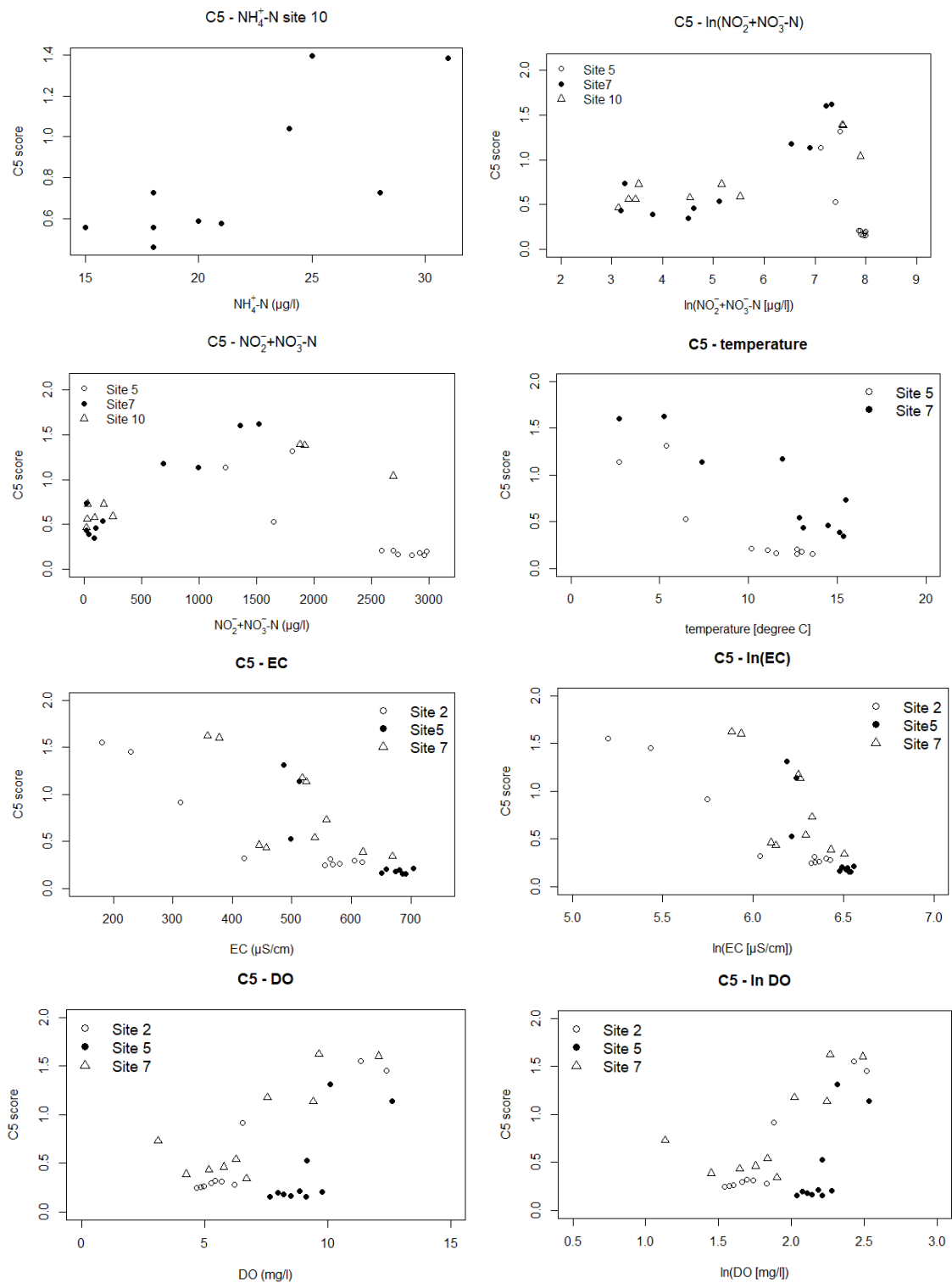


Figure B18. Plots of significant correlations between C5 score and water chemistry variables on a temporal scale.